Reduction of Internal Phosphorus Loading in Agricultural Drainages Using Iron-Incorporated Sediment Microbial Fuel Cells

Graduate School of Environmental and Life Science
(Doctor's Course)

OKAYAMA UNIVERSITY

Gamamada Liyanage Erandi Priyanagika Perera

March 2024

TABLE OF CONTENTS

ABSTRACT

Excessive phosphorus (P) in aquatic environments promotes eutrophication in closed-water bodies. Under anaerobic conditions, microbial reduction of ferric (Fe^{3+}) to ferrous (Fe^{2+}) ions releases redox-sensitive P from sediment. For better water quality management, it is essential to suppress internal P loading. In this study, we determined the effect of mixing amorphous FeOOH, biochar (BC), and Fe-treated biochar (Fe-BC) with agricultural drainage sediment to suppress P release under different dissolved oxygen conditions. The addition of FeOOH significantly suppressed P release from the sediment. On the other hand, Fe-BC and BC addition suppressed P release under high-dissolved oxygen conditions. However, low-dissolved oxygen conditions increased P release from sediment. Our study suggested that FeOOH has a better potential to suppress P release than biochar. Furthermore, we investigated the potential effect of adding Fe^{2+} or Fe^{3+} ions to sediment microbial fuel cells (SMFCs) on the suppression of P release. Mixing Fe^{3+} with sediment in SMFCs enhanced electricity generation and reduced P release from the sediment. In contrast, Fe^{2+} addition showed similar electricity to sediment-only treatment. Our findings suggest that incorporating Fe^{3+} in SMFCs is more effective in mitigating P release. Furthermore, we investigated the P suppression by Fe^{3+}-incorporated SMFCs on different sediments. Results indicated higher P release from organic matter-rich sediment than from sediment with a lower total P content. During SMFC operation, P release decreased until day 42. Afterward, P concentrations became similar to no SMFC condition. Moreover, Fe addition increased P release from sediment probably because of the P mineralization. Our research revealed that Fe precipitation caused by SMFCs efficiently suppressed P release for 42 days. However, SMFC operation or Fe addition would increase organic matter decomposition in organic matter-rich sediment after a long-time, which in turn enhances P release into the overlying water. The findings of these experiments suggested the effectiveness and limitations of SMFCs as a technology for suppressing P release from agricultural drainage sediment.

Keywords: *Iron hydroxide, Iron treated biochar, Electricity, Nitrate, Iron ions, Sulfur oxidation, Ammonium.*

ACKNOWLEDGEMENTS

I am truly grateful to the wonderful individuals who supported and inspired me throughout the completion of my doctoral thesis.

I would like to express my deepest appreciation to my mentor, Professor Morihiro Maeda, and his family for their tremendous patience and unwavering support. Without the guidance and assistance from my supervisor, I would not be able to make this journey a success. His valuable feedback and encouragement have been instrumental in shaping the direction of my work.

In addition, I am deeply indebted to my co-supervisors, Assistant Professor Hiroaki Somura and Professor Yasushi Mori, for their unceasing feedback and inspiration during these three years. Their expertise and mentorship have been invaluable in helping me navigate challenges and achieve my research goals.

I am extremely grateful to Prof. Yuta Nishina for his invaluable assistance in conducting biochar production, and analysis, and for providing guidance and access to laboratory facilities. I would also like to extend my deepest gratitude to Prof. Satoshi Akao and Prof. Takashi Tamura for their assistance and contribution throughout the microbial analysis process. I am deeply appreciative of Assistant Professor Nakano's commitment to my academic growth and development, and I look forward to continuing to learn from her expertise in the future. I have the utmost gratitude to Assistant Professor Chiyu Nakano for his tremendous guidance in helping me conduct property analysis and biochar production. My special thanks to Associate Professor Yasushiko Benino, who has provided me with significant support in XRF analysis. It was always an amazing experience to collaborate with experts in different fields.

I am immensely thankful to the Ministry of Education, Culture, Sports, Science, and Technology (MEXT) and the OU Fellowship for their kind assistance in funding this research and providing living expenses. Their support has played a crucial role in the successful fulfillment of our research project.

Next, my sincere appreciation goes to my undergraduate supervisor, Prof. Bandunee Athapattu, who introduced me to Prof. Morihiro Maeda and never stopped encouraging me to pursue overseas studies. She has been more than just a teacher, but more of a mother figure.

I want to express my heartfelt thanks to Mrs. Tomoko Yabe for her warm help and support during these years. I am truly grateful for her kindness and assistance.

Many thanks to my lab mates for embracing me as part of their family. Their camaraderie and support have made my experience in the lab truly special. I am grateful for their kindness, teamwork, and friendship, which have made every day a joy to be in the lab. Thank you for being an amazing group of colleagues and friends.

I cannot forget to thank my family, for their endless love and understanding. Their presence in my life has been a source of strength and comfort. I am truly blessed to have such a wonderful family in my life. Though he is no longer with me, I am eternally grateful to my father, Mr. Bernard Perera, for the values, wisdom, and inspiration he instilled in me to shape the person I am today. Finally, I want to sincerely thank my husband, Mr. Prabath Thennakoon, for being my pillar of support and for his patience, encouragement, and companionship. Thank you for always believing in me and for standing by me through thick and thin.

LIST OF TABLES

LIST OF FIGURES

ABBREVIATIONS

P: Phosphorus

Fe: Iron

Fe^{3+}: Ferric ion

Fe^{2+}: Ferrous ion

FeOOH: Amorphous ferric oxyhydroxide

FeS: Iron sulfide

BC: Prestine biochar

ZVI: Zero valent iron

SMFCs: Sediment microbial fuel cells

Fe-BC: Iron-treated biochar

DO: Dissolved oxygen

EC: Electrical conductivity

LS: Livestock area

PS: Pasture grown area

OC: Open circuit (act as a control without SMFC)

CC: Closed circuit (act as a SMFC)

CHAPTER 1
INTRODUCTION

1.1 Background

Phosphorus (P) is an essential nutrient for plant growth and a common element in agricultural fertilizers. However, when it is exceeding in surface waters causes eutrophication, leading to overgrowth of algae and phytoplankton (Schindler et al., 2008; Carpenter, 2008). Although external P inputs are well controlled by water treatment techniques, lake water quality has not entirely recovered (Munch et al., 2024). Remobilization of P stored in sediment has obscured the effects of water conservation measures, leading to continuous eutrophication (Stackpoole et al. 2019; Sharpley et al. 2013; Sharpley et al. 2011). The iron (Fe) redox cycle plays a major role in the P release from anaerobic sediment (Nguyen et al., 2016). Under oxic conditions, ferric ions (Fe^{3+}) would fix P in sediment by sorption and precipitation (Robertson and Lombardo, 2011). As the oxygen concentration depletes, bacteria in sediment switch their energy metabolism and reduce Fe^{3+} to Fe^{2+} causing phosphate (PO_4^{2-}-P) release from sediment (Yin et al., 2022; Ohmura et al., 2002).

Agricultural drainages are one of the primary pathways of P into waterways. In many countries, it has been determined that the primary cause of eutrophication in aquatic bodies is agricultural runoff (Marella et al., 2022). Phosphorus fertilizer in Italy accounts for 71% of the overall P load, and P release from non-point agricultural sources accounts for 67% of total pollution discharge in China (Luo et al., 2023). The large quantity of P that agricultural runoff releases into waterways has been accumulating in sediment for years (Zhang and Baoqing, 2008). Due to continuous P runoff from fertilized or manure-applied lands, sediment in agricultural drainages may have a high P content. Phosphorus in sediment serves as a hidden P source that leads to water eutrophication if it is released into the overlying water under reductive conditions. To regulate and restore eutrophic waterways, it is essential to remediate P release from sediment in agricultural drainages.

Many studies have reported on the pros and cons of Fe addition in lowering internal P loading from lake sediment (Bakker et al., 2016; Immers et al., 2015; Burley et al., 2001). In some cases, Fe addition was not efficient in P suppression because Fe^{3+} and

sulfate reduction under anaerobic conditions released PO_4^{2-}-P trapped by Fe (Munch et al., 2024; Kleeberg et al., 2013). On the other hand, Fe is often used for biochar modification because it is naturally abundant and has minimal toxicity (Qian et al. 2021). Although Fe-treated biochar has shown a high affinity to P and a low tendency to desorb (Strawn et al., 2023), its applicability to suppress internal P loading was not well discussed. To improve the management of internal P release using Fe-oxides or Fe-treated biochar sediment characteristics and redox reactions must be further investigated.

Sediment microbial fuel cells (SMFCs) are bio-electrochemical systems that produce electricity from anaerobic organic matter decomposition (Algar et al., 2020; Guo et al., 2019). These systems are made up of a cathode submerged in water with a high oxygen content above an anode embedded in anaerobic sediment (Liu et al., 2022; Liu et al., 2019; Schamphelaire et al., 2008). Electrons produced during microbial organic matter decomposition are accepted by the anode and transferred to the cathode via an external circuit (Hong et al., 2009). These electrons will be consumed at the cathode along with protons and oxygen to produce water (Pergola et al., 2023). The release of P from anaerobic sediment can be prevented by SMFCs (Takemura et al., 2021). In SMFCs, P was retained in sediment because of microbial Fe^{2+} oxidation and redox potential increment that prevented Fe^{3+} reduction (Wang et al., 2022; Qi et al., 2022; Yang et al., 2021; Haxthausen et al., 2021; Yang et al., 2016; Martins et al. 2014). According to the hypothesis of this study, SMFCs may increase the redox potential at the sediment surface, which will prevent redox-sensitive P release, particularly of Fe-bound P. The major bottle neck of SMFC field application is high internal resistance in sediment (Wang et al., 2023; Guo et al., 2022). To suppress P release from sediment with SMFCs, electrons should be effectively transferred from sediment. Iron incorporation with the anode was better in catalytic activities when used in SMFCs, which enhanced electricity production (Kim et al., 2022; Okavitri et al., 2021; Zhou et al., 2014). However, the effect on P release from agricultural drainage sediment by applying Fe-added SMFCs has not been well explored. Sediment properties such as organic matter content and nutrient availability can influence the activity and composition of microbial communities in the sediment. These microbial communities play a crucial role in the release and cycling of nutrients, including P. Therefore, variations in sediment properties may impact the efficiency and dynamics of P release in SMFC systems.

1.2 Objectives and Organization of the Thesis

This thesis aimed to suppress P release from agricultural drainage sediments with the use of Fe as a P adsorbent and an electron shuttle in SMFCs. Determining the limitations of common P adsorbents, such as Fe-oxides and Fe-treated biochar, under different field conditions is also crucial.

The present thesis has been structured (Fig. 1) to address the following objectives in particular chapters:

I. to determine the effectiveness of adding Fe hydroxide or Fe-treated biochar to sediment for reduction of P release from sediment when the O_2 supply is varied (Chapter 3),

II. to identify the effectiveness of adding different Fe ions to SMFCs as electron donors and P-fixing agents (Chapter 4), and

III. to assess the effect of Fe-added SMFC on P release from different sediments (Chapter 5).

Chapter 2 covered the mechanism of internal P release from sediment under anaerobic conditions, as well as typical remedial techniques and their limits. Along with the literature, biochar production techniques, P-adsorbing mechanisms, Fe treatment for biochar, and their possible uses were addressed in detail. Based on supporting data from the literature, the application of SMFCs to P reduction, usage of Fe to increase SMFC performances, difficulties to be overcome, and current knowledge gaps were explained. This chapter outlines the originality of the research.

Chapter 3 demonstrated how different dissolved oxygen (DO) conditions affect P release from Fe-hydroxides, biochar, or Fe-treated biochar-amended sediments. Previous studies suggested adding Fe-hydroxide or Fe-treated biochar as an approach to manage internal P loading. To the best of our knowledge, this is the first study that investigated the effect of DO conditions in the overlying water on P sorption of Fe-treated biochar-amended agricultural drainage sediments. Our study showed that Fe-hydroxide addition has the highest P adsorption under low DO conditions. However, continual low DO conditions released P and Fe under low amending rates. Iron-treated biochar effectively reduced P release when the DO is high whereas lower DO conditions increased

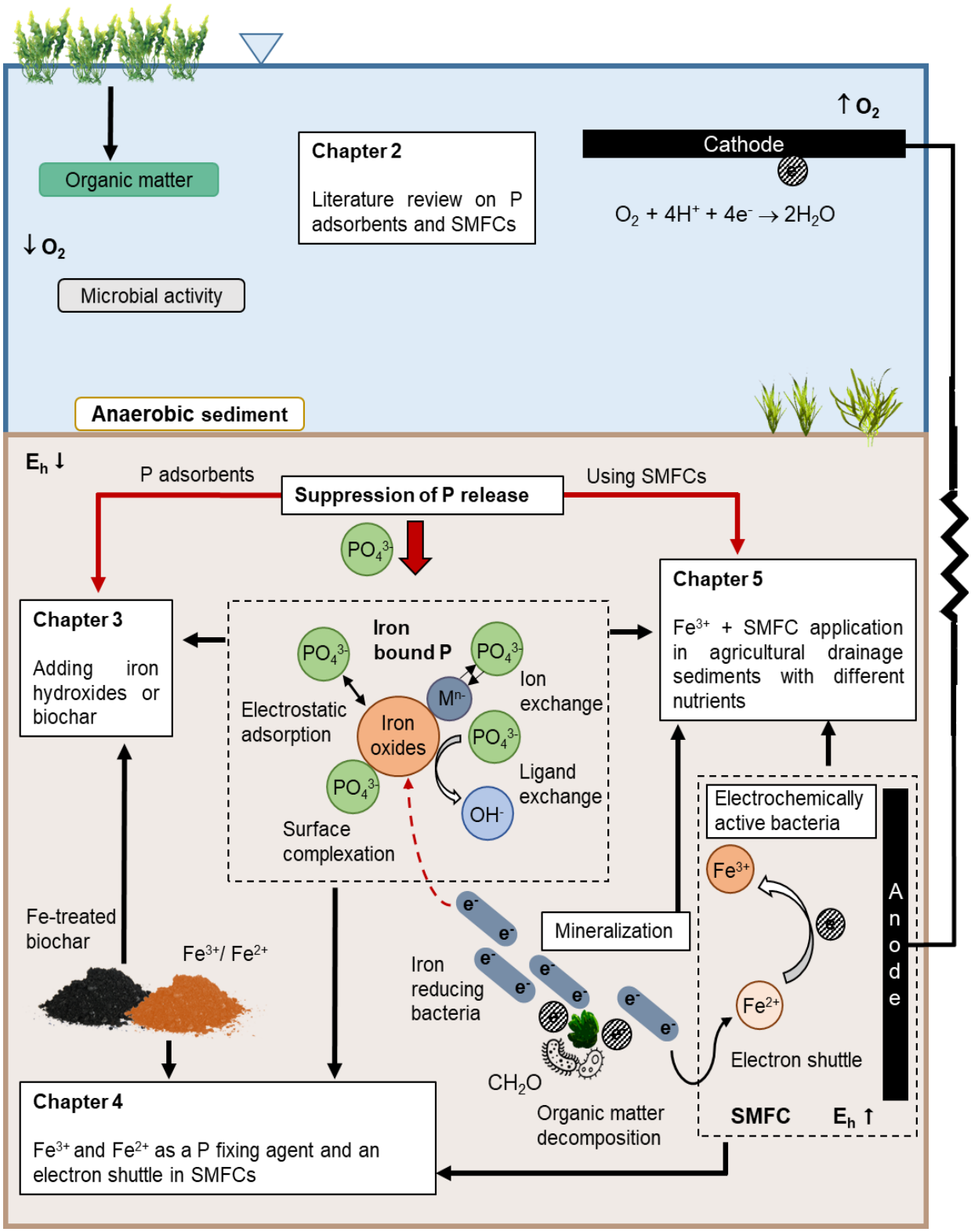

Figure 1.1 Organization of the thesis

P release from Fe-treated biochar added sediment. These findings indicated that Fe^{3+} and

sulfate reduction under anaerobic conditions inhibited long-term suppression of P release with lo w rates of Fe-hydroxides, biochar, or Fe-treated biochar-amended sediments.

Chapter 4 investigated the addition of Fe^{3+} and Fe^{2+} in a dual chamber SMFC as an electron shuttle or an electron donor. Many studies investigated the power enhancement by Fe-incorporated SMFCs. So far, none of the studies identified the suitability between Fe^{3+} and Fe^{2+} as an anode amendment in SMFCs to suppress P release from sediment while enhancing electricity. In this study SMFCs, Fe^{3+} addition showed higher electricity whereas Fe^{2+} showed similar electricity with the sediment-only treatment. During 49 days of the experiment, Fe-added sediments reduced P release from sediment. Our research found that Fe^{3+} addition in SMFCs suppressed P release and increased electricity production, acting as an electron shuttle. However, adding Fe^{2+} did not act as an electron donor in SMFCs because Eh increased by SMFCs was not high enough to oxidize Fe^{2+}.

Chapter 5 explored the reduction of P release from sediment by SMFCs, or Fe-added SMFCs for agricultural drainage sediments with two different nutrient contents. Before utilizing SMFCs in the field, it is important to determine their impact on P reduction from sediments with various characteristics. According to our results, SMFCs suppressed P release from sediment. The release of P from sediment with high nutrient content was higher than the sediment with low P content. In the latter period, SMFCs showed a similar P concentration to sediment-only treatment while Fe-added SMFCs increased P release more than that was in sediment-only treatment. In addition, SMFCs increased Fe release into the overlying water, and sulfur-oxidizing bacteria were abundant under SMFC operation. Iron addition or SMFC application in sediments with high nutrient contents may increase P release from the sediment to the overlying water due to P mineralization resulting from enhanced organic matter decomposition.

Chapter 6 provides a summary of the novel findings of the current study. The use of Fe-hydroxides, biochar, and Fe-treated biochar to suppress internal P loading from sediment and the impact of different DO conditions on the success of P suppression were concluded. Suppression of P release and enhancing electricity production with Fe-incorporated SMFCs and their interaction with different chemical properties of sediment were summarized. Lastly, additional studies required for further evaluations and novel perspectives for future research were proposed.

CHAPTER 2
LITERATURE REVIEW

2.1 Eutrophication Due to Phosphorus Release from Sediment

Eutrophication is described as "*an increase in the rate of supply of organic matter to an ecosystem.*" It is a severe environmental issue that causes ecosystem imbalance in lakes, rivers, and reservoirs. Phosphorus (P) is generally referred to as a "limiting nutrient" in aquatic environments (Maberly et al. 2020; Conley et al. 2009; Schindler et al. 1977). High P inputs alone caused continued eutrophication by supporting nitrogen-fixing cyanobacterial blooms at low nitrogen concentrations (Schindler et al., 2008). Hence, it is crucial to regulate P in the surface water for the success of lake water management.

Eutrophication is mostly caused by P release from sediment in shallow lakes because of the large surface area to water column ratio of the sediment (Munch et al., 2024; Sondergaard et al., 2003). During the summer, induced algal blooms in shallow lakes can make the sediment surface anaerobic, which causes P release from sediment (Dael et al., 2020).

$$3FePO_4 \rightarrow Fe_3(PO_4)_2 + \mathbf{PO_4^{3-}} \uparrow \text{ (by iron-reducing bacteria)} \quad \text{Eq 1}$$

As the sulfide concentration increases, Fe-hydroxide dissolution is accelerated by anoxic conditions in the sediment. Thereby, Fe^{3+} reduction prompts the release of PO_4^{3-} from sediment and curtails the P binding capacity by forming Fe-sulfides (Smolders and Roelofs, 1993; Roden and Edmonds, 1990).

$$SO_4^{2-} + 8e^- + 8H^+ \rightarrow S^{2-} + 4H_2O \text{ (Sulfate reducing bacteria)} \quad \text{Eq 2}$$

$$Fe_3(PO_4)_2 + 3S^{2-} \rightarrow 3FeS + \mathbf{2PO_4^{3-}} \uparrow \quad \text{Eq 3}$$

It was reported that reducing P concentration in the waterways can remediate eutrophication (Schindler et al., 2016).

2.2 Remediation Strategies

Various methods have been used to mitigate internal P release such as biological

processes, dredging, in-situ capping, artificial aeration, and chemical adsorption. Dredging and the addition of chemical adsorbents are commonly used methods to regulate internal P release from sediment (Yin et al., 2021). However, most of them are not applicable due to the inconvenience of practical application, environmental toxicity, or high cost (Wang et al., 2021). In general, chemical adsorption is widely used to reduce P in eutrophic lakes n (Ye et al., 2017). Adding chemical compounds has reduced P release from sediment by precipitating P in the overlying water while enhancing P sorption in the lake sediment. Iron, aluminum, calcium, or lanthanum-enriched bentonite clay including chemical compounds are usually used to control P removal from sediment. Among others, Fe has been recognized as an inexpensive, readily available, and environmentally harmless P adsorbent (Liu et al., 2011; L. Wang et al., 2021).

2.2.1 Iron-based materials

For many years, Fe has been added to lakes in a variety of forms, including Fe(III)-hydroxides, $FeCl_3$, $FeCl_2$, $FeSO_4$, and $FeClSO_4$ (Bakker et al., 2016; Smolders et al., 2006). In addition, materials based on Fe have been found to be effective at limiting P release from sediments such as Fe-salts, Fe-oxides, and zero-valent Fe. Iron can capture P by co-precipitation and adsorption (Munch et al., 2024).

2.2.1.1 Iron oxides

Iron oxides are rich in pore structure, have a large specific surface area, and are abundant in hydroxyl functional groups and magnetic properties. The three primary mechanisms of P sorption onto Fe-oxides are electrostatic adhesion, precipitation, and ligand exchange (Mao et al., 2012). Gong et al. (2019) showed that adding Fe-oxides inhibits P release from Lake Erhai Lake, China, attributed to the changes that occurred in pH, Eh, and dissolved organic matter in the sediment. Furthermore, according to Xi et al. (2017), Fe_2O_3 coating reduced the total P content of the sediment in Erhai Lake by converting active P to inert P. In addition, previous studies reported that the use of Fe-oxides modified materials effectively reduced internal P release from sediment (Wu et al. 2020; Lin et al., 2020; Liu et al., 2017). Amorphous Fe-oxyhydroxides have exhibited a higher PO_4^{3-} adsorption capacity than crystallized Fe-oxyhydroxides due to the availability of more adsorption-reactive sites (Zhang et al., 2021).

2.2.1.2 Addition of Iron ions (Fe^{3+}/ Fe^{2+})

Iron ions reduce P by precipitating with PO_4^{2-} directly. Iron ions primarily remove P by chemical precipitation and adsorption onto corresponding Fe-hydroxides (Wang et al., 2021). Phosphorus release from sediment was effectively inhibited by the addition of $FeCl_3$, mainly due to the precipitation of Fe-oxyhydroxide and the subsequent P adsorption by ligand exchange (Li et al., 2020). According to Perkins and underwood 2001 $Fe_2(SO_4)_3$ addition has significantly reduced dissolved P content in sediment. The maximum P adsorption capacity was achieved when the molar ratio of Fe^{3+} to PO_4^{3-} was 4:1 (Wang et al. 2021). Although oxidation of Fe salt addition enhanced P immobilization, those fixed P can be released under different environmental conditions such as pH changes and anaerobic conditions (Wang et al., 2021).

2.2.1.3 Zero valent iron

Zero valent iron (ZVI) also has been identified as a potential element to reduce P release from sediment. The primary mechanism via which ZVI immobilized P was the formation of Fe-P precipitates (Zhao et al., 2016). However, high pH and low dissolved oxygen conditions would inhibit the corrosion reaction of ZVI and consequently inhibit P adsorption (Li et al., 2019).

2.2.1.4 Limitations of Phosphorus suppression by adding iron

Adding Fe was generally considered successful in P suppression if the redox cycle of Fe was not affected by sulfate reduction and organic matter degradation (Bakker et al., 2016). Sulfate reduction results in sulfide (H_2S), which precipitates Fe-sulfides and removes Fe^{2+}, sequestering Fe in the sediment. However, Fe-addition can improve P retention if the ferrous PO_4^{2-} mineral vivianite ($Fe_3(PO_4)2{\cdot}8H_2O$) is formed or organic-metallic compounds are produced by combining with organic matter, which is particularly stable in anoxic conditions (Munch et al., 2024).

2.2.2 Biochar as a P adsorbent

Biochar is a high-carbon substance that is produced by thermochemically converting biomass under low or no oxygen conditions (Gokalp and Sancar et al., 2022). Wastes from forestry processes, sewage treatment plants, and agriculture can be used to

produce biochar. (Panwar et al., 2019). Biochar is considered a low-cost, beneficial, and sustainable material that can be used for soil conditioning, pollutant treatment, and agricultural purposes.

Biochar has a great potential for P recovery from high P-concentrated wastewater (Wang and Wang, 2019) because of its porous structure, large number of surface groups, high concentration of mineral components, and abundant active sites (Mohan et al., 2014; Wang et al., 2020). Recently, a number of studies have been conducted on using biochar as a P adsorbent. The mechanisms of P adsorption by biochar include physical adsorption, surface precipitation, complexation, electrostatic attraction, and ion exchange (Dai et al., 2020). The adsorption capability of biochar is primarily associated with its physicochemical characteristics.

2.2.2.1 Functional biochar

Recently, various biochar modification methods have been suggested to improve the adsorption characteristics (Wang et al., 2017). Loading metals such as Mg, Ca, Fe, La, and Bi has been recognized as a successful method to obtain better adsorption properties (Luo et al., 2022). Functional biochar is more effective than pristine biochar for environmental management, soil remediation, and energy storage (Jiao et al., 2021). The primary methods of functional biochar preparation are pre-treatment, the thermochemical process, and post-treatment.

- Pre-treatment

Pre-treatment is the process of modifying raw feedstocks to improve the preferred characteristics of biochar. Commonly used pre-treatment methods are washing, drying, crushing, and enhancement of the intended elements. The main purpose of washing and drying biomass feedstocks is to eliminate impurities and moisture. A crushing process is followed to acquire the appropriate particle size. The biomass was dipped solutions to increase the availability of specific elements in biochar.

- Thermochemical process

Gasification, combustion, pyrolysis, hydrothermal carbonization, and other processes can be used to produce biochar (Tripathi et al., 2016). A deeper understanding of each of these

processes was given by Luo et al. 2023. Pyrolysis seems to be widely used in biochar production. Pyrolysis is a process that yields primarily charcoal by heating biomass in the absence of oxygen (Lamichhane et al., 2023). Physicochemical properties of biochar such as pore structure, surface area, functional groups, and zeta potential vary on the biomass feedstocks, heating rate, residence time, and pyrolysis temperature (Sun et al., 2014).

- Post-treatment

Post-treatment defines a range of physicochemical processes used to improve the adsorbent properties of biochar. The most common physical modifications are ball milling and steam activation (Wang et al., 2017). These processes increase the surface area and result in more microporous and mesopores in modified biochar, which enhances its adsorption ability for heavy metals, nutrients, and organic pollutants (Lyu et al., 2018).

2.2.2.2 Iron modified biochar

Iron is frequently utilized to modify biochar because of its natural abundance and low toxicity (Qian et al., 2021; Han et al., 2021). When the pH of water is neutral, P mostly exists as $H_2PO_4^-$. Biochar treated with Fe primarily fixed P by ligand exchange between OH^- and $H_2PO_4^-$ formed surface complexes with Fe (Yuan et al., 2020). The amorphous hydroxide, amorphous hematite, and metal hydroxyl groups served as active PO_4^{3-} adsorption sites in biochar (Ren et al., 2015). The increased zeta potential of the Fe-modified biochar promoted electrostatic attraction. Phosphate adsorption was aided by ligand exchange, which occurred when the OH^- group was replaced with $H_2PO_4^-$ (Luo et al., 2023).

2.2.3 Sediment microbial fuel cells

Sediment microbial fuel cells (SMFCs) are a type of microbial fuel cell that produces electricity using electrons resulting from anaerobic microbial respiration in sediment. The anode is buried in the sediment, where organic matter in the soil is decomposed and produces CO_2, H^+, and electrons (Kaur et al., 2014). Electrons move from the anode to the cathode via an external circuit, while the positive charge of a cation, which is generally H^+, moves via the electrolyte to the cathode (Haxthausen et al., 2021). Dissolved oxygen at the cathode reacts with electrons and H^+ to create water molecules.

Thereby, SMFCs reduce the oxygen demand and limit reductive reactions in the sediment.

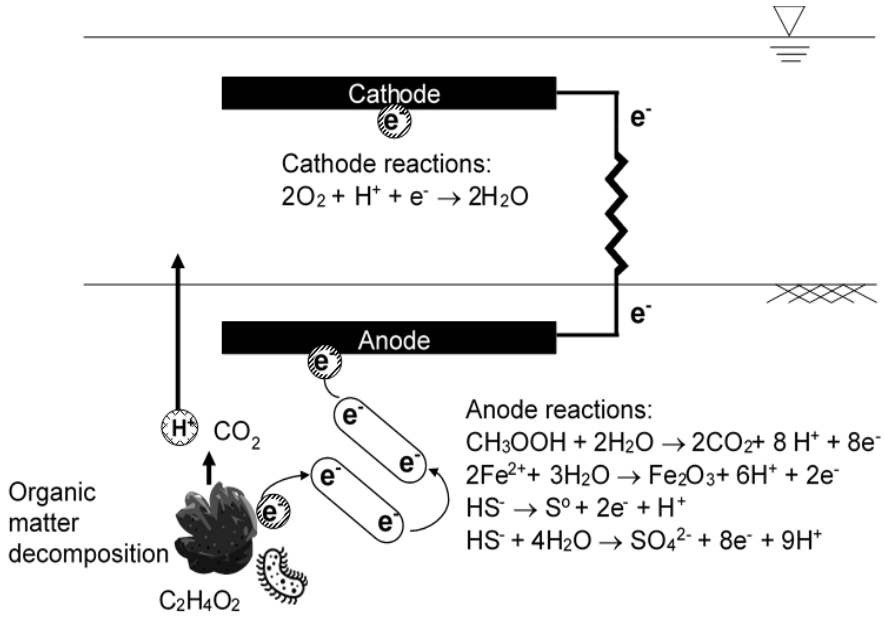

Figure 2.1: Electricity generation from SMFCs

Studies on SMFCs have identified various reactions that contribute to the production of electrical current. These include (i) the chemical oxidation of reductants produced by microorganisms, such as humic acids, Fe^{2+}, and particularly sulfur compounds at the anode, (ii) the microbial oxidation of organic substances like acetate, and (iii) the microbial oxidation of S^0 to SO_4^{2-} (Schamphelaire et al., 2008). These processes release electrons that are captured by the anode, resulting in the generation of current within an electrical circuit. The operating factors of SMFCs include the type and abundance of microbial species present in the sediment, the availability of organic matter for microbial metabolism, the design and configuration of the fuel cell system, and environmental conditions such as temperature, pH, and salinity (Hamdan and Salam, 2023; Schamphelaire et al., 2008). These factors can influence the efficiency and performance of SMFCs in generating electricity. Researchers are continuously studying and optimizing these operating factors to enhance the effectiveness of SMFC technology for sustainable energy production.

2.2.3.1 Types of SMFC designs

Many implementation designs have been put in place to increase the efficiency of

microbial fuel cells. Among those, single-chamber and dual-chamber microbial fuel cells are commonly used for research purposes.

- Single chamber SMFC

A single-chamber SMFC is a type of microbial fuel cell that consists of a single chamber where both the anode and cathode are located. In this design, the sediment serves as the electrolyte, allowing for direct interaction between the microbial community and the electrodes. Single-chamber SMFCs are relatively simple in design and operation, making them easy to deploy and maintain. However, they may face challenges related to oxygen crossover and limited control over the electrochemical reactions.

- Dual chamber SMFC

A dual chamber SMFC consists of two separate chambers: an anode chamber and a cathode chamber, separated by a proton exchange membrane. In this design, the sediment serves as the electrolyte in the anode chamber, while an external electrolyte solution is used in the cathode chamber. Dual chamber SMFCs offer better control over the electrochemical reactions, reducing issues such as oxygen crossover and pH imbalance. This design allows for improved efficiency and performance compared to single-chamber SMFCs, but it may be more complex to operate and maintain.

2.2.3.2 Effect of sediment type on SMFC performance

The characteristics of sediment play a crucial role in influencing the catalytic abilities of the sediment microbial community and the overall power output of the system. Factors such as particle size distribution can influence the performance of bioremediation by affecting the availability of substrates and nutrients in the sediment pore water. Additionally, sediment properties determine the composition of the microbial community in the sediment, which in turn impacts the establishment of an electrochemically active biofilm (Hamdan and Salam, 2023).

The conductivity of the sediment is another important factor that affects the function of SMFCs. Marine sediments, with their higher conductivity due to salinity, tend to have better electron and proton transfer processes, leading to improved bioremediation performance (Song et al. 2012; Guo et al. 2021). However, marine sediments may lack

the necessary Fe-reducing microbial community for the formation of an electrochemically active biofilm (Wang and Tam 2019; Hamdan and Salam 2020). This is attributed to the low Fe concentration in marine environments and the prevalence of sulfate-reducing microbial populations.

Furthermore, the presence and concentration of organic matter, nutrients, and secondary pollutants in sediment can also significantly impact the performance of microbial fuel cells by influencing the sediment microbial ecosystem (Mathuriya et al. 2018).

2.2.3.3 Phosphorus immobilization in sediment using SMFCs

In the context of P fixation, Fe-oxidation plays a significant role. Within the sediment, Fe minerals, such as Fe-sulfides (e.g., pyrite) or Fe-oxides (e.g., ferrihydrite), can serve as electron acceptors for microbial respiration. According to Martins et al. (2014), electrons from Fe^{3+} hydroxide were transported to the anode in sediment and then to the cathode in the oxygenated water, by which P was stabilized in sediment. When microorganisms oxidize Fe^{2+} to Fe^{3+}, they release electrons that can be harvested by the SMFCs to generate electricity. The process of Fe^{2+} oxidation in SMFCs creates a favorable environment for P fixation. Moreover, the operation of the SMFC increased the sedimentary redox potential, preventing Fe^{3+} reduction and ultimately resolving the Fe-bound P release from the sediment under reductive conditions (Qi et al., 2022). Thus, redox-sensitive P release from anaerobic sediment can be controlled with the use of SMFCs.

In SMFCs, the P fixation of the sediment can also be increased by inhibiting Fe-scavengers such as sulfide. An SMFC-increased redox potential may prevent sulfide formation in sediment under anaerobic conditions (Kubota et al., 2019). Microorganisms capable of oxidizing sulfur can transfer electrons from the SMFC anode (Bond et al., 2003). Algar et al., (2020) showed a reduction of sulfide in sediment pore water due to the SMFC operation. Thereby, Fe-sulfide (FeS) formation can be controlled by SMFCs and available Fe^{2+} will increase P fixation in sediment.

2.2.3.4 Iron addition into SMFCs

One of the primary obstacles to be overcome in the practical application of SMFCs

is low electricity generation due to higher internal resistance (Emalya et al., 2021). To improve the performance of SMFCs, adding conductive materials is a simple but efficient approach that can be easily applied in the field (Zabihallahpoor et al., 2015). The addition of Fe to SMFCs has been shown to improve electron transfer efficiency, leading to increased power output. Most Fe-oxides are conductive or semi-conductive and may act as electron carriers between bacterial cells and long-distance electron acceptors, such as the electrodes in electrochemical cells (Kato et al., 2013).

The presence of Fe has been shown to not only enhance the degradation of organic pollutants but also promote the growth of electrochemically active bacteria, ultimately leading to increased electricity production (Nosek et al., 2023). In addition, Zhou et al. (2014) showed that adding colloidal Fe-oxyhydroxide increased the electricity produced from sediment with low organic matter. In addition to its role as a conductive material, the introduction of zero-valent Fe into sediment has been suggested for utilization in SMFCs to increase the potential difference and serve as a voltage booster (Kim et al., 2023; Okavitri et al., 2021; Cai et al., 2018).

2.3 Lack of Knowledge to be Explored

The effectiveness of Fe addition for lake restoration has long been questioned. According to previous studies, adding Fe would potentially be able to reduce the amount of total P in the water column (Immerse et al., 2015; Smolders et al. 2001; Groenenberg). However, certain field variables, such as redox potential, the presence of Fe scavengers such as sulfide, and the availability of Fe with P, may have a significant impact on the efficiency of P fixation (Bakker et al., 2016; Kleeberg et al., 2013). The effectiveness and durability of Fe treatment may differ according to environmental characteristics, including sediment geochemistry. For better water quality management, understanding the long-term effect of P suppression due to Fe addition and how it impacts sediment biogeochemical processes is vital. Thus, it is necessary to evaluate the success of Fe addition in P suppression according to the sediment characteristics before directly applying it to the field.

Although Fe-treated functional biochar has demonstrated greater success in removing P from water (Qian et al., 2023), the detrimental consequences of biochar on sediments are still unknown (Gao et al., 2021). Biochar itself has the potential for P

desorption under certain conditions, such as pH increments. However, the success of Fe-treated biochar in an anaerobic environment to control P is questionable. Therefore, the risk of P release from Fe-treated biochar-loaded lake water under depleting O_2 concentration cannot be ignored. Therefore, to avoid endangering the ecological balance of lakes, it is necessary to examine the dynamic changes in sediments and water bodies before using biochar for lake restoration.

According to Wang et al. (2021), the efficiency of P immobilization in sediment by adding Fe ions can be increased if the sediment redox potential could be changed from a reductive to an oxidative condition. As discussed in Section 2.2.3, SMFC operation enhances sedimentary redox potential and thereby suppresses P release from sediment. Efficient electron transport from the sediment is required to counteract reductive conditions in anaerobic sediment. In SMFC systems, adding conductive material is essential for bioremediation as well as power generation. However, previous SMFC studies mainly focused on power enhancement from conductive material incorporation. Thus, the effect of P immobilization from Fe-added SMFCs is still unclear. Different Fe-compounds in SMFCs have shown varying effects on the generation of electricity. Zhou et al. (2014) showed colloidal Fe addition increased electricity generation, but crystalline and amorphous Fe-oxyhydroxides were not effective. On the other hand, the addition of zero-valent Fe or steel slag significantly increased electricity generation. Although it was evidenced that microbial Fe^{2+} oxidation can be facilitated by SMFCs, the potential of Fe^{2+} to act as an electron donor is uncertain.

Additionally, the performance of SMFCs may vary according to their sediment properties (Hamdan and Salam, 2023). It was mentioned that high electricity generation from SMFCs would enhance organic P mineralization due to induced organic matter decomposition (Haxthausen et al., 2021). Therefore, it is necessary to understand the interactions between electricity generation and suppression of P release according to the sediment properties. Adding Fe has increased organic matter decomposition in SMFCs (Kim et al., 2021). But its impact on the P release is yet to be discovered. Thus, it is important to evaluate the success of Fe addition in SMFCs for P suppression according to the sediment characteristics before directly applying it to the field.

CHAPTER 3
REDUCING PHOSPHORUS RELEASE FROM SEDIMENT BY ADDING IRON-HYDROXIDE OR IRON TREATED BIOCHAR

3.1 Introduction

Excessive nutrient loading in surface water causes eutrophication, endangering the aquatic environment in both freshwater and marine ecosystems (Liu et al., 2019; Wilkinson, 2017; Chislock et al., 2013). Eutrophication mitigation measures for lake systems can be controlled by reducing a single nutrient input, which is phosphorus (P) (Schindler et al., 2016). Transportation of P from agricultural fields to irrigational drainages is one of the primary contributors to watershed eutrophication (Wildemeersch et al., 2022; Haque, 2021; King et al., 2015). Phosphorus has accumulated in agricultural drainage sediment for decades due to high manure and fertilizer application, and remobilization of this legacy P can further deteriorate water quality, masking the efforts of water conservation initiatives (Stackpoole 2019; Sharpley et al. 2013). According to Seidel et al., (2021) and Sondergaard, (2003), seasonal changes such as oxygen depletion by induced microbial activity in summer, would promote eutrophication. Under prolonged anoxic conditions, P was suspected to be released due to the microbially mediated reductive iron (Fe) oxyhydroxides dissolution (Ding et al., 2016). Therefore, to maximize the utility of sustainable water treatment efforts, it is vital to investigate P removal efficiency in water resource management protocols.

In terms of controlling internal P release from sediment, various adsorptive were suggested in previous studies (Liu et al., 2017; Xie et al., 2014; Reitzel et al., 2013). However, many of those have drawbacks, such as lack of resource availability, high cost, and the development of toxicity. Recently, Fe addition was recognized as a reliable method to suppress internal P flux when the external P loading, organic matter availability, and sulfate (SO_4^{2-}-S) concentration were low (Bakker et al., 2016). In addition, several studies have also discovered the potential of Fe-based materials for lake restoration through P removal (Xia et al., 2022; Wang et al., 2021; Groenenberg et al., 2013; Smolders et al., 2001). Moreover, Fe-hydroxide has been shown to effectively immobilize phosphate (PO_4^{3-}-P) through adsorption and precipitation mechanisms, reducing its

availability for release into the water column. However, the effectiveness of P fixing in sediment by adding Fe-incorporated materials differed according to the sediment characteristics and environmental conditions such as redox potential and pH.

Additionally, biochar has been recognized as a material that can remove and recover P from wastewater by adsorption (Qin et al., 2022; Liu et al., 2022). Currently, Fe addition has gained attention as a cost-effective and ecologically friendly organic and inorganic pollutant adsorbent (Nobaharan et al., 2021). Biochar is a carbon-rich charcoal-like substance formed through pyrolysis, which involves the process of heating biomass in a limited oxygen atmosphere (Das and Ghosh, 2020). However, PO_4^{2-}-P adsorption in biochar can be influenced by several factors, including the surface area, pore structure, pH, and functional groups present in the material. Biochar without treatment may not be as effective at P removal due to its limited surface area and lack of specific functional groups that can facilitate PO_4^{3-}-P binding.

Almanassra et al., (2021) and Bolster, (2021) identified Fe included biochar composites improved the P adsorption capacity. The Fe in the treated biochar acts as a catalyst for PO_4^{2-}-P adsorption and precipitation reactions, enhancing the material's ability to immobilize PO_4^{2-}-P in sediment. This synergistic effect between Fe and biochar increases the surface area available for PO_4^{3-}-P binding and promotes stronger chemical interactions between PO_4^{3-}-P and the material. One of the most convenient and straightforward methods to introduce Fe onto biochar is pretreating feedstock biomass with a Fe solution (Gao and Wan, 2023). There is a notable lack of studies investigating the potential of fixing P in sediment by adding Fe-treated biochar, highlighting a promising area for future research in environmental remediation.

While implementing remedial measures to prevent eutrophication in aquatic systems, internal P loading should be considered in addition to external P loading. However, so far, the capability of Fe-treated biochar to combat internal P release from sediment has not been discovered. The present study was aimed at investigating how P release from agricultural drainage sediment changed under different dissolved oxygen (DO) concentrations, after Fe hydroxide, biochar, or Fe-treated biochar was amended.

3.2 Materials and Methods

3.2.1 Sediment sampling

Kojima Lake is a hypereutrophic lake located in Okayama, Japan. The Kojima Lake surface sediment contained more Fe-bound, redox-sensitive P than the deep sediment, suggesting that large P fluxes may occur under anaerobic environments (Jin et al., 2020). Sediment samples were collected at an agricultural drainage in Miyakko Rokku, Okayama, Western Japan (34° 34' 9" N, 133° 54' 11" E) which falls into Kojima Lake. The samples were immediately transported to the laboratory, where the debris and stones were removed by passing through a 2 mm sieve. Then those were homogenized and stored at 4°C until experimental use. The total Carbon (TC), total nitrogen (TN), and total P contents in sediment were 25.2, 2.8, and 4.7 g kg^{-1} respectively.

3.2.2 Preparing iron oxides and biochar

Amorphous ferric oxyhydroxide (FeOOH) was prepared by adjusting 0.4 *M* $FeCl_3$ solution to pH 7 using 1 *M* NaOH (Zhou et al., 2014). After allowing the precipitate to settle, the supernatant was removed, and the residue was washed three times with deionized water.

Cedar saw wood was used as the feedstock for biochar production. Biochar (BC) was made by pyrolyzing the cedar saw dust at 850°C at a rate of 10°C min^{-1}. To produce Fe-treated biochar (Fe-BC), cedar saw dust was pre-impregnated in a 1:3 $Fe(NO_3)_3$ aqueous solution and after drying at 50°C, pyrolyzed at an 800°C maximum temperature at 20°C min^{-1} temperature acceleration.

3.2.3 Experimental design

For the sediment incubation test, a 14.6 cm high acrylic column with a 45 mm internal diameter was used with a silicon stopper. Then 5 g of Toyoura sand was used to fill up the gaps around the edges, followed by 65 g of sediment. A platinum electrode made of 2 cm platinum wire coupled to 10 cm copper wire, was embedded at 1 cm below the sediment surface. Then 150 mL of deionized water was filled as the overlying water. For the incubation under high DO conditions, the top of the acrylic column was kept open from day 0 to 36 to facilitate oxygen diffusion from the atmosphere. Then from day 37 to 72, a low DO condition was formed by closing the columns by placing a silicon stopper.

All the treatments were incubated at 25°C in a dark room.

3.2.4 Analytical methods

The overlying water samples were collected on day 0, 3, 7, 14, 21, 28, 36, 39, 43, 50, 57, 64 and 72 and replenished with deionized water. pH in the overlying water was measured using a pH meter (F-23, Horiba, Japan). Sedimentary Eh was measured on each sampling day by connecting a platinum electrode with a KCl-saturated Ag/AgCl reference electrode (PRN-41, Fujiwara, Japan). The concentrations of PO_4^{3-}-P and SO_4^{2-}-S were measured by using a continuous flow analyzer (2-HR, AutoAnalyzer QuAAtro, Bltec, Japan) while determining Fe concentrations using an atomic absorption spectrometer (ICE 3300 AA, Thermo Scientific, America). Contents of TN TC of dry sediment were measured using a CN coder (MT700, Yanaco, Kyoto).

According to Lukkari et al. (2007) and Rydin (2000), five fractionations of P in sediment were recovered after the SMFC operation. To extract loosely bound P (Loose-P), 0.4 g of sediment was shaken for 1 h at 175 rpm with 0.46 *M* NaCl (pH 7) and then for another hour with 0.11 *M* $NaHCO_3/Na_2S_2O_4$ to extract Fe-bound P (Fe-P). The residue was then agitated for 16 hours with 0.1 *M* NaOH to extract aluminium-bound P (Al-P) from the supernatant. The TP of the solution was measured after digesting with $K_2S_2O_8$, and organic P was derived by subtracting Al-P from TP. Calcium-bound P (Ca-P) was produced by stirring the residue for 16 hours in 0.5 *M* HCl. All the collected suspensions were centrifuged for 15 minutes at 4000 rpm before being filtered. The difference between the TP and P-fractions denotes the residual - P**.**

The N_2 adsorption isotherms at 77 K with the Langmuir equation were used to determine the specific surface area of biochar (Belsorp II, Bel, Japan). Biochar characteristics were determined by scanning electron microscope (SEM) (S-5200, Hitachi, Japan) and X-ray photoelectron spectroscopy (XPS) analysis. Biochar (2 g) was mixed with 0.4 mL of 1-methyl-2pyrrolidinone (NMP) and PVDF resin in a 10% NMP solution. The mixture was distributed uniformly on a glass plate and dried for 24 h in a desiccator. The conductivity was then determined using a 4-point probe (PSP probe, Loresta-GPMCP-T610, Mitsubishi Chemical, Japan).

Turkeys HSD test was performed using R software (R i386 3.6.0) to analyze statistical significance among treatments $p = 0.05$.

3.3 Results

3.3.1 Properties of sediment and biochar

Table 3.1 shows the P fractions in the sediment. The sediment contained the most P in the form of Al-P, followed by Fe and Ca-P. Aluminium-bound P content was the highest while the Fe-bound and calcium-bounds were the next. Contents of organic P and loosely bound P were the lowest P fractions in Kojima Lake sediment.

Table 3.1 Phosphorous fractions in sediment

P fractions	P content (g kg^{-1})
Loosely bound P	0.11
Fe-bound P	0.43
Aluminium-bound P	3.21
Calcium-bound P	0.43
Organic P	0.15

The properties of BC and Fe-BC are given in Table 3.2. pH was high and similar between both types of biochar. Moreover, electrical conductivity was lower in BC than in Fe-BC. In addition, the specific surface area was slightly higher in BC than that of Fe-BC.

Table 3.2 Characteristics of biochar

Parameter	BC	Fe-BC
pH	9.74	10.39
Electrical conductivity (mS cm^{-1})	74.27	255.84
Specific surface area (m^2 g^{-1})	535.61	475.03

Figure 3.1 depicts the Raman spectra of two types of biochar. In Fe-BC, band D and G were higher than that of BC. Band 2D was formed only in Fe-BC.

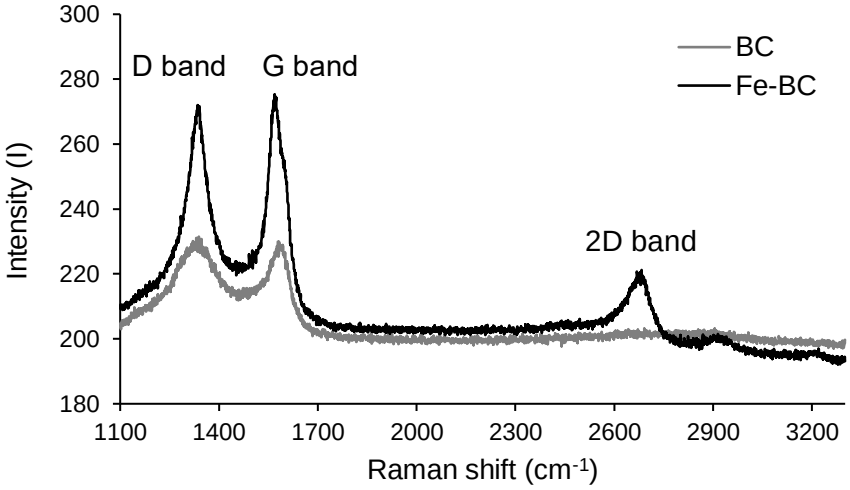

Figure 3.1 The Raman Spectra for BC and Fe-BC. D, G, and 2D bands represent structural disorder, graphitic, and layered structure of graphite.

The SEM images of the two types of biochar are shown in Figure 3.2. Iron precipitation on the Fe-BC used in this study, was not as high as it was in Qian et al., 2021 (Fig 3.2 a, c). The pore sizes of BC were larger than Fe-BC (Fig 3.2 b, d).

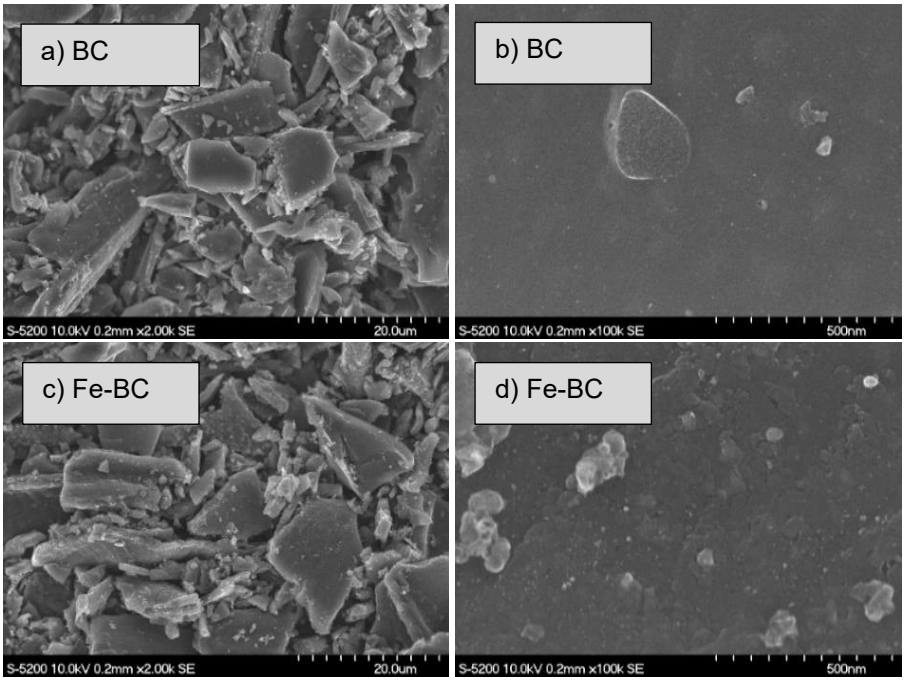

Figure 3.2 Scanning electron microscope (SEM) images of BC a) 2.0K, b) 100K magnifications and Fe-BC c) 2.0K, d) 100K magnifications.

The XPS spectra showed valance states of BC and Fe-BC (Fig 3.3). Although XPS peaks of Fe were discovered in both BC and Fe-BC those peaks were lower in BC than in Fe-BC.

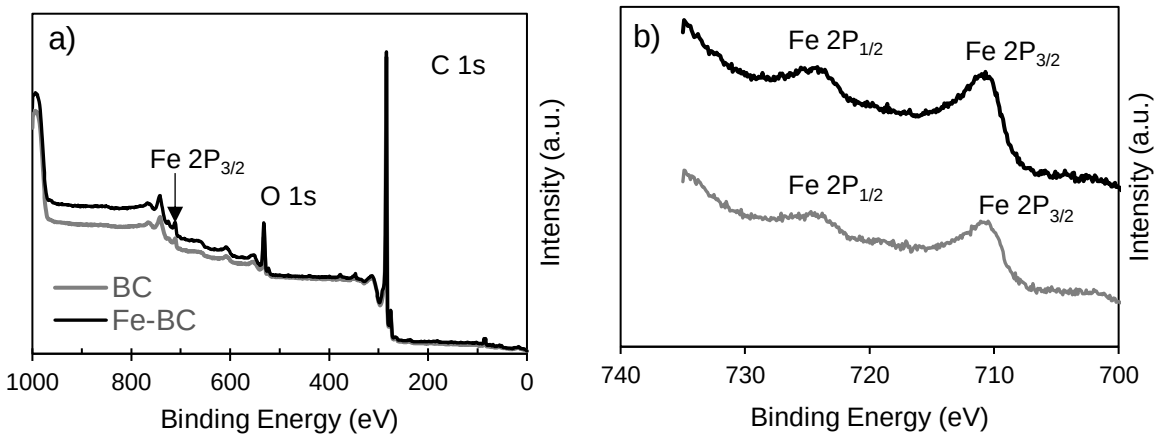

Figure 3.3 a) XPS spectra of cedar (BC) and pre-treated biochar (Fe-BC and b) XPS Fe 2P spectra

3.3.2 Amount of PO_4^{3-}-P released into the overlying water

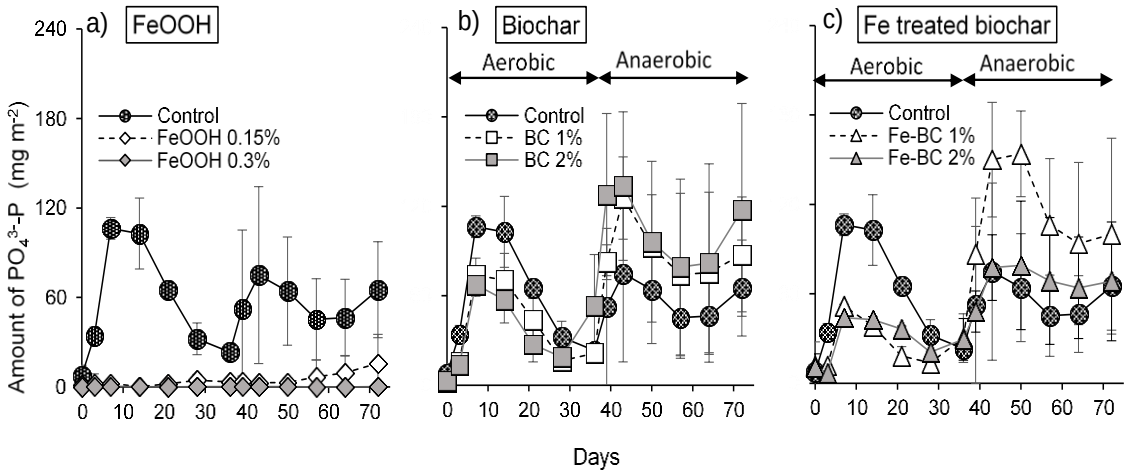

Figure 3.4 PO_4^{3-}-P released from sediment to the overlying water in a) FeOOH, b) BC, and c) Fe-BC added treatments (n=3)

Throughout the whole experiment the PO_4^{3-}-P amounts were very low in FeOOH added treatments (Fig 3.4a). Differently, in control, BC, and Fe-BC treatments the PO_4^{3-}-P amount increased till day 7 and then gradually decreased until day 36 (Fig 3.4 b, c).

After changing to low DO conditions (day 37), PO_4^{3-}-P amounts in those once increased until day 43 and then decreased. In FeOOH 0.15% treatment, PO_4^{3-}-P amount started to increase again after day 56.

During the high DO condition (day 0-36), the highest amount of PO_4^{3-}-P in the overlying water resulted on day 7. All the treatments reduced PO_4^{3-}-P amounts released from sediment to the overlying water more than the control treatment ($p < 0.05$). The reduction of PO_4^{3-}-P among treatments was 1% FeOOH < 1% Fe-BC < 1% BC ($p < 0.05$). There was no difference in PO_4^{3-}-P release among different amending ratios under high DO conditions.

At the end of the low DO incubation (day 72), amounts of PO_4^{3-}-P in the overlying water were higher than that was under high DO conditions (day 36; Fig 3.4). Our results agreed with Van et al. (2016) and James (2017), who documented anaerobic conditions cause higher P release from sediment than aerobic sediment. When the incubation condition was changed to low DO conditions, PO_4^{3-}-P amounts in FeOOH 0.15% increased after day 49 (Fig 3.4 a). However, FeOOH 0.3% treatment showed the lowest PO_4^{3-}-P amount. Amounts of PO_4^{3-}-P in BC 1%, BC 2%, and FeBC 1% treatments were the highest while control and Fe-BC 2% added treatments showed similar amounts of PO_4^{3-}-P (Fig 3.4 b, c).

3.3.3 Iron diffusion into the overlying water

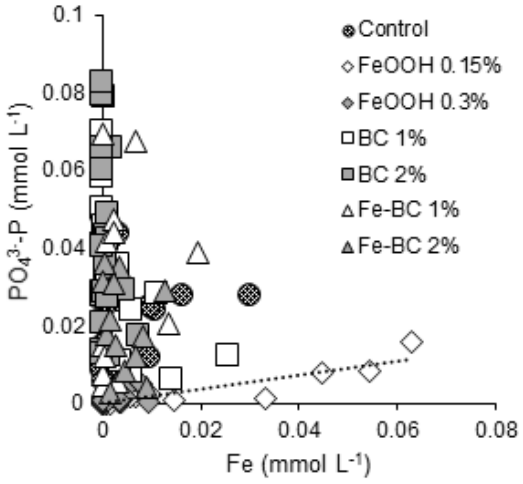

Treatment	Correlation (R^2)
Control	0.002
FeOOH 0.15%	0.821
FeOOH 0.3%	0.294
BC 1%	0.355
BC 2%	0.087
Fe-BC 1%	0.039
Fe-BC 2%	0.050

Figure 3.5 Relationship of Fe release with PO_4^{3-}-P release from sediment to the overlying water under low DO conditions

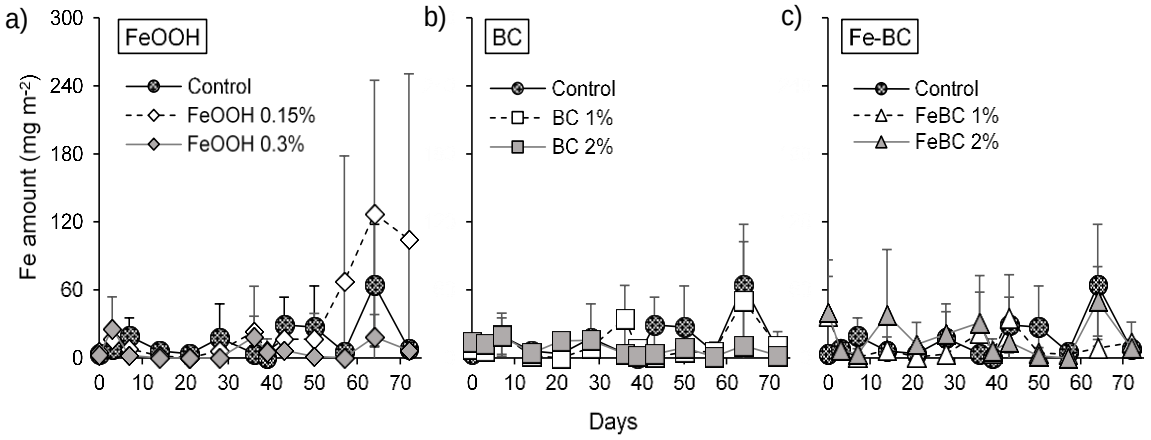

Figure 3.6 Amount of iron released to the overlying water in a) FeOOH, b) BC, and c) Fe-BC added treatments (n=3).

The correlation of Fe and PO_4^{3-}-P amounts in the overlying water under low DO conditions is shown in Figure 3.5. Only the FeOOH 0.15% treatment showed a strong correlation between PO_4^{3-}-P and Fe concentrations, while the other treatments exhibited very weak relationships. Although Fe amount in the overlying water increased in FeOOH 0.15% treatment after day 49. There was no clear variation of Fe amount in the overlying water of other treatments under both the incubation conditions (Fig. 3.6).

3.3.4 Variation of sedimentary Eh

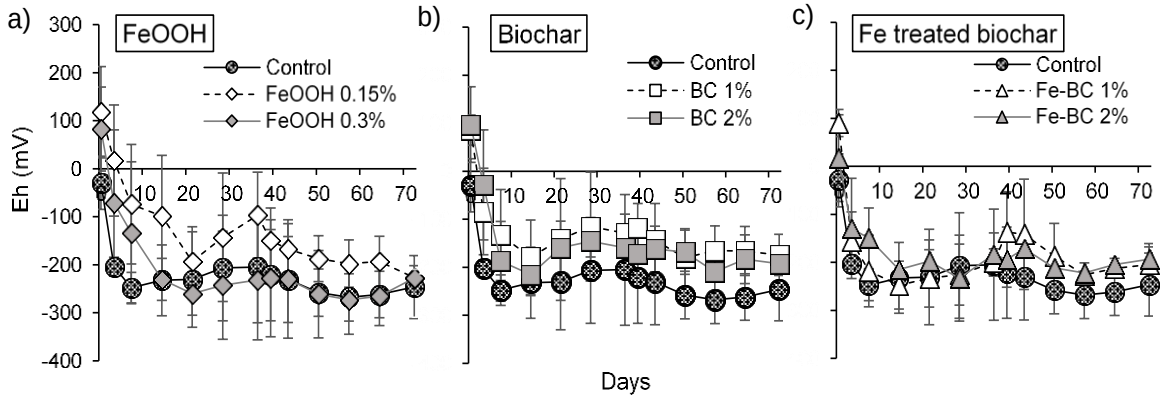

Figure 3.7 sedimentary Eh variation at 1 cm below the sediment surface in a) FeOOH, b) BC, and c) Fe-BC added treatments.

Under high DO conditions (day 0-36), Eh at 1 cm below the surface gradually

decreased in all treatments (Fig 3.7). After changing to low DO condition (day 37-72), Eh slowly reduced further below -200 mV.

3.3.5 Amounts of SO_4^{2-}-S released into the overlying water

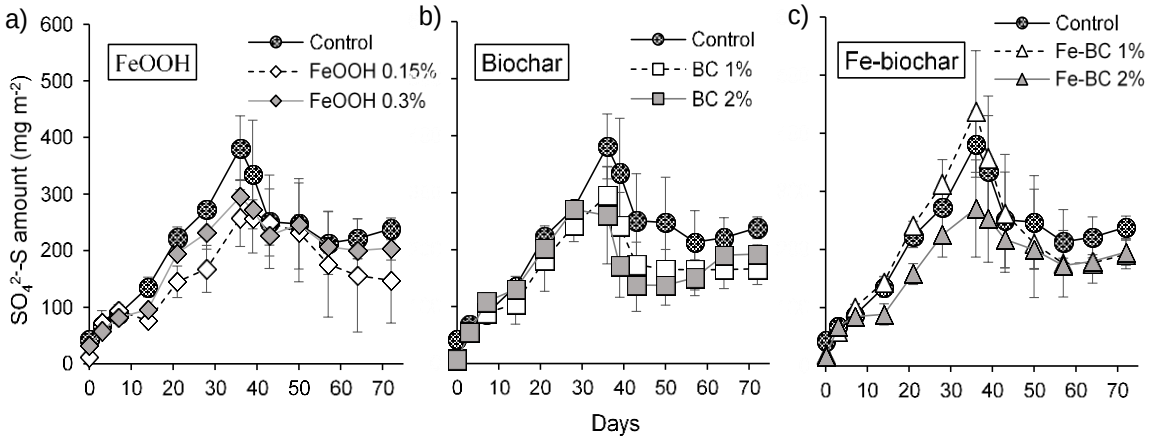

Figure 3.8 Amount of SO_4^{2-}-S released into the overlying water in different treatments from a) FeOOH, b) BC, and c) Fe-BC added treatment.

In all treatments, SO_4^{2-}-S gradually increased under high DO conditions (day 0-36) and decreased when switched to low DO conditions (day 37-72; Fig. 3.8). The highest SO_4^{2-}-S amount was in the control treatment. However, SO_4^{2-}-S amounts in the overlying water were not significantly different among treatments ($p > 0.05$).

3.3.6 Changes of pH in the overlying water

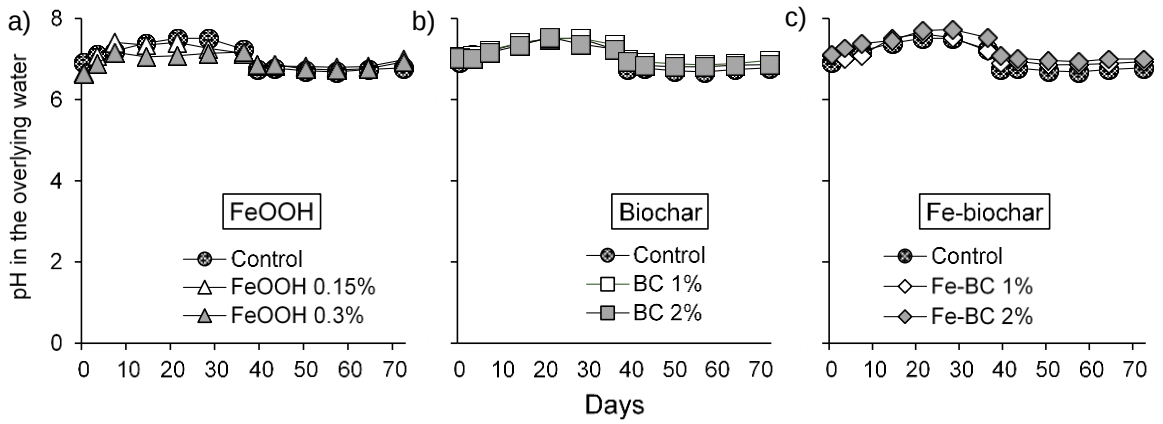

Figure 3.9 Temporal variation of pH in the overlying water of a) FeOOH, b) BC, and c) Fe-BC added treatment.

The pH in the overlying water changed in-between 6.5 to 8.0 in all the treatments during the experimental duration (Fig. 3.9). Under high DO conditions (day 0-36), pH in FeOOH 0.3% treatment mostly had lower pH values. After changing to low DO condition (day 37-72), pH slightly decreased. However, pH was not affected among different treatments.

3.3.7 The concentrations of NH_4^+-N and NO_3^--N

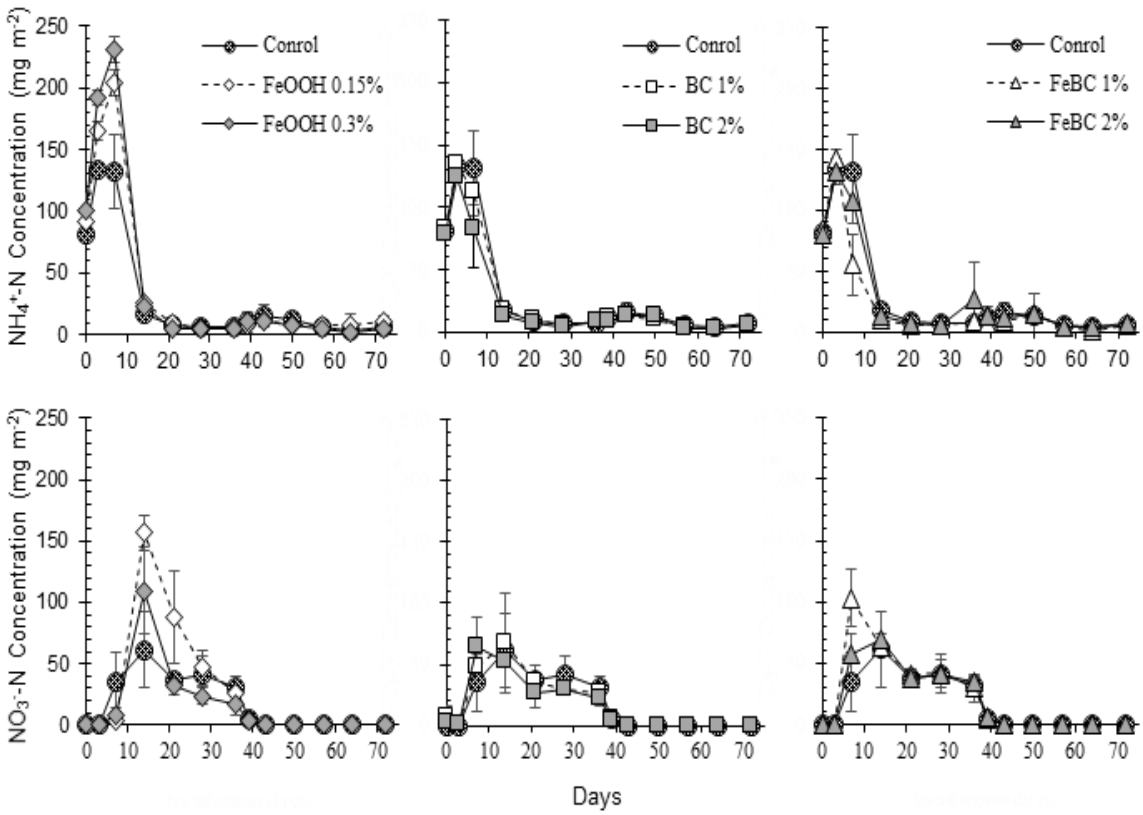

Figure 3.10 Amount of NH_4^+-N or NO_3^--N released into the overlying water in different treatments from a,d) FeOOH, b,e) BC, and c,f) Fe-BC added treatment.

On day 0, NH_4^+-N amounts in the overlying water were similar among treatments. At first, the amount of NH_4^+-N in the overlying water gradually increased in each treatment and then decreased within the first three weeks. After switching to low DO conditions (day 43), a second NH_4^+-N peak was observed, which is significantly lower than the high DO conditions ($p < 0.005$).

At the start of the experiment, NO_3^--N was not found in the overlying water. NO_3^-

-N amount gradually increased and then decreased. After day 39, NO_3^--N amount in the overlying water of each treatment remained negligible until the end of the experiment.

The maximum NH_4^+-N amount in FeOOH treatments was significantly higher than the other treatments ($p < 0.05$). Moreover, the NH_4^+-N peak for FeOOH appeared on day 7, while in the other treatments, it was on day 3. On the other hand, on day 7, NO_3^--N amount in FeOOH added treatment remained low whereas it was increased in the other treatments. However, the different amending rates of FeOOH, BC, or Fe-BC did not affect the NH_4^+-N or NO_3^--N accumulations in the overlying water.

In general BC and Fe-BC amended treatments showed similar temporal variation of NH_4^+-N and NO_3^--N amounts in the overlying water as that of the control treatment.

3.4 Discussion

3.4.1 Properties of Biochar

Biochar showed alkaline pH regardless of pretreatment probably due to high pyrolysis temperatures (Table 3.2). pH increment would result when the pyrolysis temperature increased because the alkali salts separated from organic materials (Al-Wabel et al., 2013). The EC in BC was lower than Fe-BC because of the formation of graphene layers in Fe-BC. In Fe-BC, the intensity ratio (I_{2D}/ I_G) was 0.8 (Fig 3.1). Lin et al. (2017) mentioned that being I_{2D}/ I_G less than one indicated the presence of multilayer graphene. The specific surface area was high in both types of biochar. However, in BC it was slightly greater than Fe-BC. Previous studies suggested that metal-loaded biochar decreases the surface area, possibly due to pore blockage with metal oxide precipitates (Ajmal et al. 2020; Cui et al. 2019).

In SEM figures, Fe precipitation was not clear in Fe-BC (Fig 3.2). However, High Fe peaks indicated the presence of higher Fe-associated surface functional groups in Fe-BC more than in BC.

3.4.2 Iron oxides to suppress PO_4^{3-}-P release from sediment

Our study suggested that the PO_4^{3-}-P release from P-rich agricultural drainage sediment was effectively suppressed by the FeOOH amendment for a longer period, especially under high DO conditions (Fig 3.4). Similarly, Zhang et al. 2021 exhibited high P absorptivity in amorphous FeOOH because of highly available adsorption reactive sites.

However, after day 49, FeOOH 0.15% treatment released PO_4^{3-}-P, showing a strong positive correlation in-between Fe and PO_4^{3-}-P amounts in the overlying water (Fig 3.5). Similarly, Ding et al., (2016) showed a strong positive relationship between Fe and PO_4^{3-}-P release which exhibited the Fe-coupled P release from reductive sediment. In our study, FeOOH treatments reduced the amount of P release in the high DO conditions, because reduced Fe in deep sediment migrated to the oxygenated sediment surface and immediately re-oxidized, trapping P in sediment. Iron reduction was evidenced by the lower Eh values regardless of incubation conditions (Fig 3.7). A slight reddish colour appeared on the sediment surfaces during the high DO conditions confirming re-precipitation of Fe. Moreover, low DO conditions caused microbial Fe reduction, stimulating P and Fe diffusion toward the overlying water.

However, FeOOH 0.3% treatment showed the lowest P release into the overlying water even under low DO conditions, perhaps due to high Fe availability. The sedimentary P release was substantially reduced when Fe: P > 30 and Fe: S > 6 (Wang et al., 2018). Rothe et al., (2015) mentioned that a higher supply of Fe and lower degree of sulphidisation (molar ratio of total sulphur: reactive Fe < 1.1) promoted vivianite ($Fe_3(PO_4)_2 \cdot 8H_2O$) formation. Previous studies suggested that Fe precipitation in the form of vivianite in eutrophic environments can immobilize P under anoxic conditions (Quevedo et al., 2021; Vuillemin et al., 2020; Rothe et al., 2016).

3.4.3 Biochar addition to control PO_4^{3-}-P release from sediment

Although the addition of BC and Fe-BC suppressed P release from sediment to the overlying water more than in the control treatment, Fe-BC showed higher P reduction under high DO conditions (Fig 3.4, c; $p < 0.05$). Qian et al., (2023) also showed high P adsorption by Fe-modified biochar made of peanut shell, soybean straw, and rape straw via electrostatic adsorption or ion exchange. In addition, Bolton et al., (2019) also reported that biochar addition decreased P adsorption by forming iron phosphate. However, on day 43, BC 1%, BC 2%, and Fe-BC % treatments showed the highest PO_4^{3-}-P release from sediment.

The higher SSA and the Fe present on the biochar adsorbed P under high DO conditions (Table 2, Fig 3.4). Higher Fe loaded on to Fe-BC increased P adsorption more

than that of the BC in which the SSA was higher ($p < 0.05$). It has been reported that Fe mineral particles loaded on to the biochar can increase the adsorption of P in water mainly through electrostatic attraction, ligand exchange, and precipitation mechanisms (Gao and Wan, 2023). During the modification, Fe^{3+} formed complexes with surface functional groups, causing a reduction in the negative charge on the biochar surface and an increase in the adsorption of negatively charged PO_4^{2-} ions (Jiao et al., 2021). Although Fe loading onto biochar reduced porosity and surface area due to pore blockage, it would increase PO_4^{2-} adsorption (Almanassara et al., 2021).

Presumably, low DO conditions lead those Fe-bound P formed under high DO conditions to release back into the overlying water due to induced Fe reduction. The addition of BC and Fe-BC would have boosted the growth of extracellular respiratory bacteria such as Fe-reducing bacteria by transferring Fe^{3+} to Fe^{2+} on its surface. Therefore, accelerated Fe- bound P release and Organic-P release due to organic matter decomposition would have encouraged P release from BC and Fe-BC added sediment. According to Xu et al., (2016), the addition of biochar to soil with a high content of organic matter increased the initial hematite reduction under anoxic conditions by reinforcing the dissimilatory metal-reducing bacteria growth. In addition, they mentioned that biochar leachate reduced hematite abiotically by acting as an extracellular electron shuttle. Moreover, Ni et al., (2023) also demonstrated that Fe^{3+} in Fe-modified biochar effectively promoted the extracellular respiration of microorganisms and enhanced the anaerobic digestion of pharmaceutical wastewater.

Although it was not significant, FeBC 2% addition reduced the P release comparative to those treatments. Higher Fe^{3+} availability in FeBC 2% treatment would have increased P fixation in sediment.

3.4.4 Effect of SO_4^{2-}-S on PO_4^{3-}-P release from sediment

In this experiment, SO_4^{2-}-S amount in the overlying water gradually increased in all treatments under high DO conditions (Fig 3.8). This evidenced the continuous oxidative reactions that occurred at the sediment surface. In contrast, an abrupt SO_4^{2-}-S reduction resulted immediately after switching to a low DO condition. Similar to our results Foti et al., (2007) also observed substantial sulfate-reducing rates for most lakes in a saline environment due to the presence of diverse and active sulfate-reducing bacteria.

While the SO_4^{2-}-S amount decreased in the overlying water PO_4^{3-}-P amount increased under low DO conditions. This evidenced that sulfate-reducing bacteria activity was the primary method for releasing P into the overlying. Furthermore, in our study, the Fe amount was extremely low even under low DO conditions and had no relationship with P release except in FeOOH 0.15% treatment (Fig 3.6). This would have resulted because reduced Fe precipitated in the form of FeS. The growth of sulfate-reducing and Fe-reducing bacteria was promoted by low DO conditions (Lei et al., 2019). Many studies revealed that Fe sulfide or hydrogen sulfide formation in anaerobic sediment induced PO_4^{3-}-P release from sediment to the overlying water (Yamamoto et al., 2021; Chen et al., 2014; Rozan et al., 2002). Yao et al., 2021 also stated that sulfide-mediated Fe reduction derived sulfide from sulfate in anoxic sediment which chemically reduced Fe oxides and formed insoluble Fe sulfide precipitates. If Fe amendment is utilized to increase the P retention in lake sediment, it is important to consider the ferrous sulfide forming over the entire management period because it may require more Fe application (Heinrich et al., 2022).

3.4.5 Effect of pH changes on PO_4^{3-}-P release from sediment

pH changes in the overlying water of our study did not affect P release from any treatment (Fig 3.9). It has been demonstrated that pH changes induced P release from sediment (Van et al., 2016; Wu et al., 2014; Li et al., 2013; Huang et al., 2005). The highest P contents in the sediment were in the forms of Al-P, Fe-P, and Ca-P respectively. Zhao et al., (2021) documented the lowest P release at pH 7, while acidic (pH = 4) and alkaline (pH = 10) promoted P release from Ca-P and Al-P respectively. Although BC and Fe-BC were alkaline, their in-corporation with sediment did not increase the pH in the overlying water. Qian et al., (2023) observed the highest PO_4^{3-}-P removal efficiency from biochar when the pH of the solution was in-between pH 6-7. Therefore, the P release that occurred during this study is likely to be primarily associated with the release of organic P and redox-sensitive P.

3.4.6 Mineral nitrogen release from sediment

During the first period of high DO conditions, NH_4^+-N amounts were increased in all treatments (Fig 3.10). This increment of NH_4^+-N release from sediment was caused by

the decomposition of organic matter. Subsequently, nitrification processes ensued, leading to a decrease in NH_4^+-N amounts and a concomitant increase in NO_3^--N amounts. This shift was indicative of the conversion of NH_4^+-N into NO_3^--N through bacterial action, which typically occurs under aerobic conditions. Following the nitrification phase, the denitrification process occurred, reducing the NO_3^--N amounts in the overlying water. At the end of high DO incubation, low mineral nitrogen concentrations should be attributed to factors such as decreased availability of organic matter for mineralization and reduced microbial activity responsible for denitrification.

The transition to low DO conditions resulted in a significant reduction in NH_4^+-N amounts. Anaerobic conditions obscured the activity of aerobic microorganisms responsible for organic matter mineralization. As a result, there is a diminished decomposition of organic matter, leading to lower NH_4^+-N production. In addition, anaerobic conditions favor the growth of anaerobic microorganisms that are specialized in metabolizing organic matter through fermentation and other anaerobic pathways. These microorganisms may produce intermediate products such as organic acids and alcohols, which are less conducive to NH_4^+-N production compared to aerobic decomposition. On the other hand, denitrification processes become more prevalent under anaerobic conditions. Denitrifying bacteria utilize NO_3^--N as an electron acceptor in the absence of oxygen, converting it to gaseous forms such as nitrogen (N_2) or nitrous oxide (N_2O). This removal of nitrate through denitrification reduces the availability of nitrate for subsequent nitrification and ultimately limits the production of NH_4^+-N.

The addition of Fe-hydroxide into sediment increased mineral N release into the overlying water. However, those amounts in BC or Fe-BC were similar to the sediment-only treatment. Ferric hydroxides can act as an electron acceptor in redox reactions with the organic matter present in the sediment. This process would have enhanced the decomposition of organic matter, promoting the release of NH_4^+-N into the overlying water.

In summary, under high DO conditions, there is a dynamic interplay between organic matter mineralization, nitrification, and denitrification processes, leading to fluctuations in NH_4^+-N and NO_3^--N concentrations within the aquatic environment. Understanding these nutrient dynamics is crucial for managing water quality in ecosystems and ensuring the health of aquatic habitats.

3.5 Conclusion

The addition of FeOOH was efficient in suppressing PO_4^{3-}-P release regardless of incubation conditions. However, lower amending ratios of FeOOH may lead to PO_4^{3-}-P release due to Fe reduction under longer periods of low DO conditions. Although BC and Fe-BC lowered P release under high DO conditions, low DO conditions in the overlying water increased P release from sediment more than the control. Our results suggested that BC and Fe-BC application is not an efficient method to suppress P release in the lakes with high organic matter containing sediment and low DO conditions may induce Fe-bound P and organic P release. Reduction of SO_4^{2-}-S under low DO conditions was the primary culprit associated with the induced P release from sediment in this study.

CHAPTER 4
EVALUATING THE EFFICIENCY OF IRON IONS AS PHOSPHORUS FIXING AGENT AND AN ELECTRON DONOR IN SMFCS

4.1 Introduction

Sediment properties and microbial activities at the sediment–water interface were identified as prime drivers of phosphorus (P) fixation or release from the sediment in reservoirs (He et al., 2017). Particularly, iron (Fe) hydroxides in the sediment provide a large surface area with a positive charge that adsorbs phosphate (PO_4^{3-}P) from the overlying water (Robertson et al., 2011). As the oxygen concentration depletes, bacteria switch their energy metabolism and transfer the electrons to alternative terminal electron acceptors such as cations, which are present in the sediment (Moodie and Ingledew, 1990). Reduction of Fe^{3+} to Fe^{2+} prompts P release from sediment under reductive conditions (Rothe et al., 2015). Therefore, it is essential to control P release from the sediment to prevent eutrophication of water bodies.

Sediment microbial fuel cells (SMFCs) are a type of bioreactor that uses anaerobic microbial activity to generate energy from organic matter decomposition. This novel technique can be used to suppress internal P fluxes from the sediment by diverting the flow of electrons from terminal electron acceptors such as Fe^{3+} to electrodes installed in the sediment (Takemura et al., 2021). Exoelectrogens are microorganisms that can transfer electrons extracellularly and are typically Fe-reducing bacteria (Logan, 2019; Logan et al., 2009). In SMFCs, an anode inserted in anoxic sediment accepts electrons and is transferred to the cathode in the oxygen-rich water layer via the external circuit (Mitov et al., 2015). Simultaneously, protons (H^+) migrate directly from the sediment to the overlying water. In this case, the O_2 present in the cathode compartment acts as the sole electron acceptor and forms H_2O molecules at the end of the cathode reaction. Therefore, SMFCs may restrain the microbial reduction of Fe^{3+} in anaerobic sediment corresponding to the improved redox conditions (Yang et al., 2016). Martins et al., (2014) observed P mobility among different sedimentary fractions and suggested that SMFC may have prevented metal-bound P release to the overlying water.

Agriculture serves as a nonpoint source that delivers P to riverine sediment and ultimately causes a risk of P release into river water (Mainstone and Parr, 2002). SMFC operation on a small scale would be simple, and pollution reduction at the source would be more efficient. Accordingly, using SMFC in agricultural drainage would be beneficial for reducing the internal P loading in eutrophic lakes. However, so far, SMFC operations to regulate P release from sediment in agricultural drainage have not been well-documented.

Electricity production from SMFCs is low because of the high internal resistance for mass and electron transport (Dumas et al., 2007; Song et al., 2011; Li and Yu, 2015). Therefore, the potential applications of SMFCs are very limited. Incorporation of granular activated carbon, steel slag, and colloidal Fe-oxyhydroxides improved low electricity production of freshwater SMFCs (Zhou et al., 2014; Sudirjo et al., 2019; Kim et al., 2020). Moreover, steel-slag added in SMFC consistently increased the power generated from SMFCs, and functioned as a redox catalyst (Kim et al., 2020). By functioning as a redox catalyst in the presence of Fe-oxidizing bacteria, Fe^{2+} in microbial fuel cells (MFCs) increased the generation of energy (Izadi et al., 2019). Moreover, Liu et al. (2017) reported electricity enhancement due to alterations in anode-associated microbial community structures after adding Fe^{2+}. However, the relationship between the inhibition of P release from sediment and the addition of Fe^{2+} and Fe^{3+} ions in SMFCs is not well understood.

Reducing P release from sediment in eutrophic lakes has been found to be satisfactorily accomplished by adding Fe^{2+} and Fe^{3+} ions (Yoo et al., 2016; Liu et al., 2009). Environmental factors affect the possibility of fixed P being released in sediment via Fe ion co-precipitation (Loh et al., 2013; Zaaboub et al., 2014). Iron reduction under anaerobic conditions has obscured the long-term effectiveness of Fe addition in organic matter and sulfur-rich sediment (Wang et al., 2021). Operation of SMFC would be advantageous in terms of P suppression and energy generation because it increases the redox potential in sediment and enhances Fe^{2+} oxidation by Fe-oxidizing bacteria. In addition, Fe^{2+} in SMFCs may have the potential to function as an electron donor and improve the production of electricity.

Accordingly, the purpose of this study is to determine the effects of SMFCs with the combination of Fe^{3+} and Fe^{2+} ions on the suppression of P release from sediment in

highly eutrophic sulfur-rich agricultural drainage. This study fills the knowledge gap pertaining to the function of Fe^{3+} and Fe^{2+} in SMFCs as electron donors or electron shuttles for the improvement of P fixation in sediment.

4.2 Materials and Methods

4.2.1 Study area and sediment sampling

Fresh sediment samples were collected from an agricultural drainage canal in a livestock area (34° 34' 9", 133° 54' 11") in Kasaoka, Japan on August 08, 2022. The sediment sample was homogenously mixed after the removal of stones and organic debris by passing through a 2 mm-sized sieve and then stored at 4°C until experimental use. To prepare Fe^{2+} or Fe^{3+} added sediment, $FeCl_3 \cdot 6H_2O$ or $FeCl_2 \cdot 4H_2O$ was mixed in 0.06% Fe on a wet sediment weight basis.

4.2.2 Experimental design

The laboratory experimental setup is shown in Figure 4.1. A dual-chamber SMFC prototype was prepared to prevent disturbance caused by oxygen exchange between the overlying water and sediment. (Kumar et al., 2017). 75g of fresh sediment was placed within an acrylic column of 14.6 cm in length and 4.5 cm internal diameter. A 3 x 3 cm (18 cm^2) sized graphite felt (G150-12, AvCarb, Lowell, USA) was placed 1 cm below the sediment surface. A platinum electrode was installed 1 cm below the anode to measure the redox potential (Eh). A 10 cm long carbon rod (C-100, Kenis, Osaka, Japan) was used as the cathode in a 100 mL glass beaker filled with 0.2 *M* KCl solution. A to balance the H^+ charges between the two chambers. The salt bridge was

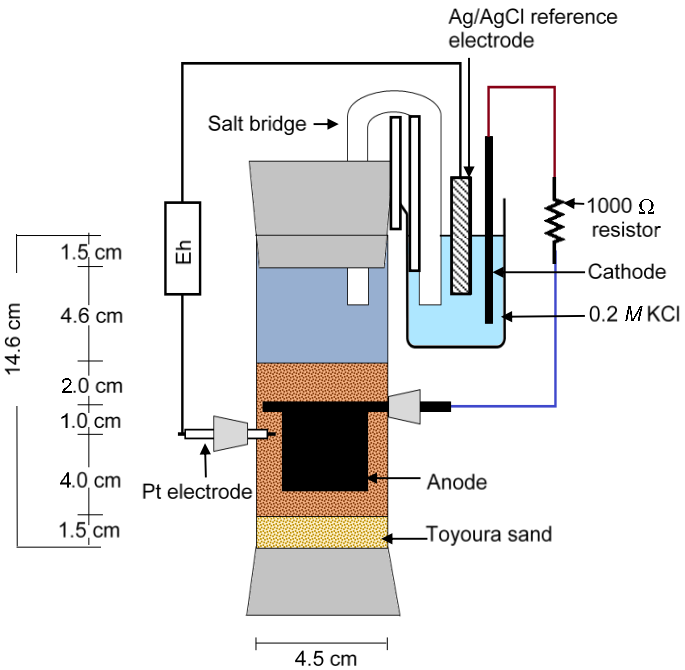

Figure 4.1 Experimental setup of SMFCs

made by filling 15% KCl and 4% agar-dissolved ultra-pure water into a glass U-tube. All treatments, including sediment only, Fe^{3+}, and Fe^{2+}-added sediment, were incubated at 25ºC in the dark under a non-SMFC or SMFC condition. Before starting the experiment, all treatments were pre-incubated for 36 h under a non-SMFC condition until the sedimentary Eh dropped to approximately -200 mV. An external circuit consisting of a 1000 Ω resistor and copper wires was used to connect the two electrodes. The resistor was replaced with 100 Ω from day 26 - 32 and day 34 - 49.

4.2.3 Analytical methods

A data acquisition system (Memory Hilogger, Hioki, LR8431, Japan) was used to record the voltage development. The current was recorded at 10-minute intervals using a voltammeter (Sanwa, Digital Multimeter, PC720M, Japan). Once the open circuit voltage was 600 mV, SMFC treatment was connected. The experiment was conducted for 49 days. The overlying water samples were collected for 0 days, 3 days, and then every 7 days. Collected water samples were stored at 4ºC until analysis. An Eh meter (PRN-41 Fujiwara, SPAD, Japan) with a KCl-saturated Ag/AgCl reference electrode was used to measure Eh in the sediment on each sampling day. The PO_4^{3-}- P concentration in the water samples was determined by a continuous flow analyzer (AutoAnalyzer QuAAtro 2-HR, Bltec, Japan) using colorimetric methods.

To measure total P in sediment, sediment samples were digested with H_2SO_4 and H_2O_2 at 300°C, and then PO_4^{3-}- P concentration was determined. An MT-700 carbon coder (Yanaco, Kyoto, Japan) was used to measure the total nitrogen (N) and carbon (C) content of dry sediment. Using a CHNS elemental analyzer (Perkin Elmer 2400II, Norwalk, USA), the total sulfur (S) content of the dry sediment was measured. Insitu measurements of agricultural drainage canal water were carried out using a pH meter (SanSyo, SPH 71, Japan), a dissolved oxygen meter (Yokogawa, SC 72, Japan), and an electrical conductivity (DKK-TOA, DO-31P, Japan).

Moles of electron flow were computed using Eq 4.1

$$\text{Electron flow (mmol)} = \frac{\sum I\Delta t \times 1000}{\text{F}} \qquad \text{Eq 4.1}$$

I: Current (A)

Δt: Time interval in measurement (600 s)

F: The Faraday constant (96, 485 C mol^{-1})

Tukey's HSD test was used to assess statistical significance at p = 0.05 using R software (R i386 3.6.0).

4.3 Results

4.3.1 Properties of sediment

The sediment samples were highly anaerobic and odorous. Total carbon, total nitrogen, and total P contents in the sediment were 102.7 g kg^{-1}, 8.9 g $kg^{-1,}$ and 1.8 g kg^{-1}, respectively. The total sulfur content in the sediment was 10.8 g kg^{-1}. Dissolved oxygen concentration in the agricultural drainage water was 1.25 mg L^{-1}, while pH and electrical conductivity were 7.35 and 1.25 mS cm^{-1}.

4.3.2 Current densities in SMFCs

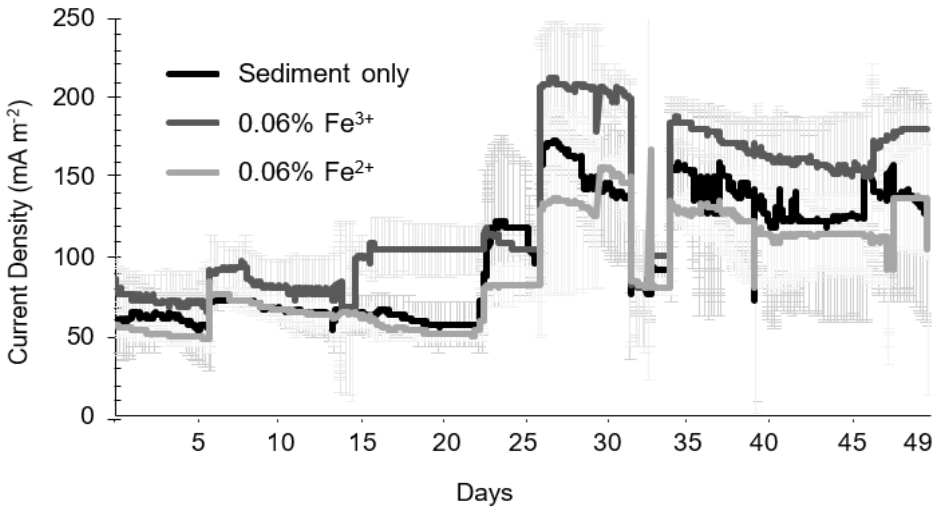

Figure 4.2 Current densities resulted from SMFCs. Day 0 denotes the beginning of the experiment after the pre-incubation. Error bars show the standard deviations (*n* = 3)

During our study, Fe^{3+}-added sediment resulted in the highest current density among the other treatments (Fig. 4.1). The total number of electrons harvested from Fe^{3+}-added sediment used SMFC was significantly higher than Fe^{2+}-added sediment used

SMFC (Table 4.1; $p < 0.05$). After replacing a 1000 Ω resistor with a 100 Ω resistor, the current density increased in all treatments.

Table 4.1 Electrons transferred by SMFCs.

Parameter	Number of electrons (mmol)
Sediment only	7.08 ± 1.26^{ab}
Fe^{3+}/ SMFC	6.38 ± 0.88^{a}
Fe^{2+}/ SMFC	9.00 ± 0.20^{b}

4.3.3 Changes of Eh in sediment

The Eh fluctuation in sediment during the experimental period is shown in Figure 4.2. At the beginning of the experiment, the initial Eh in the sediment was less than -150 mV in all treatments. Sedimentary Eh seemed to be increased in Fe^{3+} or Fe^{2+}-added SMFCs (Fig 4.2b, c). However, Eh in sediment-only treatment was similar between with and without SMFC operation (Fig 4.2a). Although Eh in Fe^{3+} added SMFC was slightly reduced at the end of the experiment still it was higher than that was in non-SMFC conditions.

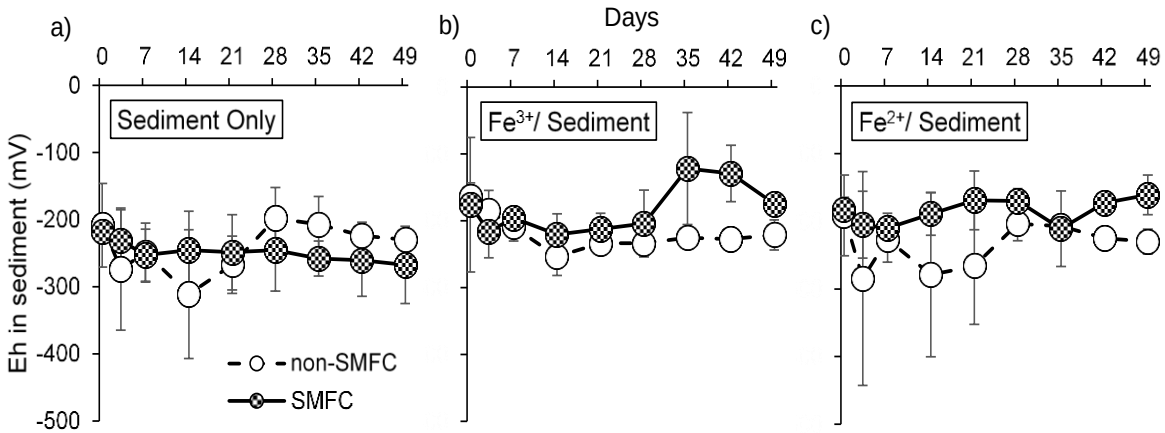

Figure 4.3 Eh changes at 2 cm below the sediment surface. Day 0 denotes the beginning of the experiment after the pre-incubation. Error bars show the standard deviations (n = 3)

4.3.4 Phosphorus immobilization in sediment

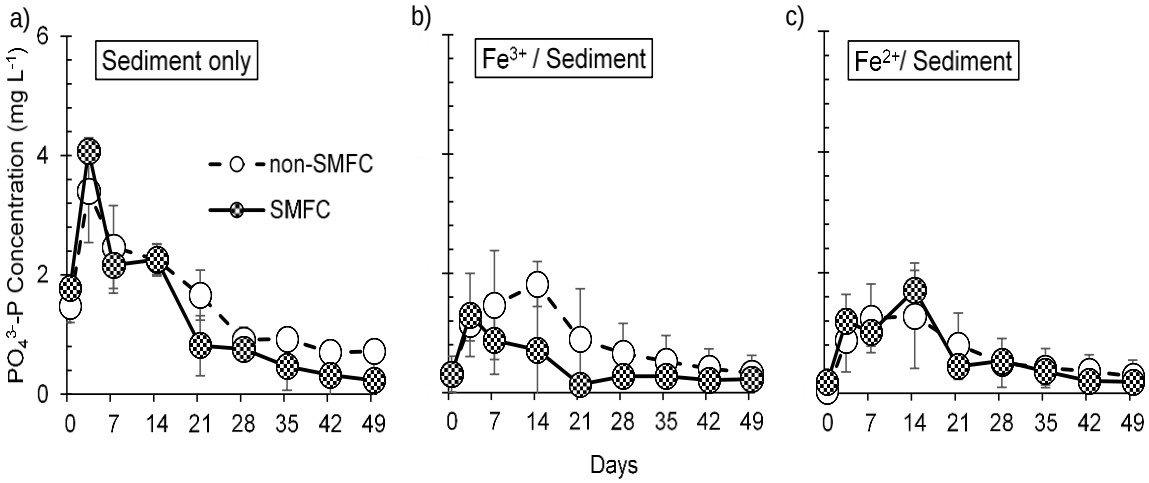

Figure 4.4 Concentrations of PO_4^{3-}-P in the overlying water. Day 0 denotes the beginning of the experiment after the pre-incubation. Error bars show the standard deviations (n = 3)

Adding Fe^{3+} or Fe^{2+} reduced the PO_4^{3-}- P concentration in the overlying water. Initial PO_4^{3-}-P concentrations in Fe-added treatments were significantly lower than in sediment-only treatments ($p < 0.05$). After day 3, Fe^{3+}-added sediment reduced PO_4^{3-}-P concentration under SMFC operation more than in the non-SMFC condition. In sediment-only treatments, SMFCs reduced PO_4^{3-}-P more than non-SMFC conditions after day 14. In contrast, Fe^{2+}-added sediment showed similar PO_4^{3-} - P concentrations regardless of the SMFC operation.

On day 3, PO_4^{3-}P release from sediment was increased in all treatments. Treatments with only sediment and Fe^{3+}-incorporated SMFC showed the highest peak on day 3, while other treatments increased PO_4^{3-}-P concentrations until day 14. Then the PO_4^{3-}-P concentration gradually decreased in all treatments.

4.4 Discussion

4.4.1 Current production from SMFCs

In our experiment, SMFCs with Fe^{3+}-added sediment produced more electricity than those with Fe^{2+}-added sediment (Fig 4.1; Table 4.1; $p < 0.05$). Contrastingly, Gonzalez-Paz et al., (2022) indicated higher current production from Fe^{2+}-added

microbial fuel cells inoculated with sulfate-reducing sludge and acetate because Fe^{3+} acted as an electron acceptor while Fe^{2+} acted as an electron donor. Moreover, Bensaida et al., 2021 showed higher electricity enhancement by both Fe^{3+} and Fe^{2+} added sludge used in a microbial fuel cell. In the present study, high electricity resulted from Fe^{3+}-added SMFC, which should be attributed to the effect of redox reactions occurring within the anode chamber (Bensaida et al., 2021). In a reductive environment, Fe^{3+} is more reactive than Fe^{2+}. The ability of an element to gain or lose electrons during a chemical process is measured by its redox potential. When Fe^{3+} is added to anaerobic sediment, Fe-reducing bacteria would participate in redox processes by reducing Fe^{3+} to Fe^{2+}. Then, as these reduced agents transferred electrons to the electrodes in SMFCs, an oxidative reaction occurred that produced electricity. As a result, the addition of Fe^{3+} increased electricity from SMFCs. However, since Fe^{2+} is already in a reduced state, it might need more energy or favorable conditions to further reduce it to an even lower oxidation state (elemental Fe). The sedimentary Eh enhanced by SMFC operation in the current study was too low to oxidize Fe^{2} Fig 4.2). Consequently, the addition of Fe^{2+} did not assist with the electricity production by serving as an electron donor in our study.

In addition, Fe^{3+} addition would have increased microbial decomposition of organic matter. Wu et al., 2013 reported that adding ferric ions to SMFCs enhanced power generation by accelerating the formation of anode biofilms, which can transfer electrons from the cytoplasmic membrane to extracellular electron acceptors including electrodes, flavins, and soluble and insoluble metals. Kim et al. (2021) also reported that Fe addition in SMFCs promotes recalcitrant organic matter degradation by thermodynamically destabilizing organic compounds in sediment.

The contrasting outcomes of adding Fe^{3+} or Fe^{2+} to SMFC are probably attributed to the differences in the redox state, the reactions of Fe species, and the ability of the microbial community to utilize these Fe forms as electron acceptors.

4.4.2 Phosphorus reduction by Fe^{3+} or Fe^{2+} addition

Our study showed adding Fe^{3+} or Fe^{2+} into sediment reduced PO_4^{3-}-P release into the overlying water (Fig 4.2). In addition, PO_4^{3-} reduction by adding Fe^{3+} or Fe^{2+} occurred through PO_4^{2-}-P precipitation or adsorption. For this study, we used ferric chloride ($FeCl_3$) or ferrous chloride ($FeCl_2$) as Fe^{3+} or Fe^{2+} supplements. Consistently, Smolder et al.

(2001) discovered the strongest decrease of PO_4^{3-} in sediment pore water due to the addition of $FeCl_3$ and $FeCl_2$. Additionally, Ann et al., (2000) found the highest P immobilization from a constructed wetland by adding $FeCl_3$. Fe oxyhydroxide would have been formed by adding Fe^{3+} and Fe^{2+} to the sediment, which would have caused adsorption of P by ligand exchange (Wang et al., 2021). $FeCl_3$ primarily suppresses P release from sediment for long terms by changing organic and unstable exchangeable P into more stable occluded PO_4^{3-} (Li et al., 2020).

The addition of Fe^{3+} or Fe^{2+} chloride can precipitate and immobilize P in the sediment, which can be advantageous for environmental management. It limits P release into the overlying water by lowering its bioavailability. As P is a crucial nutrient that encourages the excessive growth of algae and aquatic plants, Fe addition would be an effective method to avoid eutrophication and prevent algal blooms.

However, factors, including pH, Fe concentration, and sediment properties such as organic matter content, may affect the ability of PO_4^{3-} immobilization via Fe addition. To achieve the intended results for P management in anaerobic sediment and to optimize the treatment technique, it is vital to comprehend these factors.

4.4.3 Phosphorus immobilization by SMFCs

Release of P was inhibited by SMFCs (Fig. 4.1 a). Similarly, Xu et al. (2018) demonstrated that SMFCs enhanced P mobilization from the overlying water to sediment. In addition, Yang et al. (2016) showed that SMFC operation reduced P concentration in the overlying water. According to Haxthausen et al. (2021), P co-precipitation with Fe caused SMFCs to decrease P release from sediment. On the other hand, Takemura et al. (2022) suggested that SMFCs reduced P in sediment pore water by electrochemically attracting dissolved P to the anode. In the present study, Fe reduction at lower Eh was avoided by SMFCs by transferring electrons via an external circuit. Thus, PO_4^{2-} release from sediment was lowered under SMFC operation.

Our results revealed that Fe^{3+}-added SMFC increased suppression of P more than that in Fe^{2+}-added SMFCs or SMFCs with sediment only. Mixed Fe^{3+} with sediment in SMFCs would have been utilized as electron acceptors during microbial respiration. Thereby, transferring electrons from sediment as an electron mediator, Fe^{3+} would adsorb PO_4^{2-} ions, reducing P release from sediment. However, Fe^{2+} showed similar electricity,

which showed the scarcity of Fe^{2+} participation in the electron transfer process of SMFC systems as it was in Fe^{3+}-added SMFCs. In this study, PO_4^{3-}adsorption by Fe^{2+} mixed with sediment would be greater than the contribution of SMFC in suppressing P release. Therefore, Fe^{2+}-added SMFCs showed similar PO_4^{3-} concentrations regardless of SMFC operation. Hence, in the current experiment, while Fe^{3+} increased electricity generation and reduced P release in SMFCs as an electron acceptor, Fe^{2+} did not typically act as an electron donor and therefore did not yield similar effects in SMFCs.

4.5 Conclusion

The present experiment was conducted to evaluate the effects of Fe^{3+} and Fe^{2+} additions in SMFCs on electricity production and suppression of P release from agricultural drainage sediment. Adding Fe^{3+} to SMFCs increased current production and suppressed P release from sediment by acting as an electron shuttle. Adding Fe^{2+} to SMFCs did not increase electricity by acting as an electron donor, probably due to the low Eh in the sediment. However, Fe^{2+} effectively reduced P release from the sediment at the beginning by adsorbing P. This study suggested that adding Fe^{3+} to sediment enhanced the efficiency of P suppression and electricity generation from SMFCs.

CHAPTER 5
EFFECT OF VARYING NUTRIENT CONTENTS IN AGRICULTURAL DRAINAGE SEDIMENTS ON PHOSPHORUS RELEASE FROM IRON-INCORPORATED SMFCS

5.1 Introduction

Phosphorus (P) in sediment has the potential to be released, leading to continued eutrophication (Li et al., 2023; Li et al., 2021, Tu et al., 2019; Wu et al., 2014; Wang et al., 2008). Even after using remediation techniques to reduce external P loadings, internal P release resulting from iron (Fe) reduction in sediment has been determined to be a primary issue against lake restoration (Tu et al., 2019; Luo et al., 2022; Chen et al., 2018; Wang et al., 2015). In summer, higher organic matter decomposition reduces O_2 concentration in the bottom water, which prompts lake sediment to become anaerobic (Yang et al., 2021; Sondergaard et al., 2021). Under reductive conditions, Fe^{3+} in sediment is transformed to Fe^{2+}, causing the dissolution of Fe^{2+} and PO_4^{3-}-P into the overlying water (Wang et al., 2022; Tammeorg et al., 2020). On the other hand, when sulfate-reducing bacteria are present in the overlying water, sulfate (SO_4^{2-}) is converted to sulfide (S^{2-}) under anaerobic conditions, promoting the formation of insoluble ferrous sulfide (FeS) compounds at the sediment surface (Duverger et al., 2020; Cui et al., 2021; Kankanamge et al., 2020; Sun et al., 2016). The approach of adding Fe^{3+} to control P release from sediment was found to be inadequate due to FeS production (Heinrich et al., 2022). Therefore, to combat eutrophication in water bodies, minimizing internal P loadings from sediment through an innovative method is crucial (Liu et al., 2018).

Sediment microbial fuel cells became increasingly attractive as both a renewable energy source and pollutant treatment technique due to their ability to oxidize reduced substances like S^{2-} or organic carbon buried in anoxic sediment (Algar et al., 2020; Guo et al., 2019). These systems consist of an anode embedded in anaerobic sediment and a cathode placed in the overlying water with high oxygen concentration Liu et al., 2022; Liu et al., 2019). The anode is the acceptor of electrons generated by electrogenesis that facilitate the decomposition of organic matter (Hong et al., 2009). The electrons are then passed to the cathode across an external circuit, where electrons react with oxygen and

protons to produce water while generating electricity (Pergola et al., 2023; Zhao et al., 2017).

Sediment microbial fuel cells have been recognized as a novel technology to immobilize P in anoxic sediment (Sondergaard et al., 2001; Takemura et al., 2022). The redox potential was increased by SMFCs, and P was retained in sediment due to microbial Fe^{2+} oxidation (Yang and Chen, 2021; Haxthausen et al., 2021; Yang et al., 2016). In addition, the meditative action of electrochemically active bacteria with SMFCs would remediate Fe^{3+} hydroxide reduction, consequently preventing Fe-bound P release (Yang and Chen 2021; Qi et al., 2022; Martins et al., 2014). Wang et al. (2022) suggested that SMFCs oxidized S^{2-} in FeS and released Fe^{2+} into the overlying water. After migrating to oxygen-rich overlying water, Fe^{2+} is re-oxidized to Fe^{3+} and precipitated with PO_4^{3-}. It would be beneficial if the mechanism of P immobilization by SMFC were further explained based on sediment properties.

Low power generation limited the practical application of SMFCs (Guo et al., 2022; Wang et al., 2023), and Fe-incorporation with the anode structure had shown better catalytic activities, which enhanced electricity production in SMFCs (Kim et al., 2022; Oktavitri et al., 2021; Zhou et al., 2014). However, the effect of P release from agricultural drainage sediment by applying Fe-added SMFCs has not been well explored. Accordingly, we set up the hypothesis that Fe^{3+} addition to SMFCs may reduce TP release from sediment while producing high electricity. Under short-term SMFC operation for 17 days, we found that high P adsorption by Fe^{3+} oxyhydroxides reduced P release from Kojima Lake sediment with high TP content (4.7 g kg^{-1}) regardless of SMFC operation until day 15 and then Fe^{3+} addition increased P release into the overlying water (Perera et al., 2023). Therefore, additional studies on long-term SMFC operations for Fe-added sediment are required. The present study investigated the performances of Fe-added SMFCs using agricultural drainage sediments with different TP contents for 98 days.

5.2 Materials and Methods

5.2.1 Sediment sampling

Surface sediment samples (0 - 10 cm) were collected from agricultural drainage canals in livestock farming (LS: 34º 28' 38" N, 133º 30' 1" E) and a pasture-grown area (PS: 34° 28' 33" N, 133° 30' 3" E) of Kasaoka reclaimed land, Japan on August 23, 2023.

Sediment properties are shown in Table 1. The drainage canal in the LS area was highly eutrophic and odorous due to the discharge from livestock farms. Contrastingly, the PS drainage canal showed low nutrient contents of sediment and dissolved oxygen in the water was over-saturated. On the other hand, both sediments had similar total sulfur (S) and total Fe contents, and the canal water from LS and PS areas showed high electrical conductivities of 2 mS cm^{-1} and 7 mS cm^{-1}, respectively, reflecting the effect of seawater intrusion.

Samples were passed through a 2 mm-sized sieve to remove stones and debris. The homogenized sediment samples were then stored at 4°C until the use of the experiment. Chemical properties of sediment samples are shown in Table 1. Total carbon (TC) nitrogen and P contents (TN, TP) were higher in the LS sediment than in the PS sediment ($p < 0.05$). To prepare 0.05% Fe-added LS (LS/Fe) and PS sediments (PS/Fe), $FeCl_3 \cdot 6H_2O$ was mixed with sediment on a wet weight basis. The moisture contents of fresh LS and PS sediments were 68% and 62% on a wet-weight basis, respectively.

5.2.2 Experimental setup

A dual-chamber SMFC was designed to prevent oxygen diffusion into the anode (Hagoss and Demeke 2015). The SMFC design was illustrated in Perera et al. (2023). The anode chamber was made of a 14.6 cm-high acrylic tube with a 4.5 cm internal diameter. After placing 5 g of Toyoura standard sand (Toyoura Keiseki Kosyo), 65 g of fresh sediment was placed in the anode chamber. Then it was topped off with N_2 gas-sparged deionized water (110 mL, at 0.2 L min^{-1} for 5 min). A 4 x 3 cm graphite-felt anode (G150-12, AvCarb, Lowell, USA) was placed 1 cm below the sediment surface, whereas a 10-cm long carbon rod (C-100, Kenis, Osaka, Japan) was used as the cathode. Before use in the experiment, surfaces of graphite felt were water-saturated. A 0.02 *M* KCl-filled 100-mL beaker was used as the cathode chamber, coupled with the anode chamber using a 15% KCl salt bridge. A platinum electrode was made by placing a copper wire crimped with a platinum wire in a glass tube (5 mm diameter), which was enclosed with epoxy resin at both ends to avoid any water seepage. Those were installed 3 cm below the sediment surface (close to the anode) to measure the sedimentary redox potential. A 1000 Ω external resistor was used for 42 days and then replaced with 100 Ω until the end of the experiment.

Two groups of sediment columns with each LS, PS, LS/Fe, and PS/Fe were prepared in triplicate. One group was left under an open circuit (OC) condition in which the anode and cathode were not connected, and the other was operated as closed circuits (CC), which work as SMFCs. Before starting the experiment, all sediment columns were pre-incubated at 25ºC for two days under OC operational conditions so that sedimentary Eh reached about -200 mV. The experiment was carried out at 25°C in the dark. 30 mL of overlying water samples were collected every 14 days, and the filtered samples (0.2 μm) were stored at 4°C for chemical analyses. After each sampling, the overlying water in the SMFCs was compensated by adding N_2-sparged deionized water. Water sampling started from day 0 before connecting SMFC circuits.

5.2.3 DNA extraction and 16s rRNA gene analysis

In this study, we examined the changes in the microbial community in sediment due to SMFC operation. Total P release was much higher in LS sediment regardless of SMFC's operation. To know the mechanism of Fe^{2+} or S^{2-} oxidation that regulates TP release in SMFCs, we measured the microbial community only in LS sediment. At the end of the experiment, the anodes of LS and LS/Fe treatments were carefully removed, and sediment samples were collected by scraping the anode surface. The DNA was extracted from the sediment samples using the FastDNA Spin Kit for Soil (MP Biomedicals, Irvine, USA). The extracted DNA (80 μL) was purified using DNA Clean and Concentrator-25 (Zymo Research, Irvine, USA). The concentrations and quality of the DNA were measured using a spectrophotometer (DS-11, Denovix, Wilmington, USA). The DNA samples were stored at -20°C.

A primer set of V3V4f_MIX and V3V4r_MIX were used for 16S rRNA gene amplification (Hugerth et al., 2014). Amplicon sequencing was performed by an external analytical laboratory (Bioengineering Lab., Sagamihara, Japan). The FASTX-toolkit (ver. 0.0.14) and FLASH (ver. 1.2.11) were used to process the raw sequence reads. Representative sequences and amplicon sequence variant (ASV) tables were prepared after removing chimeric and noisy sequences with the dada2 plugin in Qiime2 (ver. 2022.8). Taxonomy assignment of the ASVs was performed using the q2-feature-classifier plugin against the EzBioCloud 16S database.

5.2.4 Analytical methods

The voltages and current were measured at 10 min intervals using a data acquisition system (LR8431, Memory Hilogger, Hioki, Nagano, Japan) and an ammeter (PC720M, Digital Multimeter, Sanwa, Tokyo, Japan), respectively. The current density was calculated by dividing the produced current by the surface area of the anode.

The water quality of the overlying water in the anode chamber was measured every 14 days. Water samples were digested with $K_2S_2O_8$ (120°C, 30 min), and iron colloids formed in the digested tubes due to oxidation were dissolved by adding 11 *M* $NaHCO_3/NaS_2O_4$ solution (shaken for 1 h) to determine the total P (TP) concentrations (Lakkari et al., 2014). Phosphate (PO_4^{3-}- P) and ammonium (NH_4^+-N) concentrations were measured using a continuous flow analyzer (2-HR, QuAAtro, AutoAnalyzer, Bltec, Tokyo, Japan) after filtration (0.2 μm). The below-mentioned anode-half reaction was considered to have occurred during organic matter decomposition (Eq 5.1).

$$CH_2O + H_2O \rightarrow CO_2 + 4H^+ + 4e^- \quad \text{Eq 5.1}$$

If Fe^{2+} was released from sediment under SMFC operation by FeS oxidation, electrons transferred via SMFCs were assumed to be produced by following anode half-reaction (Eq 5.2).

$$FeS \rightarrow Fe^{2+} + S^0 + 2e^- \quad \text{Eq 5.2}$$

If Fe^{2+} was released due to corrosion of the anode connection, the chemical reaction may occur owing to the charge recovered from zero-valent iron (Fe^0) in steel slag.

$$Fe \rightarrow Fe^{2+} + 2e^- \quad \text{Eq 5.3}$$

The amount of Fe^{2+} that can be released by the above half-reactions was computed using Eq (5.4).

$$Fe^{2+} \text{ released by FeS or Fe oxidation (g m}^{-2}) = \frac{\sum I \Delta t \times M_{Fe}}{2F \times A} \quad \text{Eq 5.4}$$

I: Current (A)

Δt: Time interval in measurement (600 s)

F: The Faraday constant (96, 485 C mol^{-1})

M_{Fe}: Mass of Fe (56 g)

A: Cross-sectional area of acrylic column (m^{-2})

Mineralization of N and P during the SMFC operation was calculated by assuming that all electrons passed through SMFC circuits were produced from organic matter decomposition.

$$N\ (\text{g m}^{-2}) = \frac{\sum I\Delta t \times M_c}{4F \times C/N \times A} \quad \text{Eq 5.5}$$

M_c: Mass of carbon (12 g)

C/N: Carbon to nitrogen mass ratio of sediment

$$P\ (\text{g m}^{-2}) = \frac{\sum I\Delta t \times M_c}{4F \times C/P \times A} \quad \text{Eq 5.6}$$

C/P: Carbon to phosphorus mass ratio of sediment

The averaged amounts of each component in the overlying water under the OC condition were reduced from those under the CC condition at the end of the study to determine observed differences in Fe^{2+}, NH_4^+-N, or TP amounts between the OC and CC conditions.

An atomic absorption spectrometer (ICE 3300 AA, Thermo Fisher Scientific, Waltham, USA) was used to measure Fe concentration in the water samples. Sulfate (SO_4^{2-}) was extracted from sediment (1:4 solid: water ratio) with distilled water by shaking at 175 rpm for 1 h and then filtered (0.2 μm). Concentrations of SO_4^{2-} were determined by ion chromatography (761 Compact IC, Metrohm, Herisau, Switzerland). At the beginning and end of the experiment, pH in the overlying water was measured using a digital pH meter (F-23, Horiba, Kyoto, Japan). Sedimentary Eh was measured every 7 days using the platinum electrode connected to the SMFC and a KCl-saturated Ag/AgCl reference electrode (PRN-41, Fujiwara, Tokyo, Japan).

The initial chemical properties of the sediment were also analyzed. Sediment samples were digested with H_2SO_4 and H_2O_2 at 300°C, and then TP content was determined by analyzing PO_4^{3-}-P concentrations. Using a CN coder (MT-700, Yanaco, Kyoto, Japan), the total nitrogen (N) and total carbon (C) content of dry sediment were determined. At the end of the experiment, the total Fe and non-soluble S contents in the sediment at the surface and the anode were measured by the X-ray fluorescence spectrometry (XRF) method (ZSX Primus II-R1, Rigaku, Tokyo, Japan). Before the measurement, sediment samples were washed with distilled water to remove SO_4^{2-} from the sediment and freeze-dried at -40ºC. Sediment water content was determined by oven-drying at 105ºC for 24 h on the dry weight basis.

Using the R software (R i386 3.6.0), Tukey's HSD test was applied to evaluate statistical significance at $p < 0.05$. Changes in microbial communities between OC and CC conditions were determined by LEfSe (Galaxy module, The Huttenhower Lab, Harvard University). The threshold for discriminative features on the logarithmic LDA score was set at 2.0, and the statistical significance of relative abundance was $p < 0.05$.

5.3 Results

5.3.1 Changes of sulfur in the overlying water and sediment

Table 5.1 Chemical properties of sediments

Parameter	LS	PS
Total C (g kg^{-1})	102.7	27.2
Total N (g kg^{-1})	8.9	2.05
Total P (g kg^{-1})	1.8	0.6
Total S (g kg^{-1})	10.8	9.35
Total Fe (g kg^{-1})	110.1	104.5
C/N	11.6	13.3
C/P	57.1	45.3

The initial properties of the sediment are shown in Table 5.1. The total C, N, and P

contents in LS sediment were higher than in PS sediment. However, S and Fe contents are similar between the two sediments.

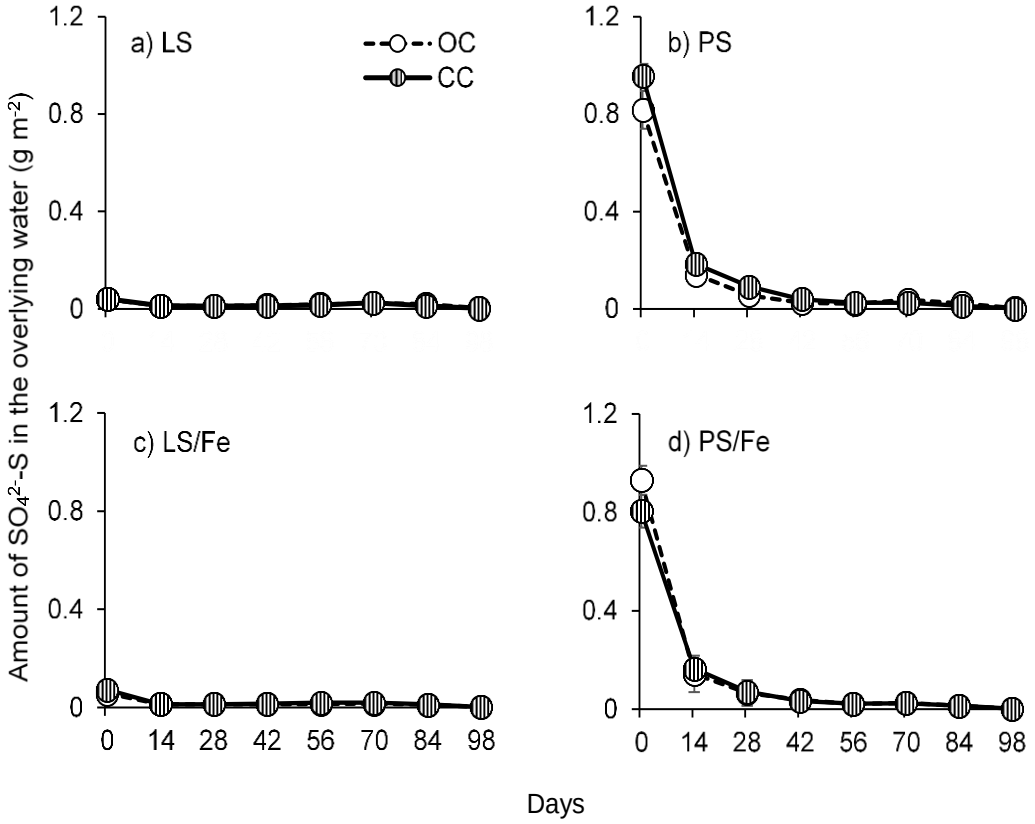

Figure 5.1 Dissolved SO_4^{2-}- S amounts in the overlying water of a) LS, b) PS, c) LS/Fe and d) PS/Fe treatments. Day 0 denotes the beginning of the experiment after the pre-incubation. Error bars show the standard deviations (n = 3)

Release of SO_4^{2-}-S from PS sediment to the overlying water was higher than LS sediment (Fig 5.1; $p < 0.05$). Amounts of SO_4^{2-}- S in the overlying water gradually decreased in PS sediment during the entire period, regardless of SMFC operational conditions. Initial SO_4^{2-}- S concentrations in LS and PS sediments were about 300 and 200 mg kg^{-1}, respectively (no data shown), which account for only a few percentages of total S in sediment (Table 1). At the end of the study, SO_4^{2-}- S content in LS sediment was 2 mg kg^{-1}, while it was 171−233 mg kg^{-1} in PS sediment. There were no differences between OC and CC conditions in both sediments. On the other hand, non-soluble S

contents in sediment were similar between 0- and 4-cm depths in both sediments (Fig 5.2).

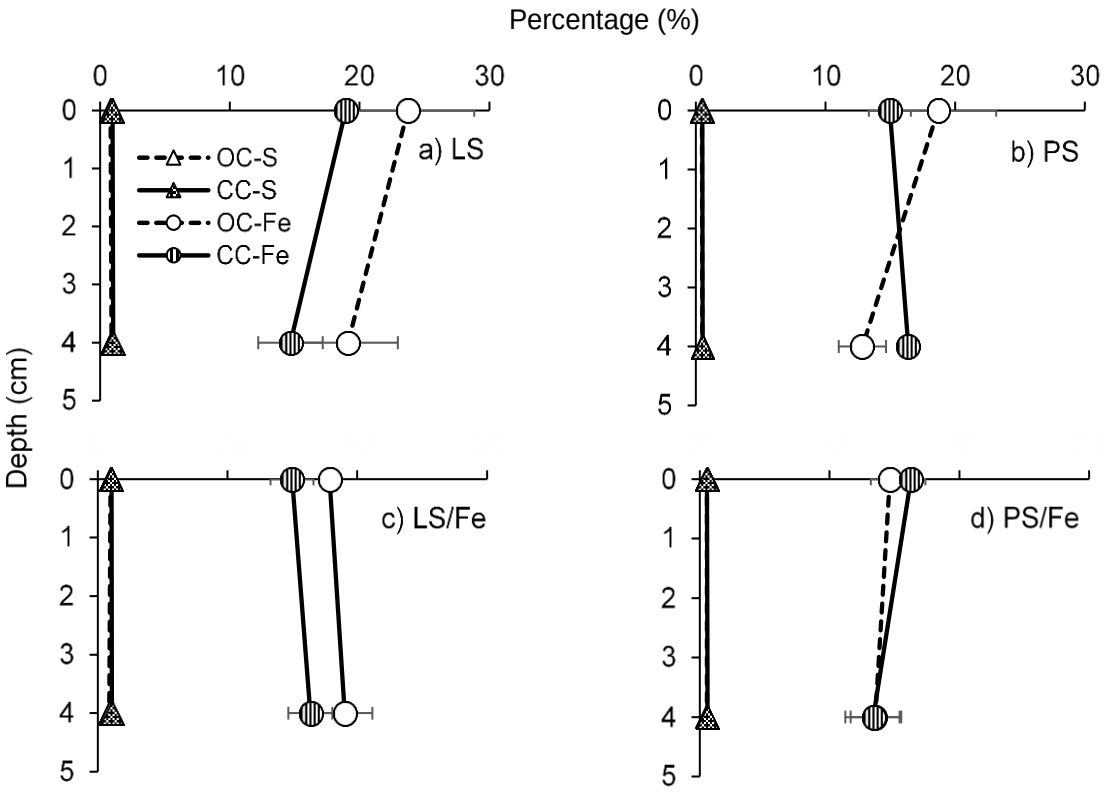

Figure 5.2 Non-soluble S and total Fe distribution in the surface and 4 cm below the sediment surface of a) LS, b) PS, c) LS/Fe and d) PS/Fe treatments at the end of the experiment. Error bars show the standard deviations (n = 3)

5.3.2 Changes in sedimentary Eh

Sedimentary Eh was negative and varied at -200 mV in all treatments (Fig. 5.3). Statistical analysis indicated no significant difference in sedimentary Eh between the OC and CC conditions. However, at the end of the experiment, sedimentary Eh in treatments under the CC condition was slightly higher than under the OC condition. Our findings deviate from previous research findings, as documented by Hong et al. (2009), Yang et al. (2021), Haxthausen et al. (2021), Yang et al. (2016), and Xu et al. (2018). These studies have consistently reported a notable increase in sedimentary Eh during the operation of SMFC systems. According to our results, the effects of Fe addition on Eh changes in OC or CC treatments were not clear in each sediment.

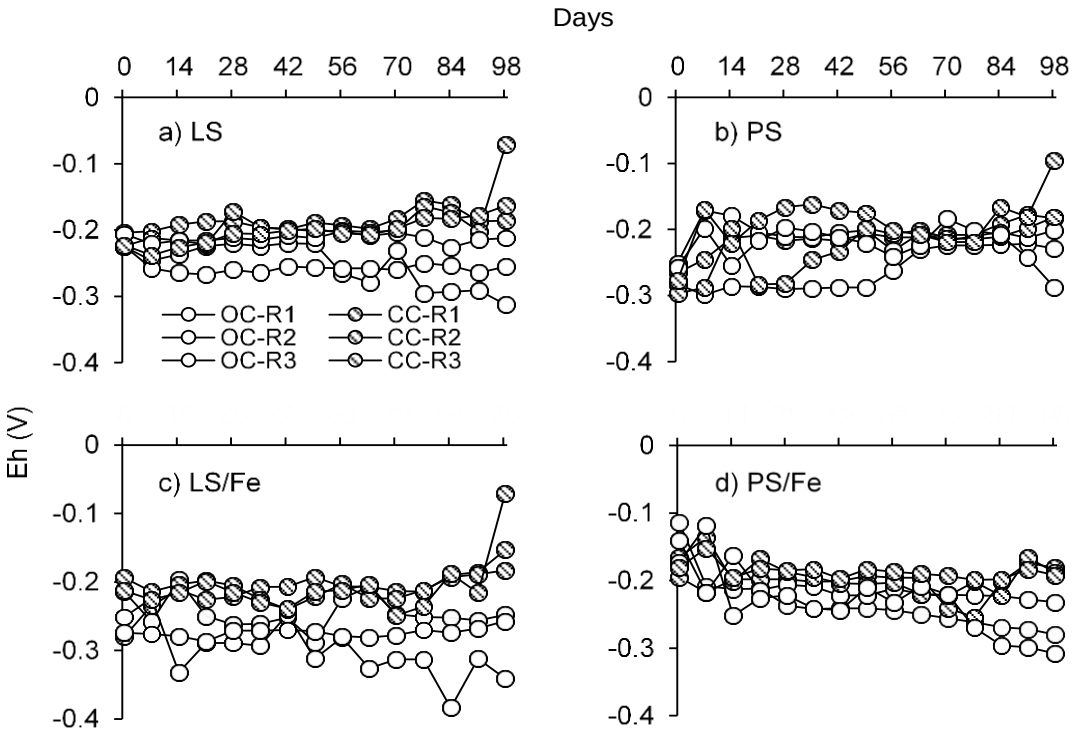

Figure 5.3 Eh changes at 3 cm below the sediment surface in a) LS, b) PS, c) LS/Fe, and d) PS/Fe treatments. Day 0 denotes the beginning of the experiment after the pre-incubation. Error bars show the standard deviations (n = 3). Replicates under the same conditions were represented by R1,2,3.

5.3.3 Release of Fe from sediment to the overlying water

Regardless of sediment type, SMFC operation (CC) significantly increased Fe release from sediment to the overlying water more than the OC condition (Fig 5.4; $p < 0.05$). Adding Fe to SMFCs with LS sediment (LS/Fe-CC) released more Fe than no-Fe SMFCs (LS-CC) from 56 - 84 days (Fig 5.4a, c; $p < 0.05$). Under OC conditions, Fe release once increased and then decreased (Fig 5.4).

At the end of the experiment, total Fe content at the sediment surface under OC conditions was higher than under CC conditions in all treatments except for PS/Fe treatment (Fig 5.4). LS-CC and PS/Fe-CC sediment showed high total Fe content at 0 cm more than at 4 cm depth. In contrast, those did not differ much in PS-CC and LS/Fe-CC.

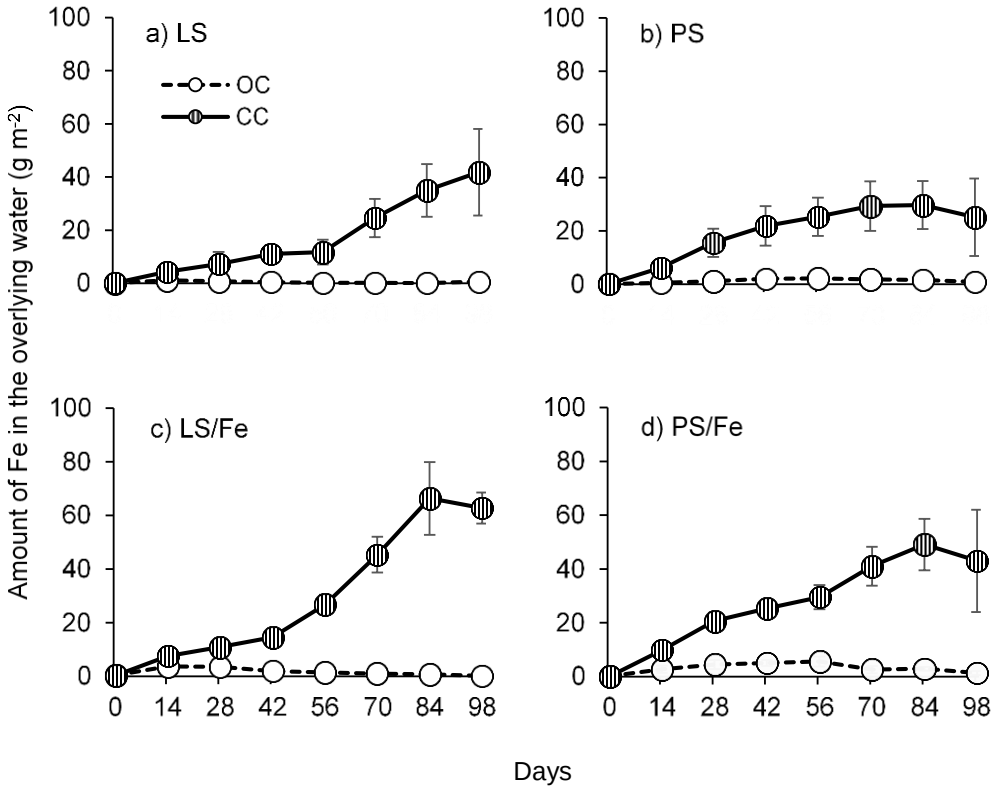

Figure 5.4 Dissolved Fe amounts in the overlying water of a) LS, b) PS, c) LS/Fe, and d) PS/Fe treatments. Day 0 denotes the beginning of the experiment after the pre-incubation. Error bars show the standard deviations (n = 3).

5.3.4 Changes in pH in the overlying water

Table 5.2 pH changes in the overlying water at the end of the experiment

LS			PS		
Treatment	Start	End	Treatment	Start	End
LS-OC	7.9^{a}	6.6^{a}	PS-OC	7.7^{a}	4.5^{a}
LS-CC	8.1^{a}	3.7^{b}	PS-CC	7.7^{ab}	4.0^{a}
LS/Fe-OC	7.8^{a}	6.2^{a}	PS/Fe-OC	7.9^{b}	4.1^{a}
LS/Fe-CC	7.7^{a}	3.7^{ab}	PS/Fe-CC	7.9^{b}	4.4^{a}

** The same lowercase letters represent no significant differences between treatments on each day based on Tukey's HSD test at $p < 0.05$ (n = 3). Average H^{+} concentrations were used to calculate the average pH among replicates.*

At the beginning of the study, pH in the overlying water was about 8 in all treatments (Table 5.2). pH values in all treatments dropped at the end of the study. The ending pH under CC conditions for LS and LS/Fe sediments was lower than that under OC conditions. Contrastingly, PS nor PS/Fe did not show significant pH differences between OC and CC conditions.

5.3.5 Amount of NH_4^+-N in the overlying water

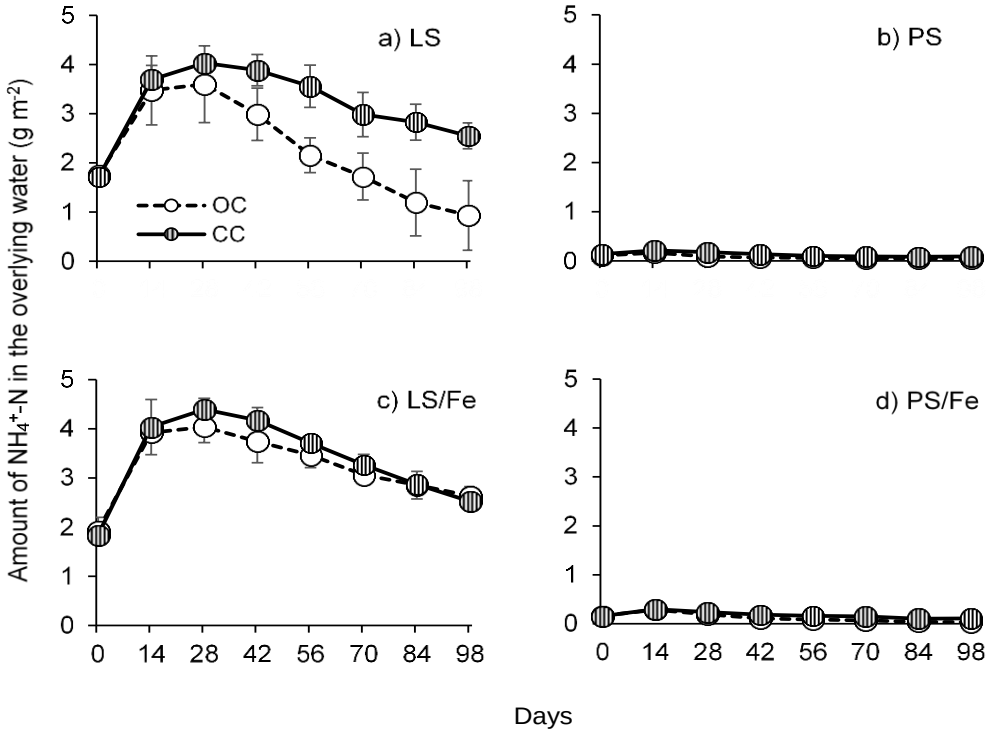

Figure 5.5 Amounts of NH_4^+-N released from sediment to the overlying water in a) LS, b) PS, c) LS/Fe, and d) PS/Fe treatments. Day 0 denotes the beginning of the experiment after the pre-incubation. Error bars show the standard deviations (n = 3)

Release of NH_4^+-N into the overlying water was higher in LS sediment than in PS sediment (Fig 5.5; $p < 0.05$). The amount of NH_4^+-N in the overlying water was increased until day 28 in LS sediment, while PS sediment showed the highest NH_4^+-N concentration on day 14 (Fig 5.5a, b**)**. Although the concentrations were reduced at the latter period, treatments under the CC condition showed higher NH_4^+-N amounts than those under OC treatments. This reduction was significant between LS-OC and LS-CC treatments ($p <$ 0.05). Adding Fe^{3+} into both sediments increased NH_4^+-N release regardless of operating

condition (Fig 5.5c, d). In the overlying water, NO_3^--N was not detected during the experimental period.

The difference between calculated N mineralization under CC condition and the difference of actual NH_4^+-N concentrations between OC and CC treatments at the end of the study were given in Table 3. Calculated N mineralization was similar to the actual amount of NH_4^+-N in the overlying water for LS-CC treatment. However, PS sediment and Fe^{3+} added treatments showed equal NH_4^+-N amounts under OC and CC treatments.

5.3.6 Release of TP from sediment to the overlying water

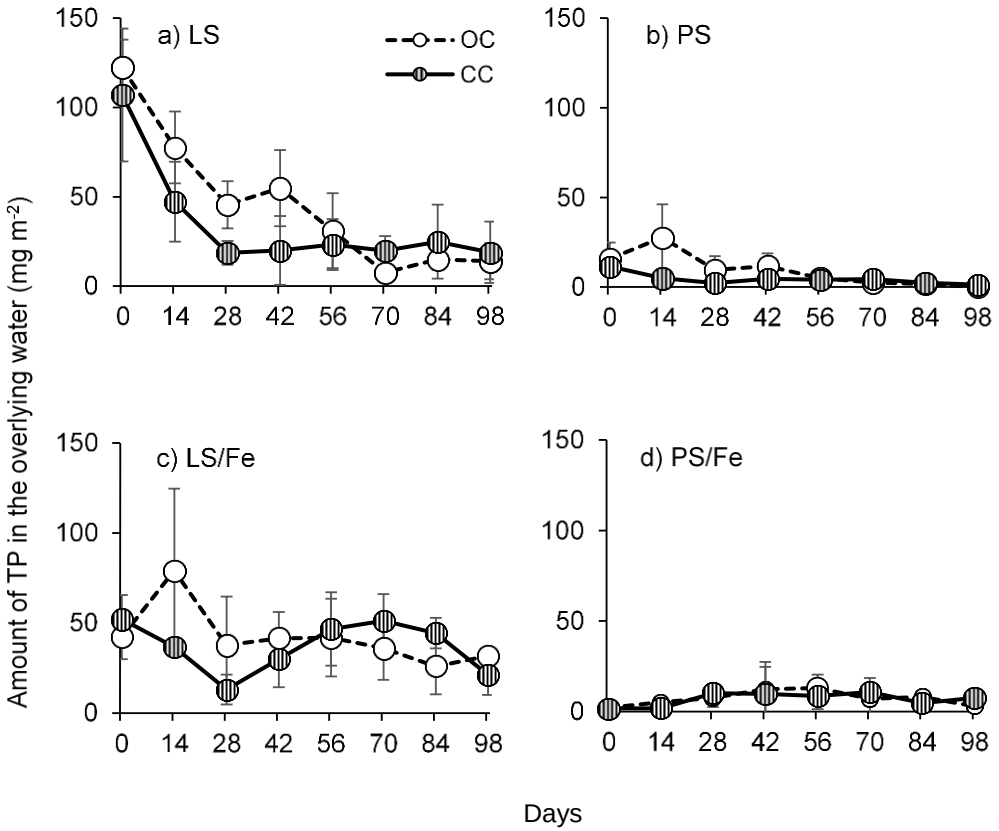

Figure 5.6 Amounts of total P released from sediment to the overlying water in a) LS, b) PS, c) LS/Fe, and d) PS/Fe treatments. The concentration of TP on each sampling day was divided by the sediment surface area to calculate the TP amount released from the sediment. Day 0 denotes the beginning of the experiment after the pre-incubation. Error bars show the standard deviations (n = 3)

The amount of TP released from the LS sediment was higher than that from the

PS sediment (Fig 5. 6a, b; $p < 0.05$). Until day 42, TP amounts under the CC condition were lower than those under the OC condition, regardless of the sediment type (Fig. 5.6a, b). On day 0, the TP amounts in LS/Fe and PS/Fe treatments were lower than in LS and PS sediments (Fig 5.6c, d; $p < 0.05$). In the latter half of the experiment, Fe^{3+} addition increased TP amounts in the overlying water, unlike the No-Fe treatments (Fig 5.6c, d). From day 56 to 70, TP release increased more in the LS/Fe-CC treatment than in the LS-CC treatment (Fig 5.6a, c; $p < 0.05$). However, the P release between PS-CC and PS/Fe-CC was not significantly different.

5.3.7 Electricity generation

Current densities were similar between the two sediments and were stable between 45 and 60 mA m^{-2} (Fig 5.7). On day 42, current densities increased in all treatments when the external resistor was replaced from 1000 to 100 Ω. Cathodes were replaced on day 70 due to KCl precipitation on the

surface. Simultaneously, current densities were immediately increased in all treatments. However, after replacing the cathodes, current densities gradually decreased. On the other hand, the current density in LS/Fe-CC treatment appeared to be higher than in LS-CC treatment (Fig 5.7a, c). However, the cumulative numbers of electrons passing through the external circuit were not significantly different in all treatments (Table 3). Drops in current densities at the end of the experiment were probably attributed to the failure of the anode connection due to corrosion.

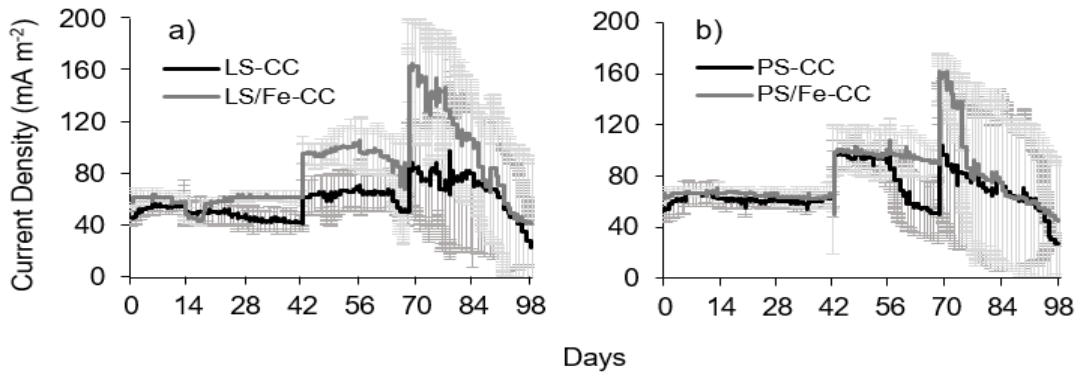

Figure 5.7 Current densities in a) LS, LS/Fe and b) PS, PS/Fe. Day 0 denotes the beginning of the experiment after the pre-incubation. Error bars show the standard deviations ($n = 3$)

Table 5.3 Calculated electron flow and nutrient mineralization from SMFCs

Treatment	Calculated electron flow in SMFCs (mmol)	Calculated carbon degradation in SMFCs (mmol)	Calculated Fe^{2+} from FeS or Fe^0 oxidation by SMFC (mmol)	Calculated Fe^{2+} release by SMFC ($g\ m^{-2}$)	Observed Fe^{2+} difference between OC and CC ($g\ m^{-2}$)	Calculated TP release by SMFC ($g\ m^{-2}$)	Observed TP difference between OC and CC ($g\ m^{-2}$)	Calculated N release by SMFC ($g\ m^{-2}$)	Observed NH_4^+-N difference between OC and CC ($g\ m^{-2}$)
LS-CC	12.5 ± 1.4^a	3.1 ± 0.4^a	6.6 ± 0.7^a	220 ± 25^a	41.15	0.4 ± 0.1^a	0.005	2.04 ± 0.23	1.62
LS/Fe-CC	17.4 ± 3.5^a	4.3 ± 0.9^a	8.7 ± 1.7^a	306 ± 62^a	62.62	0.6 ± 0.1^a	-0.010	2.83 ± 0.57	- 0.11
PS-CC	14.5 ± 2.9^a	3.6 ± 0.7^a	7.3 ± 1.5^a	256 ± 52^a	24.27	0.6 ± 0.1^a	0.001	2.05 ± 0.42	0.05
PS/Fe-CC	16.8 ± 4.4^a	4.2 ± 1.1^a	8.4 ± 2.2^a	296 ± 77^a	41.67	0.7 ± 0.2^a	0.005	2.38 ± 0.62	0.07

5.3.8 Microbial community

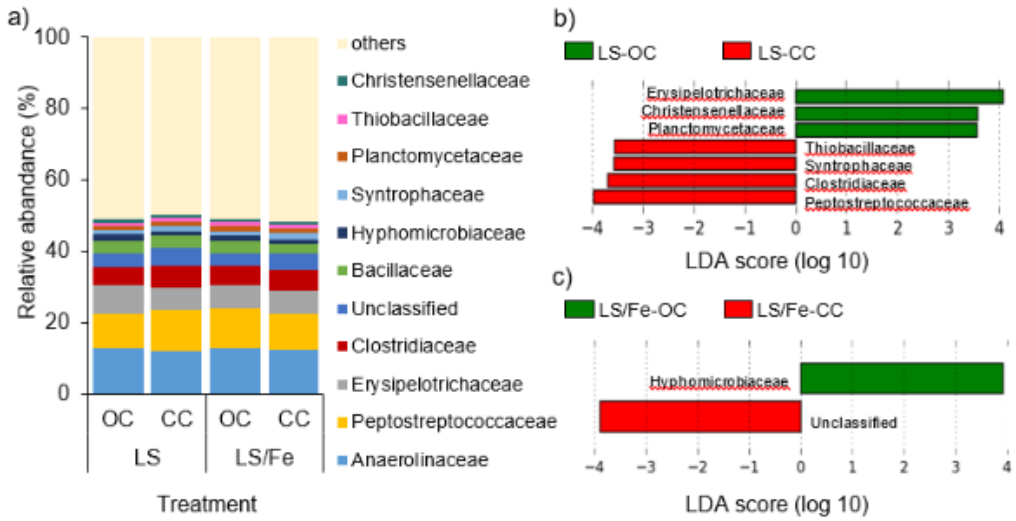

Figure 5.8 a) 16S rRNA gene sequence for the microbial community in sediment near the anode of LS and LS/Fe sediments (family level). Taxa with significantly different microbial abundances in b) LS and c) LS/Fe were detected by LEfSe analysis with an LDA threshold score of 2.0 and a significance level of $p < 0.05$.

** Horizontal bars show the effect size for each taxon. Log 10 transformed LDA scores are in Fig. 5.8b, c. Green and red colors represent more abundant taxa in OC and CC treatments, respectively. The negative LDA values under CC conditions were due to the order of the numerator and dominator when calculating the effect size.*

Relative abundances of the microbial community at the family level in LS and LS/Fe sediment are shown in Fig 5.8a. Anaerolinaceae, Peptostreptococcaceae, Erysipelotrichaceae, Clostridiaceae, and Bacteroidales were dominant in all treatments (relative abundance > 3%). Most of the microbial families enriched in LS sediment represented phylum Firmicutes (>35%), Proteobacteria (>15%), Chloroflexi (>19%), and Bacteroides (>5%). The linear discriminant analysis (LDA) score shows the effect size of each abundant microbial family under OC and CC conditions in LS (Fig. 5.8b) and LS/Fe sediments (Fig. 5.8c). For LS sediment, Erysipelotrichaceae, Chistensellaceae, and Planctomycetaceae were abundant under OC conditions, while Clostroiadaceae, Peptostreptococcaceae, and Thiobacillaceae, Syntrophaceae families were predominant

under CC conditions (Fig. 5.8b; $p < 0.05$). The genera *Clostridium* and *Romboutsia* were dominated by the Clostroiadaceae and Peptostreptococcaceae families, respectively. Furthermore, the genus *Thiobacillus* represented the whole Thiobacillaceae family (belonging to Beta-proteobacteria), while *Smithella* and *Syntrophorhabdus* dominated the Syntrophaceae (belonging to Delta-proteobacteria). Only the unclassified bacteria under order Bacteroidales were abundant in Fe-added SMFCs (Fig 5.8c; $p < 0.05$). In this study, Fe addition in sediment did not significantly affect the microbial community.

5.4 Discussion

5.4.1 Sulfur and iron dynamics

Regardless of sediment type and SMFC operations, amounts of SO_4^{2-}- S in the overlying water decreased and became undetectable at the end of the experiment (Fig 5.1). They did not differ between OC and CC conditions. At lower Eh (Fig 5.3), SO_4^{2-}- S in the overlying water was probably reduced to S^{2-} by sulfur-reducing bacteria (Richards and Pallud 2016). Contradictory to our findings, Wang et al. (2022) showed increased SO_4^{2-} concentrations in the overlying water or sediment under SMFC operation. This discrepancy presumably originated from low oxygen in dual chamber SMFCs, which would have prevented S^{2-} oxidation to SO_4^{2-}. In our study, SO_4^{2-}- S reduction to S^{2-} in the overlying water and S^{2-} oxidation to elemental sulfur (S^0) in sediment would have concurrently occurred under CC conditions. Similarly, Angelov et al., (2012) and Perez-Diaz et al., (2020) demonstrated concurrent reactions of S^{2-} oxidation to S^0 in a dual chamber MFC and reduction of SO_4^{2-} to S^{2-}. Ryckelynck et al. (2005) also reported S^0 deposition on the graphite anodes of an SMFC installed on a seafloor. In SMFCs, SO_4^{2-} reduction would produce S^{2-} by consuming organic substances under anaerobic conditions. According to Perez-Diaz et al. (2020) and Daghio et al. (2018), sulfur-reducing bacteria presumably acted as electron shutters, and S^{2-} was oxidized to S^0 at the anode.

At the surface sediment, total Fe increased under OC conditions more than under CC conditions, except in the PS/Fe treatment (Fig 5.2). At low sedimentary Eh (Fig 5.3), Fe^{3+} was reduced to Fe^{2+}, which was released from the sediment to the overlying water (Tammeorg et al., 2020). Under OC conditions, Fe^{2+} is probably coprecipitated in the

form of FeS on the sediment surface. As a result, dissolved Fe amounts in the overlying water remained low under OC conditions (Fig 5.4; $p < 0.05$). Similarly, Wang et al. (2022) and Pan et al. (2020) demonstrated that S^{2-} formed in anaerobic sediment fixed Fe^{2+} as FeS while SO_4^{2-} decreased in the overlying water. However, in the present study, non-soluble S in the surface sediment did not increase due to FeS formation (Fig 5.2). The non-soluble S increment at the surface sediment due to SO_4^{2-} reduction to S^{2-} in the overlying water should be small, as SO_4^{2-}-S on day 0 was less than 1% of total S in both sediments (Fig 5.1). LS sediments initially contained high S^{2-} contents due to higher organic matter (Table 1) and severe eutrophic conditions in the sampling area. In contrast, PS sediment showed low carbon and nutrient contents (Table 1). In PS sediment, rapid SO_4^{2-} reduction was seen in the overlying water until day 14. This indicates that high rates of SO_4^{2-} reduction took place in PS sediment. Production of S^{2-} in pore water is high if anaerobic microbial respiration of SO_4^{2-} occurs in sediment (Pollman et al., 2017). In both sediments, Fe^{2+} diffused from sediment to the overlying water would have immediately been trapped by high S^{2-} initially present in the surface sediment. Thus, non-soluble S in sediment did not change, unlike total Fe.

In all treatments, Fe concentration in the overlying water was significantly increased by SMFCs (Fig 5.4; $p < 0.05$). As mentioned above, those canals are located in a sea-reclaimed area. Both sediments used in our study had high non-soluble S and total Fe contents (Fig 5.2) and probably high FeS because marine sediments show high FeS contents (Wu et al., 2017). Consistently, Kim et al. (2021) reported that Fe^{2+} release was more increased under CC conditions or steel slag-added SMFCs than under OC conditions. In SMFCs, Fe^{2+} produced from the oxidation of FeS in sediment should have diffused into the overlying water. Ryckelynck et al. (2005) mentioned that SMFCs released Fe^{2+} into the overlying water while it oxidizes S^{2-} in FeS or pyrite. Another possible reason for Fe increment in SMFCs is that low pH (Table 2) at the anode of SMFCs caused the dissolution of Fe^{2+} or Fe^{3+} from sediment (Wang et al., 2022; Algar et al., 2020, Touch et al., 2017). Additionally, if pH reduction was induced by SMFCs, FeS would be dissolved in the overlying water (Algar et al., 2020), which may cause Fe^{2+} dissolution. At the end of our study, similar low pH values were seen in PS and PS/Fe treatments under both OC and CC conditions, in which Fe^{2+} amounts were significantly different (Table 2; Fig 5.4). Therefore, Fe accumulation in the overlying water did not

occur in our study at lower pH. Instead, pH reduction probably exhibited alkalinity removal by utilizing HS^- and proton production under SMFC operation (Algar et al., 2020).

5.4.2 Amount of NH_4^+-N in the overlying water

The amount of NH_4^+-N released from LS sediment was higher than that from PS sediment due to its higher TC and TN contents (Table 1; Fig 5.5). In the beginning, NH_4^+-N gradually increased in the overlying water, indicating N mineralization. Then, it reduced in the latter period, presumably due to weakened organic N mineralization and microbial assimilation. In the overlying water, NO_3^-- N was not detected during the experiment. Inhibited nitrification due to oxygen limitation in dual chamber SMFCs and enhanced denitrification increased ammonia accumulation.

Under CC conditions, NH_4^+- N release from sediment was higher than under OC conditions. These results were consistent with Perera et al. (2023) and Xu et al. (2017). In LS-OC treatment, NH_4^+- N reduced significantly at the end due to N immobilization. Although microbial assimilation took place in LS-CC treatments, the rate of NH_4^+- N decrease was masked by the higher N mineralization. Equivalent N amounts between calculated and actual NH_4^+-N release from SMFCs further explained high N mineralization under SMFC operation (Table 3). This NH_4^+- N increment under CC operation was not significant for PS sediment. Because of the low N availability in PS sediment, inorganic N was used for microbial respiration without being released into the overlying water. On the other hand, the amount of NH_4^+- N in LS/Fe and PS/Fe treatments showed no difference between OC and CC treatments (Fig 5.5c, d). Nitrogen mineralization would have been induced with Fe^{3+} addition to sediment regardless of SMFC operation, resulting from increased microbial activity.

5.4.3 Phosphorus release from sediment

The release of P from LS sediment was higher than that from PS sediment due to its higher TP content (Table 1; Fig 5.6). The amount of TP reduced over time regardless of OC or CC condition. During the experiment, reduction of NH_4^+-N and TP exhibited nutrient immobilization due to microbial respiration.

For LS and PS sediments, P release under CC conditions was lower than under

OC conditions until 42 days (Fig 5.6a, b) when the external resistance was reduced. Increased Fe concentrations induced PO_4^{3-} precipitation under CC conditions, which caused a reduction of TP in the overlying water (Fig 5.4). This was explained by the increased total Fe at the surface sediment more than at the anode in LS-CC treatment (Fig 5.2). However, total Fe did not increase in PS-CC treatment because Fe precipitation did not occur due to the low TP amount in the overlying water. After day 56, P amounts in the overlying water were similar between OC and CC conditions for both sediments. In contrast, the calculated TP release due to organic matter decomposition was larger than the observed TP increment under SMFC operation (Table 3). Similar TP amounts between OC and CC conditions would have resulted from P equilibrium in the sediment-water system. When the P release into the overlying water is excessive under CC conditions, P is absorbed into the sediment to reconstruct the equilibrium status (Peng et al., 2021; Nguyen et al., 2016).

Adding Fe^{3+} into sediment decreased P release from sediment on day 0 (Fig 5.6c, d). Previous studies (Wang et al., 2021; Natarajan et al., 2021; Chen et al., 2016; Smolders et al., 2001) demonstrated that Fe addition immobilized P in sediment due to its high P absorptivity. At the beginning of our experiment, Fe^{3+} hydroxides that were formed by Fe^{3+} addition absorbed PO_4^{3-}-P. However, the Fe^{3+}-added treatments showed higher TP amounts than the sediment-only treatments under OC conditions. Wang et al. (2016) reported that Fe addition to suppress P release from sediment is less effective when organic matter and S^{2-} concentrations are high. Anaerobic fermentation of $FeCl_3$-added sludge increased P release due to accelerated SO_4^{2-} reduction (Yang et al., 2019). In the present study, Fe^{3+} addition would have increased microbial activity in sediments such as sulfur-reducing and Fe-reducing bacteria. Increased microbial organic matter decomposition would have released more P from Fe^{3+}-added sediment.

In the latter period, LS/Fe-CC treatment increased P release more than in LS-CC (Fig 5.6a, c; $p < 0.05$). Oktavitri et al. (2021) indicated that adding 0.06% of nano-zero-valent Fe to SMFCs did not reduce P released from the sediment. Rapid decomposition of organic matter by Fe^{3+}-added SMFCs released more P into the overlying water (Lu et al., 2021). For PS/Fe-CC treatment, this TP increment from SMFCs was not significantly different than PS-CC treatment. Lower TP content limited P mineralization in PS sediment (Table 1).

In this experiment, Fe^{3+} was not involved in P suppression under SMFC operation. Previous studies (Yang et al., 2021; Qi et al., 2022; Martins et al., 2014) reported that SMFCs increased the redox potential in sediment, and thereby P concentrations in the overlying water were lowered. In contrast, Eh in the SMFCs of this study was not adequately increased to avoid Fe^{3+} reduction (Fig 5.3). When the organic matter content and the S^{2-} contents are abundant in sediment, Fe^{2+} might not be oxidized under CC conditions. Instead, the Fe^{2+} would be released into the overlying water under CC conditions (Algar et al., 2020). If oxygen concentration in the overlying water was high, these released Fe^{2+} may oxidize to Fe^{3+} and precipitate PO_4^{3-} in the overlying water to sediment.

5.4.4 Electricity generation

All SMFCs immediately started to produce electricity, which varied around 45 - 65 mA m^{-2} (Fig 5.7a, b). Tran et al. (2019) reported similar results from an SMFC with sediment collected from a semi-enclosed bay. Oktavitri et al. (2021) reported starting current density from SMFCs similar to our study. In our experiment, current densities were similar between different sediments. Song et al. (2019) showed different voltage outputs from SMFCs according to the sediment type after 80 days of operation. Kim et al. (2020) demonstrated that sedimentary Eh in steel slag-added SMFCs fluctuated around -200 mV for 160 days. They further mentioned that increased Eh differences between electrodes resulted in higher and more stable electricity production. A steel clip used to connect the anode would have acted as Fe^0 addition under CC conditions. This would have led to higher electricity production from SMFCs. Another critical factor that affects electricity production from a dual chamber system is the proton exchange system. Min et al. (2005) documented a 2-fold power reduction due to a salt bridge in an MFC. Higher internal resistance exerted by the salt bridge would have forced a similar proton transfer rate under both sediments. Significant pH reduction under SMFC with LS or LS/Fe sediment indicated a weakened proton transferring rate through the salt bridge. Similar current densities from the two sediments were attributed to similar electron transfer rates under CC conditions.

Adding Fe^{3+} seemed to enhance current densities from SMFCs (Table 3; Fig 5.7a, b). Stimulated organic matter decomposition due to Fe-reducing microorganisms would

have increased the electron production under CC conditions. Our results were compatible with Kim et al. (Kim et al., 2021), who demonstrated that Fe addition induced electricity production from SMFCs due to enhanced oxidative organic matter degradation at low pH with high S^{2-} content. In this study, using the iron clip for the anode clip might have acted as Fe^0 addition to sediment. If Fe^{2+} released under CC condition in this experiment occurred due to FeS or Fe^0 oxidation, its contributions to total electron flow under CC conditions were approximately 10%, 14%, 6%, and 9% in LS-CC, LS/Fe-CC, PS-CC and PS/Fe-CC treatments, respectively (Table 3). Actual N mineralization in the LS-CC treatment showed 79% of calculated N mineralization due to electron flow under CC conditions. This difference was not clear for other treatments because Fe^{2+} addition increased NH_4^+-N released regardless of operational condition, and low NH_4^+-N release from PS sediment masked the effect of SMFCs. Electron transferred by LS/Fe-CC was approximately 39% higher than LS-CC treatments and only around 16% for PS/Fe-CC treatment. Low carbon and nutrient contents in PS sediment (Table 1) would have hampered the decomposition of organic matter, resulting in a 16% current enhancement under Fe^{3+} addition. On the other hand, Fe^{2+}-added SMFCs increased electron production by 4% for LS sediment by releasing $Fe^{2+,}$ while it was about 3% for PS sediment. Accordingly, we can conclude that electricity generation in Fe^{3+}-added SMFCs primarily occurred by decomposing organic matter despite the sediment type. However, sulfur oxidation by Fe^{3+}-added SMFCs should be investigated more in future studies.

5.4.5 Changes in microbial communities in SMFCs

Regardless of the operational condition, LS sediment was enriched with Anaerolineaceae, which is an electrochemically active bacterial family (Fig 5.8a). This family of bacteria has been found to be acidogenic fermenters with the ability to remove organic matter from wastewater (Wang et al., 2019). In this study, the operation of SMFCs supported the growth of Clostridiaceae, Peptostreptococcaceae, Thiobacillaceae, and Syntrophaceae at anode-associated sediment (Fig 5.8b; $p < 0.05$). Clostridiaceae and Peptostreptococcaceae come under the phylum Firmicutes, whereas Thiobacillaceae and Syntrophaceae are the families belonging to the phylum Proteobacteria. The abundance of electrochemically active bacteria under phylum Firmicutes and Proteobacteria primarily supported electricity production and voltage increment of plant microbial fuel

cells because of the plant root exudates (Lin et al., 2022). The family Clostridiaceae can hydrolyze cellulose from dead plant roots into less-complex substances like fatty acids, which electrochemically activated bacteria can use (Lu et al., 2015). Like our findings, Song et al. (2019) found an abundance of genus *Clostridium* in sediments from SMFCs. These bacteria are known to ferment various carbohydrates, including starches, organic acids, monosaccharides, and disaccharides (Dos-Passos et al., 2019; Kouzuma et al., 2013). Plant residues in agricultural drainage sediments probably promoted the growth of these bacteria due to the SMFC's operation. Bhatti et al. (2022) reported that electricigens genus *Romboutsia* increased in microbial fuel cells with higher molasses and acetate, which might be a reason for the increased electricity production from MFCs. The abundance of this genus would have supported electricity generation in our study. Previous studies mentioned that several species of the genus *Thiobacillus* have been identified as bacteria that derive energy from Fe or sulfur oxidation in anaerobic environments (Chen et al., 2016; Smolders et al., 2001; Wang et al., 2016). On the other hand, *Thiobacillus* can remove N from sediment by denitrification (Wu et al., 2022). Additionally, Aida et al. (2014) showed that the genus *Smithella* was possibly able to aid in the sulfur oxidation in up-flow anaerobic sludge blanket reactors. In this study, the operation of SMFC probably supported S^{2-} oxidation at the anode.

In LS/Fe-CC, unclassified bacteria under the order Bacteroidales were dominated (Fig 5.8c; $p < 0.05$). This bacterial group might have indicated an electrochemically active bacterium.

5.5 Conclusion

This study aimed to investigate the long-term effects of Fe-added SMFC on electricity generation and P release from sediment with different T contents. The SMFCs had the potential to reduce P release from sediment due to accumulating dissolved Fe in the overlying water. However, TP release from sediment was increased in the late period by Fe^{3+} addition under CC conditions due to high organic matter decomposition and thereby P mineralization. This phenomenon was not clear in the short-term experiment. Although power generation was not affected by the organic matter content in different sediments, the amount of P released into the overlying water depended upon initial TP contents in sediment. Sulfur-dependent bacteria abundance in sediment associated with

SMFCs suggested S^{2-} oxidation by SMFCs. When the sulfur content in sediment is high, Fe^{2+} oxidation by SMFCs may not occur efficiently. This study indicated that Fe^{3+} addition to sediment stimulated organic P release from sediment while increasing electricity production. The effect of SMFC with Fe and sulfur-rich sediment should be further studied in the future.

CHAPTER 06
GENERAL DISCUSSION, CONCLUSIONS, AND IMPLICATIONS FOR FURTHER STUDY

6.1 General discussion and conclusions

In our research, we investigated the effects of adding FeOOH to sediment on phosphorus (P) release under different dissolved oxygen (DO) conditions (Chapter 3). Our findings revealed that FeOOH addition effectively reduced P release from the sediment, demonstrating strong P adsorption capabilities under different DO conditions. However, when exposed to prolonged low DO conditions, both P and Fe are released into the overlying water, particularly at a 0.15% FeOOH treatment. In addition, under low DO conditions, P amounts released from FeOOH 0.15% treatment had a strong correlation with the amount of Fe released into the overlying water. This phenomenon was attributed to the prolonged anaerobic conditions leading to the release of P from the sediment due to Fe^{3+} reduction. However, P release from FeOOH 0.3% treatments was low even under low DO oxygen conditions, probably due to the strong adsorption capabilities of FeOOH. When FeOOH is added to sediment at high concentrations, it has a greater capacity to adsorb and retain PO_4^{2-} ions, preventing their release into the surrounding environment. This strong adsorption ability allows FeOOH to effectively sequester PO_4^{2-} even in anaerobic conditions, where other factors may lead to PO_4^{2-}-P release. Therefore, the high amending rates of FeOOH create a protective barrier that inhibits P release, ensuring that the nutrient remains bound to the FeOOH particles rather than being released into the overlying water.

On the other hand, under high-dissolved oxygen conditions, the addition of Fe-BC and BC suppressed P release respectively (Chapter 3). In contrast, under low-dissolved oxygen conditions, BC 1%, BC2%, and Fe-BC 1% treatments showed the highest P release from the sediment. Moreover, there was no relationship between the release of Fe and P in the treatments and the addition of Fe-BC or BC treatments. Our results indicated that in those treatments, sulfate reduction under anaerobic conditions resulted in the formation of FeS, which induced P release. Furthermore, we observed that high amending rates of Fe-BC were more effective in reducing P release compared to low

amending rates, perhaps due to the high P adsorption characteristics of Fe. Overall, our study suggests that FeOOH has a greater potential to suppress P release from sediment than biochar under varying DO conditions.

In Chapter 4, the addition of Fe^{2+} or Fe^{3+} to the sediment decreased P release more than in the original sediment conditions by adsorbing P. When Fe^{3+} was mixed with sediment in sediment microbial fuel cells (SMFCs), there was an enhancement in electricity generation along with a reduction in P release from the sediment. On the other hand, the addition of Fe^{2+} resulted in electricity generation levels similar to those in the sediment-only treatment, indicating a less pronounced impact on SMFC performance. These findings underscore the potential benefits of incorporating Fe^{3+} into SMFC systems for effectively managing P release in sediment environments. The increased electricity production would be due to Fe^{3+} aiding in electron transfer and supporting the growth of electro-active microbes. The rise in sedimentary Eh indicates the effective transport of electrons in SMFCs with added Fe^{3+}, showcasing enhanced efficiency in electron movement. As a result, the SMFCs suppressed the reduction of Fe^{3+} and subsequently decreased the release of P from the sediment. In contrast, the limited impact of Fe^{2+} on electricity generation and P release mitigation suggests that Fe^{3+} may be more effective in promoting beneficial outcomes in SMFC systems. The distinct behavior of Fe^{2+} and Fe^{3+} in sediment emphasized the importance of considering the specific properties and reactivity of different Fe species when designing strategies for nutrient management and energy production in SMFCs.

Findings of Chapter 5 indicated that P release was higher from organic matter-rich sediment than the pasture-grown area sediment with lower total P content. Initially, the SMFC operation led to a reduction in P release up to day 42. The SMFC operation significantly increased the Fe concentration in the overlying water. In our study, the higher Fe concentrations in the overlying water would have fixed P in sediment, lowering P release from sediment. Afterward, P concentrations in the overlying water became similar between with or without SMFC conditions. At the latter period, Fe addition into sediment also enhanced the P release from the sediment. This increment resulted due to enhanced organic matter decomposition and subsequent P mineralization. Under SMFC operation, an abundance of sulfur-using microbial families was found in sediments rich in organic matter. These findings suggest that sulfide oxidation by SMFCs may have occurred,

potentially releasing Fe2+ bound in the form of FeS. Consequently, Fe^{2+} release from sediment might have increased under SMFC conditions. The study showed that the formation of Fe precipitates by SMFCs successfully inhibited the release of P for 42 days. However, in organic matter-rich sediment, SMFC operation or Fe addition would accelerate organic matter decomposition, which may enhance P release into the overlying water.

In conclusion, this thesis revealed that FeOOH addition to sediment effectively inhibits P release from sediment, but Fe-treated biochar promotes P release from sediment in low-DO environments. On the other hand, using Fe^{3+}-added sediment in SMFCs enhanced electricity production more than Fe^{2+}. Operation of SMFCs or Fe^{3+}-incorporated SMFCs reduced P release. However, enhanced organic matter decomposition in nutrient-rich agricultural sediment by SMFCs or Fe^{3+}-incorporated SMFCs may in turn release P into the overlying water. The knowledge obtained from this study can be applied to internal P management tactics in agricultural drainage sediment.

6.2 Implication for further study

In our study, we observed that the release of P from sediment is intricately linked to the dynamics of Fe and sulfur within the sediment. Specifically, our results showed that in sulfur-rich sediment, sulfide oxidation is more prominent compared to Fe oxidation processes. This suggests that the presence of sulfur influences the redox reactions occurring in the sediment, potentially affecting P release mechanisms. To effectively address the issue of P suppression by SMFCs, it is essential to delve deeper into the anode reactions associated with sulfur and Fe oxidation. By conducting further research in this area, while considering the specific properties of the sediment involved, we can gain a more comprehensive understanding of how sulfur and Fe dynamics impact P release and how they can be manipulated to enhance SMFC performance in managing P concentrations. This future implication underscores the significance of optimizing the interactions between sulfur, Fe, and sediment properties to improve the efficiency and effectiveness of SMFCs in mitigating P-related issues. By elucidating the complex interplay between these factors, we can develop more targeted strategies for P management in aquatic environments.

In our study, we observed that the addition of Fe to sediment in SMFCs increased

P release. This phenomenon can be attributed to the enhanced decomposition of organic matter facilitated by the presence of Fe. When Fe was mixed with sediment, it likely accelerated the organic matter decomposition in sediment, leading to higher levels of P release. Based on these findings, it is suggested that modifying the anode with Fe would be a more favorable approach compared to simply adding Fe into the sediment as a conductive material. Anode modification by Fe might potentially provide the benefits of enhanced organic matter decomposition without directly influencing P release from the sediment. This approach allows for more targeted control over the processes involved in P dynamics within SMFCs, offering a more efficient and effective strategy for managing P concentrations in aquatic environments.

REFERENCES

Aida AA, Hatamoto M, Yamamoto M, Ono S, Nakamura A, Takahashi M, Yamaguchi T: Molecular characterization of anaerobic sulfur-oxidizing microbial communities in up-flow anaerobic sludge blanket reactor treating municipal sewage. *J. Biosci. and Bioeng.*, **118**, 540-545, 2014.

Ajmal Z, Muhmood A, Dong R, Wu S: Probing the efficiency of magnetically modified biomass-derived biochar for effective phosphate removal. *J. Environ. Manag.,* **253**, 109730, 2020,

Algar CK, Howard A, Ward C, Wanger G: Sediment microbial fuel cells as a barrier to sulfide accumulation and their potential for sediment remediation beneath aquaculture pens. *Sci. Rep*., **10**, 13087, 2020.

Almanassra IW, Mckay G, Kochkodan V, Ali Atieh M, Al-Ansari T: A state of the art review on phosphate removal from water by biochars. *Chem. Eng. J.*, **409**, 128211, 2021.

Al-Wabel, MI, Al-Omran E, El-Naggar AH, Nadeem M, Usman AR: Pyrolysis temperature induced changes in characteristic and chemical composition of biochar produced from conocarpus wastes. *Bioresour. Technol.*, **131**, 374–379, 2013.

Angelov A, Bratkova S, Loukanov A: Microbial fuel cell based on electroactive sulfate-reducing biofilm. *Energy Convers. Manag.*, **67**, 283-286, 2012.

Ann Y, Reddy KR, Delfino JJ: Influence of chemical amendments on phosphorus immobilization in soils from a constructed wetland, *Ecol. Eng*., **14**, 157-167, 2000.

Bakker ES, Van Donk E, Immers AK: Lake restoration by in-lake iron addition: a synopsis of iron impact on aquatic organisms and shallow lake ecosystems. *Aquat. Ecol.*, **50**, 121-135, 2016.

Bensaida K, Falyouna O, Maamoun I, Eljamal, O: Understanding the effect of Fe(II) and Fe(III) in generating electricity from real waste sludge in microbial fuel cells. Proceedings of International Exchange and Innovation Conference on Engineering & Sciences (IEICES), Kyushu University, 2021. doi.org/10.5109/4738584

Bhatti, ZA, Syed, M, Maqbool, F, et al. Potential of molasses substrate for bioelectricity production in microbial fuel cell with the help of active microbial community. *Int J Energy Res.* **46**(8), 11185-11199, 2022.

Bolster CH: Comparing unamended and Fe-coated biochar on removal efficiency of bacteria, microspheres, and dissolved phosphorus in sand filters. *Biochar*, **3**, 329-338, 2021.

Bolton L, Joseph S, Greenway M, Donne S, Munroe P, Marjo CE: Phosphorus adsorption onto an enriched biochar substrate in constructed wetlands treating, *Ecol. Eng*., **142**, 100005, 2019.

Bond DR, Lovley DR: Electricity production by Geobacter sulfurreducens attached to electrodes. *Appl.Environ. microbiol*., **69**, 1548-1555, 2003.

Burley KL, Prepas EE, Chambers PA: Phosphorus release from sediments in hardwater eutrophic lakes: the effects of redox-sensitive and -insensitive chemical treatments. *Freshw Biol*., **46**, 1061–1074, 2001.

Cai L, Zhang H, Feng Y, Wang Y, Yu M: Sludge decrement and electricity generation of sludge microbial fuel cell enhanced by zero valent iron. *J. Clean. Prod*., **174**, 35-41, 2018.

Carpenter, SR: Phosphorus control is critical to mitigating eutrophication. Proceedings of the National Academy of Sciences of the United States of America, **105**, 11039-11040, 2008. doi.org/10.1073/pnas.0806112105

Chen M, Ding S, Chen X, Sun Q, Fan X, Lin J, Ren M, Yang L, Zhang C, Mechanisms driving phosphorus release during algal blooms based on hourly changes in iron and phosphorus concentrations in sediments. *Water. Res.*, **133**, 153-164, 2018.

Chen M, Sun HQ, Jiang H: The addition of FeOOH binds phosphate in organic matter-rich sediments. *Chem. Ecol.*, **32**(5), 432-445, 2016.

Chislock MF, Doster E, Zitomer R, Wilson AE: Eutrophication: Causes, consequences, and controls in aquatic ecosystems. *Nature Education Knowledge*, **4**(4) **(**, 10, 2013.

Conley DJ, Paerl HW, Howarth RW, Boesch DF, Seitzinger SP, Havens KE, Lancelot C, Likens GE: Controlling eutrophication: nitrogen and phosphorus. *Science*, **323**(5917), 1014-1015, 2009.

Cui J, Jin Z, Wang Y, Gao S, Fu Z, Yang Y, Wang Y: Mechanism of eutrophication process during algal decomposition at the water/sediment interface. *J. Clean Prod.*, **309**, 127175, 2021.

Cui Q, Jiao G, Zheng J, Wang T, Wu G, Li G: Synthesis of a novel magnetic caragana korshinskii biochar/mg–al layered double hydroxide composite and its strong

adsorption of phosphate in aqueous solutions. *RSC Adv.*, **9**, 18641–18651, 2019.

Dael TV, De Cooman T, Verbeeck M, Smolders E: Sediment respiration contributes to phosphate release in lowland surface waters. *Water Res.,***168**, 115168, 2020

Daghio M, Vaiopoulou E, Aulenta F, Sherry A, Head I, Franzetti A, Rabaey K: Anode potential selection for sulfide removal in contaminated marine sediments, *J. Hazard. Mater*, **360**, 498-503, 2018.

Dai Y, Wang W, Lu L, Yan L, Yu D: Utilization of biochar for the removal of nitrogen and phosphorus. *J. Clean. Prod.,* **257**, 120573, 2020.

Das SK, Ghosh GK: Soil Health Management Through Low Cost Biochar Technology. In: Singh, J. S. & Singh, C. (eds.) Biochar Applications in Agriculture and Environment Management. Cham: Springer International Publishing, 2020.

De Schamphelaire L, Rabaey K, Boeckx P, Boon N, Verstraete W. Outlook for benefits of sediment microbial fuel cells with two bio-electrodes. *Microb. Biotechnol.,***1**(6), 446-62, 2008. doi: 10.1111/j.1751-7915.2008.00042.x.

Ding S, Wang Y, Wang D, Li YY, Gong M, Zhang C: In situ, high-resolution evidence for iron-coupled mobilization of phosphorus in sediments. *Sci. Rep.*, **6**, 24341, 2016. doi: 10.1016/j.biortech.2019.122174

Dos-Passos VF, Marcilio R, Aquino-Neto S, Santana FB, Dias ACF, Andreote FD, de Andrade AR, Reginatto V: Hydrogen and electrical energy co-generation by a cooperative fermentation system comprising Clostridium and microbial fuel cell inoculated with port drainage sediment. *Bioresour. Technol.,* **277**, 94–103, 2019.

Dumas C, Mollica A, Féron D, Basséguy R, Etcheverry L, Bergel A: Marine microbial fuel cell: use of stainless steel electrodes as anode and cathode materials. *Electrochimica acta*, **53**, 468-473, 2007.

Duverger A, Berg JS, Busigny V, Guyot F, Bernard S, Miot J: Mechanisms of pyrite formation promoted by sulfate-reducing bacteria in pure culture. *Front. Earth Sci.*, **8**, 2020.

Emalya1 N, Munawar E, Suhendrayatna S, Fathanah U, Yunardi Y: An overview of recent advances in sediment microbial fuel cells for wastewater treatment and energy production, IOP Conf. Ser.: Earth Environ. Sci., **922**, 012002, 2021.

Foti, M, Sorokin DY, Lomans B, Mussman M, Zacharova EE, Pimenov NV, Kuenen JG, Muyzer G: Diversity, activity, and abundance of sulfate-reducing bacteria in saline

and hypersaline soda lakes. *Appl. Environ. Microbiol.*, 73, 2093-100, 2007.

Gao AL, Wan Y: Iron modified biochar enables recovery and recycling of phosphorus from wastewater through column filters and flow reactors. *Chemosphere*, **313**, 137434, 2023.

Gokalp Z, Bulut S: Potential use of biochar in wastewater treatment operations and soil improvement. *Current Trends in Natural Sciences*, **11**, 161-169, 2022.

Gong JJ, Ni ZK, Xiao SB, Zhao HC, Xi Y, Wang SR: Effects and differences of the release of dissolved organic and inorganic phosphorus in different sediments covered by different materials of Erhai Lake. Huan Jing Ke Xue **40** (4), 1826–1833, 2019. (In Chinese). 10.13227/j.hjkx.201807243.

González-Paz, JR, Del Carmen Monterrubio–Badillo M, Ordaz A, García-Peña EI, Guerrero-Barajas C: Influence of Fe^{2+} and Fe^{3+} on the performance and microbial community composition of a MFC inoculated with sulfate-reducing sludge and acetate as electron donor. *J. Chem.,* 5685178, 2022.

Groenenberg JE, Chardon WJ, Koopmans GF: Reducing Phosphorus Loading of surface water using iron-coated sand. *J. Environ. Qual.,* **42**, 250-259, 2013. doi.org/10.2134/jeq2012.0344

Guo F, Luo H, Shi Z, Wu Y, Liu H: Substrate salinity: a critical factor regulating the performance of microbial fuel cells, a review. *Sci. Total Environ*., **763**, 143021, 2021.

Guo F, Shi Z, Yang K, Wu Y, Liu H: Enhancing the power performance of sediment microbial fuel cells by novel strategies: Overlying water flow and hydraulic-driven cathode rotating. *Sci. Total Environ.*, **15**, 533-542, 2019

Guo H, Ren W, Huang C, Yang Q, Tang S, Geng X, Jia X: Effect of the Anode Structure on the Performance of Oily Sludge Sediment Microbial Fuel Cells. *ACS Omega*, **7**, 29959-29966, 2022.

Hagoss Y, Demeke A: Review on microbial fuel cell. *Basic Research J. Microb.*, **2**, 13, 2015.

Hamdan HZ, Salam DA, Hari AR, Semerjian L, Saikaly PE: Assessment of the performance of SMFCs in the bioremediation of PAHs in contaminated marine sediments under different redox conditions and analysis of the associated microbial communities. *Sci. Total Environ*., **575**, 1453–1461, 2017.

Hamdan HZ, Salam DA: Response of sediment microbial communities to crude oil

contamination in marine sediment microbial fuel cells under ferric iron stimulation. *Environ. Pollut.,* **263**, 114658, 2020.

Hamdan HZ, Salam DA: Sediment microbial fuel cells for bioremediation of pollutants and power generation: a review. *Environ. Chem. Lett.,* **21**, 2761–2787, 2023.

Han B, Song L, Li H, Song H: Immobilization of Cd and phosphorus utilization in eutrophic river sediments by biochar-supported nanoscale zero-valent iron. *Environ. Technol.,* **42**(26), 4072–4078, 2021.

Haque SE: How Effective Are Existing Phosphorus Management Strategies in Mitigating Surface Water Quality Problems in the U.S.? *Sustainability*, **13**, 6565, 2021.

Haxthausen K, Lu X, Zhang Y, Gosewinkel U, Petersen D, Marzocchi U, Brock A, Trapp S: Novel method to immobilize phosphate in lakes using sediment microbial fuel cells. *Water Res.*, **198**, 117108, 2021.

He J, Su D, Lv S, Diao Z, Xie J, Luo Y: Effects of Sediment Chemical Properties on Phosphorus Release Rates in the Sediment-Water Interface of the Steppe Wetlands. *Int. J. Environ. Res. Public Health,* **14**, 1430, 2017.

Heinrich L, Dietel J, Hupfer M: Sulphate reduction determines the long-term effect of iron amendments on phosphorus retention in lake sediments. *J. Soils Sediments*, **22**, 316-333, 2022.

Hong SW, Chang IS, Choi YS, Kim BH, Chung TH: Responses from freshwater sediment during electricity generation using microbial fuel cells. Bioprocess *Biosyst. Eng.,* **32**(3), 389-95, 2009.

Hong Z, Baoqing S: Historical distribution and partitioning of phosphorus in sediments in an agricultural watershed in the Yangtze-Huaihe region, *China Environ. Sci.Technol.*, **42** (7), 2328-2333, 2008.

Huang Q, Wang Z, Wang C, Wang S, Jin X: Phosphorus release in response to pH variation in the lake sediments with different ratios of iron-bound P to calcium-bound P. *Chem. Spec. Bioavailab.*, **17**, 55-61, 2005.

Hugerth LW, Wefer HA, Lundin A, Jakobsson HE, Lindberg M, Rodin S, Engstrand L, Andersson AF: DegePrime, a program for degenerate primer design for broad-taxonomic-range PCR in microbial ecology studies. *Appl. Environ.l Microbial.*, **80**(16), 5116–5123, 2014.

Immers AK, Bakker ES, Van Donk E, Ter Heerdt GNJ, Geurts JJM, Declerck SAJ:

Fighting internal phosphorus loading: An evaluation of the large scale application of gradual Fe-addition to a shallow peat lake. *Ecol. Eng.*, **83**, 78-89, 2015.

Izadi P, Fontmorin JM, Fernández LFL, Cheng S, Head I, Yu EH: High performing gas diffusion biocathode for microbial fuel cells using acidophilic iron oxidizing bacteria. *Front. Energy Res*., **7**, 2019.

James WF: Diffusive phosphorus fluxes in relation to the sediment phosphorus profile in big traverse bay, Lake of the Woods. Lake and Reservoir Management, **33**, 360-368, 2017.

Jiao GJ, Ma J, Li Y, Jin D, Ali Z, Zhou J, Sun R: Recent advances and challenges on removal and recycling of phosphate from wastewater using biomass-derived adsorbents. *Chemosphere*, ***278***, 130377, 2021.

Jiao Y, Li D, Wang M, Gong T, Sun M, Yang T: A scientometric review of biochar preparation research from 2006 to 2019. *Biochar*, **3**(3):283–298, 2021.

Jin G, Onodera SI, Saito M, Shimizu Y: Sediment phosphorus cycling in a nutrient-rich embayment in relation to sediment phosphorus pool and release. *Springer japan KK*, **21**(3), 415-425, 2020. doi: 10.1007/s10201-020-00627-x

Kankanamge NR, Bennett WW, Teasdale PR, Huang J, Welsh DT: A new colorimetric DET technique for determining mm-resolution sulfide porewater distributions and allowing improved interpretation of iron(II) co-distributions. *Chemosphere*, **244**, 125388, 2020.

Kato S, Hashimoto K, Watanabe K: Iron-oxide minerals affect extracellular electron-transfer paths of Geobacter spp. *Microb. Environ*., **28**, 141 – 148, 2013.

Kaur A, Boghani HC, Michie I, Dinsdale RM, Guwy AJ, Premier GC: Inhibition of methane production in microbial fuel cells: Operating strategies which select 68 electrogens over methanogens. *Bioresour. Technol.*, **173**, 75–81, 2014. https://doi.org/10.1016/j.biortech.2014.09.091

Kim K, Nakashita S, Hibino T: Enhanced power performance of an in situ sediment microbial fuel cell with steel-slag as the redox catalyst: i. electricity generation. *Sustain. Energy Fuels*, **4**, 1363-1371, 2020.

Kim K, Nakashita S, Yoshimura K, Hibino T: In situ electrochemical remediation of brackish river sediment rich in aromatic organic matter using steel-slag-combined sediment microbial fuel cells. *Journal of Clean. Prod.*, **315**, 128206, 2021.

Kim K, Takahashi T, Yumioka R, Hibino T: Sediment microbial fuel cells in oxidative sedimentary environments using iron substrate as voltage booster. *J. Power Sources*, **557**, 232510, 2022.

King K, Williams M, Macrae M, Fausey NR, Frankenberger J, Smith D, Kleinman P, Brown L: Phosphorus transport in agricultural subsurface drainage: *A Review. J. Environ. Qual*., **44**, 2015.

Kleeberg A, Herzog C, Hupfer M: Redox sensitivity of iron in phosphorus binding does not impede lake restoration. *Water Res*., **47**, 1491-1502, 2013.

Kouzuma A, Kasai T, Nakagawa G, Yamamuro A, Abe T, Watanabe K: Comparative metagenomics of anode-associated microbiomes developed in rice paddy-field microbial fuel cells. PLoS One, **8**(11), e77443.

Kubota K, Watanabe T, Maki H, Kanaya G, Higashi H, Syutsubo, K: Operation of sediment microbial fuel cells in Tokyo Bay, an extremely eutrophicated coastal sea. *Bioresour. Technol. Rep.*, **6**, 39-45, 2019.

Lamichhane B, Dunn B, Ouedraogo A, Singh H: Preparation of Biochar for Use as a Soil Amendment, Division of Agricultural Sciences and Natural Resources, Oklahoma Cooperative Extension Service, HLA-6502, 2023.

Lei P, Nunes L, Liu YR, Zhong H, Pan K: Mechanisms of algal biomass input enhanced microbial Hg methylation in lake sediments. *Environ. Int.,* **126**, 279-288, 2019.

Li H, Liu L, Li M, Zhang X: Effects of pH, temperature, dissolved oxygen, and flow rate on phosphorus release processes at the sediment and water interface in storm sewer. *J. Anal. Methods in Chem.,* 104316, 2013.

Li R, Gao L, Wu O., Liang Z, Hou L, Yang Z, Chen J, Jiang T, Zhu A, Li M: Release characteristics and mechanisms of sediment phosphorus in contaminated and uncontaminated rivers: A case study in South China. *Environ. Pollut.*, **268** (A), 115749, 2021.

Li S, Lin Z, Liu M, Jiang F, Chen J, Yang X., Wang S: Effect of ferric chloride on phosphorus immobilization and speciation in Dianchi Lake sediments. *Ecotoxicol. Environ. Saf*., **197**, 110637, 2020.

Li WW, Yu HQ: Stimulating sediment bioremediation with benthic microbial fuel cells. *Biotechnol. Adv.,* **33**, 1-12, 2015.

Li XC, Huang L, Fang HW, He GJ, Reible D, Wang CH: Immobilization of phosphorus

in sediments by nano zero-valent iron (nZVI) from the view of mineral composition. *Sci. Total Environ,.* **694**, 133695, 2019. doi.org/10.1016/j.scitotenv.2019.133695.

Li Y, Zhang C, Li P, Wang J, Zhou W, Zhang Y: Study on phosphorus releasing and releasing kinetics of sediments in Dongping Lake. *J. Hazard. Mater. Adv.*, **9**, 100234, 2023.

Lin CW., Alfanti L, Cheng YS, Liu SH: Enhancing bioelectricity production and copper remediation in constructed single-medium plant sediment microbial fuel cells. *Desalination*, **542**, 116079, 2022.

Lin JW, Zhao YY, Zhan YH, Wang Y: Control of internal phosphorus release from sediments using magnetic lanthanum/iron-modified bentonite as active capping material. *Environ. Pollut.* **264**, 15, 2020. https://doi.org/10.1016/j.envpol.2020.114809.

Lin Z, Ps K, Hada M, Nishikawa T, Hayashi Y: Simple technique of exfoliation and dispersion of multilayer graphene from natural graphite by ozone-assisted sonication. *Nanomater. (Basel)*, **7**(6), 125, 2017. doi: 10.3390/nano7060125.

Liu B, Zhai H, Liang Y, Ji M, Wang R: Increased power production and removal efficiency of polycyclic aromatic hydrocarbons by plant pumps in sediment microbial electrochemical systems: A preliminary study. *J. Hazard Mater.*, **380**, 120896, 2019.

Liu M, Li R, Wang J, Liu X, Li S, Shen W: Recovery of phosphate from aqueous solution by dewatered dry sludge biochar and its feasibility in fertilizer use. *Sci. Total Environ*., **814**, 152752, 2022.

Liu M, Li R, Wang J, Liu X, Li S, Shen W: Recovery of phosphate from aqueous solution by dewatered dry sludge biochar and its feasibility in fertilizer use. *Sci. Total Environ*., **814**, 152752, 2022.

Liu Q, Liu B, Li W, Zhao X, Zuo W and Xing D: Impact of ferrous iron on microbial community of the biofilm in microbial fuel cells. *Front. Microbiol.* **8**, 920, 2017. doi: 10.3389/fmicb.2017.00920

Liu SH, Su YH, Chen CC, Lin CW, Huang WJ: Simultaneous enhancement of copper removal and power production using a sediment microbial fuel cell with oxygen separation membranes. *Environ. Technol. Innov.*, **26**, 102369, 2022.

Liu TZ, Wang H, Zhang Z, Zhao D: Application of synthetic iron-oxide coated zeolite for

the pollution control of river sediments. *Chemosphere,* **180**, 160–168, 2017. doi.org/10.1016/j.chemosphere.2017.04.023.

Liu X, Tao Y, Zhou K, Zhang Q, Chen G, Zhang X: Effect of water quality improvement on the remediation of river sediment due to the addition of calcium nitrate. *Sci Total Environ*, **575**, 887-894, 2017.

Liu X, Zhang G, Sun G, Wu Y, Chen Y: Assessment of Lake Water Quality and Eutrophication Risk in an Agricultural Irrigation Area: A Case Study of the Chagan Lake in Northeast China. *Water*, **11**, 2380, 2019.

Liu Y, Shi H, Li W, Hou Y, He M: Inhibition of chemical dose in biological phosphorus and nitrogen removal in simultaneous chemical precipitation for phosphorus removal. *Bioresour. Technol.* **102** (5), 4008–4012, 2011.

Liu Z, Zhang Y, Han F, Yan P, Liu B, Zhou Q, Min F, He F, Wu Z: Investigation on the adsorption of phosphorus in all fractions from sediment by modified maifanite. *Sci. Rep.,* **8**, 15619, 2018.

Liu, GR, Ye CS, He JH, Qian Q, Jiang H: Lake sediment treatment with aluminum, iron, calcium and nitrate additives to reduce phosphorus release. *J. Zhejiang Univ. Sci. A,* **10** (9), 1367–1373, 2009. doi.org/10.1631/jzus.A0920028.

Logan B, Logan BE: Exoelectrogenic bacteria that power microbial fuel cells. Nat Rev Microbiol 7: 375-381. Nature reviews. *Microbiol.*, **7**, 375-81, 2009.

Logan BE, Rossi R, Ragab A, Saikaly PE: Electroactive microorganisms in bioelectrochemical systems. Nat. Rev. *Microbiol.,* **17**(5), 307-319, 2019.

Loh PS, Molot LA, Nurnberg GK, Watson SB, Ginn B: Evaluating relationships between sediment chemistry and anoxic phosphorus and iron release across three different water bodies. *Inland Waters*, **3**, 105–118, 2013. doi.org/10.5268/iw3.1.533.

Lu L, Xing D, Ren Z: Microbial community structure accompanied with electricity production in a constructed wetland plant microbial fuel cell. *Bioresour. Technol.*, **195**, 115-121, 2015.

Lu X, Von Haxthausen KA, Brock AL, Trapp S: Turnover of lake sediments treated with sediment microbial fuel cells: a long-term study in a eutrophic lake. *Sci. Total Environ.*, **796**, 148880, 2021.

Lukkari K, Leivuori M, Hartikainen H: Fractionation of sediment phosphorus revisited: ii. changes in phosphorus fractions during sampling and storing in the presence or

absence of oxygen. *Limnol. Oceanogr. Methods*, **5**, 445-456, 2007.

Luo CY, Wen SL, Lu YH, Dai JR, Du YX: Coprecipitation of humic acid and phosphate with Fe(III) enhances the sequestration of carbon and phosphorus in sediments. *Chem. Geol.*, **588**, 120645, 2022.

Luo D, Wang L, Nan H, Cao Y, Wang H, Kumar TV, Wang C: Phosphorus adsorption by functionalized biochar: a review. *Environ. Chem. Lett.*, **21**(1), 497-524, 2023.

Lyu H, Gao B, He F, Zimmerman AR, Ding C, Huang H, Tang J: Effects of ball milling on the physicochemical and sorptive properties of biochar: experimental observations and governing mechanisms. *Environ. Pollut.,* **233**, 54–63, 2018.

Maberly SC, Pitt JA, Davies PS, Carvalho L: Nitrogen and phosphorus limitation and the management of small productive lakes. *Inland Waters*, **10**(2), 159-172, 2020.

Mainstone, C, Parr W: Phosphorus in rivers - Ecology and management. *Sci. Total Environ.*, **282-283**, 25-47, 2002.

Mao YP, Pham AN, Xin YJ, Waite TD: Effects of pH, floc age and organic compounds on the removal of phosphate by pre-polymerized hydrous ferric oxides. *Sep. Purif. Technol.* **91**, 38–45, 2012. https://doi.org/10.1016/j.seppur.2011.09.045.

Marella TK, Saxena A, Tiwari A, Datta A, Dixit S: Treating agricultural non-point source pollutants using periphyton biofilms and biomass volarization. *J. Environ. Manage.*, **301**, 113869, 2022.

Martins G, Peixoto L, Teodorescu S, Parpot P, Nogueira R, Brito AG: Impact of an external electron acceptor on phosphorus mobility between water and sediments, *Bioresour. Technol.*, **151**, 419-423, 2014.

Mathuriya AS, Jadhav DA, Ghangrekar MM: Architectural adaptations of microbial fuel cells. *Appl. Microbiol. Biotechnol*. **102**, 9419–9432, 2018.

Min B, Cheng S, Logan BE: Electricity generation using membrane and salt bridge microbial fuel cells. *Water Res*., **39**(9), 1675-86. 2005.

Mitov M, Bardarov I, Mandjukov P, Hubenova Y: Chemometrical assessment of the electrical parameters obtained by long-term operating freshwater sediment microbial fuel cells. *Bioelectrochem*., **106**(Pt A): 105–114, 2015. doi.org/10.1016/j.bioelechem.2015.05.017

Mohan D, Sarswat A, Ok YS, Jr PC: Organic and inorganic contaminants removal from water with biochar, a renewable, low cost and sustainable adsorbent- -a critical

review. *Bioresour. Technol.,* **160**, 191-202, 2014.

Moodie AD, Ingledew WJ: Microbial anaerobic respiration. *Adv Microb Physiol.*, **31**, 225-69, 1990.

Münch, MA, Van Kaam R, As K, Peiffer S, Heerdt GT, Slomp CP, Behrends T: Impact of iron addition on phosphorus dynamics in sediments of a shallow peat lake 10 years after treatment. *Water Res.*, **248**, 120844, 2024.

Natarajan P, Gulliver J, Arnold W: Iron filings application to reduce lake sediment phosphorus release. Lake *Reserv. Manag.*, **37**, 1-19, 2021.

Nguyen HV, Maeda M: Effects of pH and oxygen on phosphorus release from agricultural drainage ditch sediment in reclaimed land. Kasaoka Bay, Japan. *Water Environ. Technol*., **14**(4), 228-235, 2016.

Ni Z, Zhou L, Lin Z, Kuang B, Zhu G, Jia J, Wang T: Iron-modified biochar boosts anaerobic digestion of sulfamethoxazole pharmaceutical wastewater: Performance and microbial mechanism. *J. Hazard. Mater.*, **452**, 131314, 2023.

Nosek D, Mikołajczyk T, Cydzik-Kwiatkowska A: Anode modification with Fe_2O_3 affects the anode microbiome and improves energy generation in microbial fuel cells powered by wastewater. *Int. J. Environ. Res. Public Health,* **20,** 2580, 2023. doi.org/10.3390/ijerph20032580

Ohmura N, Sasaki K, Matsumoto N, Saiki H: Anaerobic respiration using Fe(3+), S(0), and H(2) in the chemolithoautotrophic bacterium Acidithiobacillus ferrooxidans. *J. bacterial.*, **184**, 2081-2087, 2002.

Oktavitri NI, Nakashita S, Hibino T, Tran TV, Jeong I, Oh TG, Kim K: Enhancing pollutant removal and electricity generation in sediment microbial fuel cell with nano zero-valent iron. *Environ. Technol. Innov.,* **24**, 101968, 2021.

Pan F, Guo z, Cai Y, Fu Y, Wu J, Wang B, Liu H, Gao A, Cyclical patterns and immobilization mechanisms of phosphorus in sediments from a small creek estuary: evidenced from in situ monthly sampling and indoor experiments. *Water Res.*, **171**, 115479, 2020.

Panwar NL, Pawar A, Salvi BL: Comprehensive review on production and utilization of biochar. SN *Appl. Sci.,* **1**, 168, 2019. doi.org/10.1007/s42452-019-0172-6

Peng H, Jiang A, Wang H: Adsorption and desorption characteristics of phosphorus on sediment in Panzhihua section of Jinsha river, China, IOP Conference Series: Earth

and Environmental Science, Shenyang city, China, **651**, 042059, 2021.

Perera GLEP, Maeda M, Hiroaki S, Nakano C, Nishina Y: Iron-added sediment microbial fuel cells to suppress phosphorus release from sediment in an agricultural drainage, *J. Water Environ. Technol.*, **accepted**.

Pérez-Díaz MI, Zárate-Segura P, Bermeo-Fernández LA, Nirmalkar K, Bastida-González F, García-Mena J, Jan-Roblero J, Guerrero-Barajas C: Bacterial consortium from hydrothermal vent sediments presents electrogenic activity achieved under sulfate reducing conditions in a microbial fuel cell. *J. Environ. Health Sci. Eng.*, **18**(2), 1189-1205, 2020.

Pérgola M, Sacco NJ, Bonetto MC, Galagovsky L, Cortón E: A laboratory experiment for science courses: Sedimentary microbial fuel cells. *Biochem. Mol. Biol. Educ.*, **51**(2): 221– 229, 2023.

Perkins R, Underwood G: The potential for phosphorus release across the sediment–water interface in an eutrophic reservoir dosed with ferric sulphate. *Water Res.* **35** (6), 1399–1406, 2001. doi.org/10.1016/S0043-1354(00)00413-9

Pollman CD, Swain EB, Bael D, Myrbo A, Monson P, Shore MD: The evolution of sulfide in shallow aquatic ecosystem sediments: An analysis of the roles of sulfate, organic carbon, and iron and feedback constraints using structural equation modeling. *J. Geophys. Res. Biogeosci.*, **122**, 2719–2735, 2017.

Qi J, Sun Z, Zhang J, Ye C. The application of sediment microbial fuel cells in aquacultural sediment remediation. *Water*, **14**(17), 2668, 2022.

Qian J, Zhou X, Cai Q, Zhao J, Huang X: The Study of optimal adsorption conditions of phosphate on Fe-Modified biochar by response surface methodology. *Molecules*, **28**, 2323. doi.org/10.3390/molecules28052323

Qian ZY, Xue SG, Cui MQ, Wu C, Li WC: Arsenic availability and transportation in soil-rice system afected by iron-modifed biochar. *J. Cent. South Univ.,* **28**(6), 1901–1918, 2021.

Qin Y, Li H, Ma S, Li K, Zhang X, Hou D, Zheng X, Wang C, Lyu P, Xu S, Zhang W: Recovery and utilization of phosphorus from fruit and vegetable wastewater. *Sci. Rep*., **12**, 617, 2022.

Reitzel K, Andersen FØ, Egemose S, Jensen HS: Phosphate adsorption by lanthanum modified bentonite clay in fresh and brackish water. *Water Res.*, **47**, 2787-2796,

2013.

Ren J, Li N, Li L, An JK, Zhao L, Ren NQ: Granulation and ferric oxides loading enable biochar derived from cotton stalk to remove phosphate from water. *Bioresour. Technol.,* **178**, 119–125, 2015.

Richards CM, Pallud C: Kinetics of sulfate reduction and sulfide precipitation rates in sediments of a bar-built estuary (Pescadero, California). *Water Res.*, **94**, 86-102, 2016.

Robertson WD, Lombardo PS: Treatment of wastewater phosphate by reductive dissolution of iron: use of ferric oxyhydroxide media. *J. Environ. Qual*., **40**, 1955-1962, 2011.

Roden E, Edmonds J: Phosphate mobilization in iron-rich anaerobic sediments: microbial fe(iii) oxide reduction versus iron-sulfide formation. *Archiv. fur. Hydrobiol.,* **139**, 347-378, 1997.

Rothe M, Kleeberg A, Grüneberg B, Friese K, Pérez-Mayo M, Hupfer M: Sedimentary Sulphur:Iron Ratio Indicates Vivianite Occurrence: A study from two contrasting freshwater systems. PLOS ONE, **10**, e0143737, 2015. doi.org/10.1371/journal.pone.0143737

Rothe M, Kleeberg A, Hupfer M: The occurrence, identification and environmental relevance of vivianite in waterlogged soils and aquatic sediments. *Earth Sci. Rev*, 158, 51–64, 2016.

Rozan T, Taillefert M, Trouwborst R, Glazer B, Ma S, Herszage J, Valdes L, Luther G: Iron-sulfur-phosphorus cycling in the sediments of a shallow coastal bay: Implications for sediment nutrient release and benthic macroalgal blooms. *Limnol. Oceanogr*., **47**, 1346-1354, 2002.

Ryckelynck N, Stecher HA, Reimers CE: Understanding the anodic mechanism of a seafloor fuel cell: Interactions between geochemistry and microbial activity. *Biogeochemistry,* **76**, 113–139, 2005.

Rydin E: Potentially mobile phosphorus in lake erken sediment. *Water Res.*, 34(7), 2037-2042, 2000.

Schamphelaire L, Rabaey K, Boeckx P, Boon N, Verstraete W: Outlook for benefits of sediment microbial fuel cells with two bio-electrodes. *Microb. Biotechnol.*, **1**, 446-62, 2008.

Schindler DW, Carpenter SR, Chapra SC, Hecky RE, Orihel DM: Reducing phosphorus to curb lake eutrophication is a success. *Environ. Sci. Technol.* **50** (17), 8923-8929, 2016.

Schindler DW, Hecky RE, Findlay DL, Stainton MP, Parker BR, Paterson MJ, Beaty KG, Lyng M, Kasian SEM: Eutrophication of lakes cannot be controlled by reducing nitrogen input: Results of a 37-year whole-ecosystem experiment. Proceedings of the National Academy of Sciences of the United States of America, **105**, 11254–11258, 2008.

Schindler DW: Evolution of phosphorus limitation in lakes. *Science*, **195** (4275), 260-262, 1977.

Seidel L, Broman E, Turner S, Ståhle M, Dopson M: Interplay between eutrophication and climate warming on bacterial communities in coastal sediments differs depending on water depth and oxygen history. *Sci. Rep.*, **11**, 23384, 2021.

Sharpley A, Jarvie HP, Buda A, May L, Spears B, Kleinman P: Phosphorus legacy: overcoming the effects of past management practices to mitigate future water quality impairment. *J. Environ. Qual.,* **42**, 1308-1326, 2013.

Sharpley AN, Kleinman PJ, Flaten DN, Buda AR: Critical source area management of agricultural phosphorus: experiences, challenges and opportunities. *Water Sci. Technol.*, **64**, 945-52, 2011.

Smolders A, Roelofs JG. M: Sulphate-mediated iron limitation and eutrophication in aquatic ecosystems. *Aquat. Bot.*, **46**, 247-253, 1993.

Smolders AJP, Lamers LPM, Moonen M, Zwaga K, Roelofs JGM: Controlling phosphate release from phosphate-enriched sediments by adding various iron compounds. *Biogeochemistry*, **54**, 219-228, 2001.

Smolders AJP, Lamers LPM, Moonen M, Zwaga K, Roelofs JGM: Controlling phosphate release from phosphate-enriched sediments by adding various iron compounds. *Biogeochemistry*, **54**, 219-228, 2001.

Sondergaard M, Jensen JP, Jeppesen E: Role of sediment and internal loading of phosphorus in shallow lakes. *Hydrobiologia*, **506**, 135-145, 2003.

Søndergaard M, Jensen P, Jeppesen E: Retention and internal loading of phosphorus in shallow, Eutrophic Lakes. *Sci. World J.*, **1**, 427-442, 2001.

Song N, Jiang H, Yan Z: Contrasting effects of sediment microbial fuel cells (smfcs) on

the degradation of macrophyte litter in sediments from different areas of a shallow eutrophic lake. *Appl. Sci.*, **9**, 3703, 2019.

Song T, Tan W, Wu X, Zhou CC: Effect of graphite felt and activated carbon fiber felt on performance of freshwater sediment microbial fuel cell. *J. Chem. Technol. Biotechnol*., **87**, 1436–1440, 2012. https://doi.org/10.1002/jctb.3764

Song T, Zaisheng Y, Zhao ZW, Jiang H: Construction and operation of freshwater sediment microbial fuel cell for electricity generation. Bioproc Biosys. Eng., **34**, 621-7, 2011.

Stackpoole SM, Stets EG, Sprague LA: Variable impacts of contemporary versus legacy agricultural phosphorus on US river water quality. Proceedings of the National Academy of Sciences, **116**, 20562-20567, 2019.

Strawn DG, Crump AR, Peak D, GarciaPerez M, Moller G: Reactivity of Fe-amended biochar for phosphorus removal and recycling from wastewater. PLOS Water, **2**(4): e0000092, 2023.

Sudirjo E, Buisman C, Strik D: Activated carbon mixed with marine sediment is suitable as bioanode material for spartina anglica sediment/plant microbial fuel cell: plant growth, electricity generation, and spatial microbial community diversity. *Water*, **11**, 1810, 2019.

Sun Q, Sheng Y, Yang J, Bonito MD, Mortimer RJG: Dynamic characteristics of sulfur, iron and phosphorus in coastal polluted sediments, north China. *Environ. Pollut.*, **219**, 588-595, 2016.

Sun Y, Gao B, Yao Y, Fang J, Zhang M, Zhou Y, Chen H, Yang L: Effects of feedstock type, production method, and pyrolysis temperature on biochar and hydrochar properties. Chem. Eng., J., **240**, 574–578, 2014.

Takemura Y, Syutsubo K, Kubota K: Suppression of phosphorus release from eutrophic lake sediments by sediment microbial fuel cells. *Environ. Technol.*, **43**(17), 2581-2589, 2021.

Tammeorg O, Nürnberg G, Niemistö J, Haldna M, Horppila J: Internal phosphorus loading due to sediment anoxia in shallow areas: implications for lake aeration treatments. *Aquat. Sci.,* **82**, 54, 2020.

Touch N, Hibino T, Morimoto Y, Kinjo N: Relaxing the formation of hypoxic bottom water with sediment microbial fuel cells. *Environ. Technol.*, **38**, 3016-3025, 2017.

Tran TV, Lee IC, Kim K: Electricity production characterization of a Sediment Microbial Fuel Cell using different thermo-treated flat carbon cloth electrodes. *Int. J. Hydrog. Energy*, **44**, 32192-32200, 2019.

Tripathi M, Sahu JN, Ganesan P, Monash P, Dey TK: Effect of microwave frequency on dielectric properties of oil palm shell (OPS) and OPS char synthesized by microwave pyrolysis of OPS. *J. Anal. Appl. Pyrolysis,* **112**, 306–12, 2015.

Tu L, Jarosch KA, Schneider T, Grosjean M: Phosphorus fractions in sediments and their relevance for historical lake eutrophication in the Ponte Tresa basin (Lake Lugano, Switzerland) since 1959. *Sci. Total Environ.*, **685**, 806-817, 2019.

Van Nguyen H, Yoden T: Maeda M: Phosphorus flux across the sediment-water interface in a drainage ditch receiving water from livestock farms in Kasaoka, Japan. *J.Water Environ. Technol.*, **14**, 191-199, 2016.

Vuillemin A, Friese A, Wirth R, Schuessler JA, Schleicher AM, Kemnitz H, Lücke A, Bauer KW, Nomosatryo S, Von Blanckenburg F, Simister R, Ordoñez LG, Ariztegui D, Henny C, Russell JM, Bijaksana S, Vogel H: Vivianite formation in ferruginous sediments from Lake Towuti, Indonesia. *Biogeosciences*, **17**, 1955-1973, 2020.

Wang B, Gao B, Fang J: Recent advances in engineered biochar productions and applications. *Crit. Rev. Environ. Sci. Technol.*, **47**(22), 2158–2207, 2017.

Wang C, Jiang HL: Chemicals used for in situ immobilization to reduce the internal phosphorus loading from lake sediments for eutrophication control. *Crit. Rev. Environ. Sci. Technol.*, **46**, 947-997, 2016.

Wang H, Xu J, Sheng L: Preparation of straw biochar and application of constructed wetland in China: a review. *J Clean Prod*., **273**, 123131, 2020.

Wang H, Ye Y, Zhang J, Ning H, Xiang Y, Xiang Y, Song X, Zhao W, Guo F: Power performance improvement in sediment microbial fuel cells: recent advances and future challenges. *Int. J. Hydrogen Energy*, **48** (63), 24426−24446, 2023.

Wang H, Zhai P, Long X, Ma J, Li Y, Liu B, Xu Z: Research progress on using biological cathodes in microbial fuel cells for the treatment of wastewater containing heavy metals. *Front. Microbiol.,* **14**, 2023. doi.org/10.3389/fmicb.2023.1270431

Wang J, Chen J, Guo J, Sun Q, Yang H: Combined Fe/P and Fe/S ratios as a practicable index for estimating the release potential of internal-P in freshwater sediment. *Environ. Sci. Pollut. Res. Int.,* **25**, 10740-10751, 2018.

Wang J, Jiang X, Zheng B, Niu Y, Wang K, Wang W, Kardol P: Effects of electron acceptors on soluble reactive phosphorus in the overlying water during algal decomposition. *Environ. Sci. Pollut. Res. Int.,* **22**(24), 19507-17, 2015.

Wang J, Wang S: Preparation, modification and environmental application of biochar: A review. *J. Clean*, **227**, 1002-1022, 2019.

Wang Q, Liao Z, Yao D, Yang Z, Wu Y, Tang C: Phosphorus immobilization in water and sediment using iron-based materials: a review. *Sci. Total Environ.*, **767**, 144246, 2021.

Wang Q, Liao Z, Yao D, Yang Z, Wu Y, Tang C: Phosphorus immobilization in water and sediment using iron-based materials: A review. *Sci. Total Environ.*, **767**, 144246, 2021.

Wang SR, Jin X, Bu Q, Jiao L, Wu F: Effects of dissolved oxygen supply level on phosphorus release from lake sediments. colloids and surfaces *A: Physicochem. Eng. Aspects - Colloid Surface A*, **316**, 245-252, 2008.

Wang X, Shen N, Zhi Y, Zhang X, Wang G, Chen Y: Sulfur oxidation process: A neglected contributor to minimize P release during sediment microbial fuel cell operation. *J. Chem. Eng.*, **449**, 137845, 2022.

Wang X, Zhi Y, Chen Y, Shen N, Wang G, Yan Y: Realignment of phosphorus in lake sediment induced by sediment microbial fuel cells (SMFC), *Chemosphere*, **291**(pt 3), 132927, 2022.

Wang, G., Guo, Y., Cai, J., Wen, H., Mao, Z., Zhang, H., Wang, X., Ma, L. & Zhu, M: Electricity production and the analysis of the anode microbial community in a constructed wetland-microbial fuel cell. *RSC Advances*, **9**, 21460-21472, 2019.

Wildemeersch M, Tang S, Ermolieva T, Ermoliev Y, Rovenskaya E, Obersteiner M: Containing the Risk of Phosphorus Pollution in Agricultural Watersheds. *Sustainability*, **14**, 171, 2022.

Wilkinson GM: eutrophication of freshwater and coastal ecosystems. In: Abraham, M. A. (ed.) Encyclopedia of Sustainable Technologies. Oxford: Elsevier, 2017.

Wu D, Xing D, Lu L, Wei M, Liu B, Ren N: Ferric iron enhances electricity generation by Shewanella oneidensis MR-1 in MFCs. *Bioresour Technol.,* **135**, 630-4, 2013.

Wu J, Lin J, Zhan Y: Interception of phosphorus release from sediments using Mg/Fe-based layered double hydroxide (MF-LDH) and MF-LDH coated magnetite as geo-

engineering tools. *Sci. Total Environ.,* **739**, 2020. doi.org/ 10.1016/j.scitotenv.2020.139749

Wu Q, Liu J, Li Q, Mo W, Wan R, Peng S. Effect of electrode distances on remediation of eutrophic water and sediment by sediment microbial fuel cell coupled floating beds. *Int. J. Environ. Res. Public Health*., **19**(16), 10423, 2022.

Wu Y, Wen Y, Zhou J, Wu Y: Phosphorus release from lake sediments: Effects of pH, temperature and dissolved oxygen. KSCE, *J Civ. Eng.*, **18**, 323-329, 2014.

Wu Z, Ren D, Zhou H, Gao H, Li J: Sulfate reduction and formation of iron sulfide minerals in nearshore sediments from Qi'ao Island, Pearl River Estuary, Southern China. *Quat. Int*., **452**, 137-147, 2017.

Xi Y, Wang SR, Zhao HC, Zhang L, Xiao SB: Impact of different capping materials on the phosphorus release from lake sediment. *Environ. Chem.,* **36** (03), 532–541, 2017. (In Chinese).

Xia L, David T, Verbeeck M, Bruneel Y, Smolders E: Iron rich glauconite sand as an efficient phosphate immobilising agent in river sediments. *Sci. Total Environ*., **811**, 152483, 2022.

Xie F, Wu F, Liu G, Mu Y, Feng C, Wang H, Giesy JP: Removal of phosphate from eutrophic lakes through adsorption by in situ formation of magnesium hydroxide from diatomite. *Environ. Sci. Technol*., **48**, 582-590, 2014.

Xu P, Xiao E, Xu D, Li J, Zhang Y, Dai Z, Zhou Q, Wu Z: Enhanced phosphorus reduction in simulated eutrophic water: a comparative study of submerged macrophytes, sediment microbial fuel cells, and their combination. *Environ. Technol.*, **39**, 1144-1157, 2018.

Xu P, Xiao ER, Xu D, Zhou Y, He F, Liu BY, Zeng L, Wu ZB: Internal nitrogen removal from sediments by the hybrid system of microbial fuel cells and submerged aquatic plants. PLoS One, **12**(2), e0172757, 2017.

Xu S, Adhikari D, Huang R, Zhang H, Tang Y, Roden E, Yang Y: Biochar-facilitated microbial reduction of hematite. *Environmen. Sci. Technol*., **50**, 2389-2395, 2016.

Yamamoto T, Orimoto K, Asaoka S, Yamamoto H, Onodera SI: A Conflict between the legacy of eutrophication and cultural oligotrophication in Hiroshima bay. *Oceans*, **2**, 546-565, 2021.

Yang H, Liu J, Hu P, Zou L, Li YY: Carbon source and phosphorus recovery from iron-

enhanced primary sludge via anaerobic fermentation and sulfate reduction: Performance and future application. *Bioresour. Technol.*, **294**, 122174, 2019.

Yang Q, Zhao H, Zhao N, Ni J, Gu X: Enhanced phosphorus flux from overlying water to sediment in a bioelectrochemical system. *Bioresour. Technol.*, **216**, 182-7, 2016.

Yang X, Chen S: Microorganisms in sediment microbial fuel cells: Ecological niche, microbial response, and environmental function. *Sci. Total Environ.*,**756**, 144145, 2021

Yang X, Zhang R, Wang J, He K, Chen J: Fluxes and mechanisms of phosphorus release from sediments in seasonal hypoxic reservoirs: a simulation-based experimental study. *J. Soils Sediments*, **21**, 3246–3258, 2021.

Yao Y, Li D, Chen Y, Liu H, Wang G, Han R: High-resolution distribution of internal phosphorus release by the influence of harmful algal blooms (HABs) in Lake Taihu. *Environ. Res*., **201**, 111525, 2021.

Yin H, Zhang M, Yin P, Li J: Characterization of internal phosphorus loading in the sediment of a large eutrophic lake (Lake Taihu, China). *Water Res.*, **225**, 119125, 2022.

Yoo JC, Shin YJ, Kim EJ, Yang JS, Baek K: Extraction mechanism of lead from shooting range soil by ferric salts. *Process Saf. Environ. Protect.,* **103**, 174–182, 2016. doi.org/10.1016/j.psep.2016.07.002.

Zaaboub N, Ounis A, Helali MA, Bejaoui B, Lillebo AI, da Silva EF, Aleya L: Phosphorus speciation in sediments and assessment of nutrient exchange at the water-sediment interface in a Mediterranean lagoon: implications for management and restoration. *Ecol. Eng.* **73**, 115–125, 2014. doi.org/10.1016/j.ecoleng.2014.09.017.

Zabihallahpoor A, Rahimnejad M, Talebnia F: Sediment microbial fuel cells as a new source of renewable and sustainable energy: present status and future prospects. *RSC Adv.*, **5**, 94171-94183, 2015.

Zhang X, Yao H, Lei X, Lian Q, Roy A, Doucet D, Yan H, Zappi ME, Gang DD: A comparative study for phosphate adsorption on amorphous FeOOH and goethite (α-FeOOH): An investigation of relationship between the surface chemistry and structure. *Environ. Res*., **199**, 111223, 2021.

Zhao Q, Ji M, Li R, Ren ZJ: Long-term performance of sediment microbial fuel cells with multiple anodes. *Bioresour. Technol.*, **237**, 178-185, 2017.

Zhao S, Shi X, Sun B, Liu Y, Tian Z, Huotari J: Effects of pH on phosphorus form transformation in lake sediments. Water Supply, 2021.

Zhao X, Liu W, Cai ZQ, Han B, Qian TW, Zhao DY: An overview of preparation and applications of stabilized zero-valent iron nanoparticles for soil and groundwater remediation. *Water Res*., **100**, 245–266, 2016. doi.org/10.1016/j.watres.2016.05.019.

Zhou YL, Yang Y, Chen M, Zhao ZW, Jiang HL: To improve the performance of sediment microbial fuel cell through amending colloidal iron oxyhydroxide into freshwater sediments. *Bioresour. Technol.*, **159**, 232-239, 2014.